Maria Vatshaug Ottermo

Virtual Palpation Gripper

Doctoral thesis
for the degree of philosophiae doctor

Trondheim, June 2006

Norwegian University of
Science and Technology
Faculty of Information Technology, Mathematics and Electrical
Engineering
Department of Engineering Cybernetics

NTNU
Innovation and Creativity

NTNU
Norwegian University of Science and Technology

Doctoral thesis
for the degree of philosophiae doctor

Faculty of Information Technology, Mathematics and Electrical Engineering
Department of Engineering Cybernetics

ISBN 82-471-7945-8 (printed ver.)
ISBN 82-471-7943-1 (electronic ver.)
ISSN 1503-8181

ITK Report 2006-4-W

Doctoral Theses at NTNU, 2006:95

Printed by Tapir Uttrykk

In the middle of difficulty lies opportunity

(Albert Einstein)

Summary

This thesis presents the design and performance of the Virtual Palpation Gripper, an early prototype of a remote palpation instrument intended for laparoscopic surgery. Psychophysical experiments related to this prototype are also described.

In minimally invasive techniques, such as laparoscopic surgery, the interventions are performed with instruments inserted into the body through small incisions. This technique has become increasingly popular and is now considered the gold standard for many surgical procedures, such as cholecystectomy. The main advantages compared to open surgery are smaller scars, reduction in pain and faster recovery. Despite the advantages, laparoscopic surgery introduces many restrictions for the surgeon, such as reduced dexterity, fewer degrees of freedom and awkward positioning of the hands. Additionally, the visual and tactile perception is severely degraded. The aim of the Virtual Palpation Gripper is to compensate for some of the lost perception by feeding tactile information back to the surgeon. The ultimate goal is to make the remote palpation instrument serve as an extension of the surgeon's fingers. This is accomplished by attaching a tactile sensor array to the end effector of a laparoscopic grasper and a tactile display to the handle of the grasper. The sensor array then aids as the tactile sense, and the tactile information is sent to the surgeon's fingers via the tactile display to provide him with a feeling of the shape,hardness, or size of an object grasped with the laparoscopic instrument.

Two different sensor arrays are discussed. The first one is based on piezoelectricity and is made from scratch in our laboratory. The second sensor is the custom made TactArray, which is based on a mature capacitive technology. Both sensor arrays are small enough to fit through a 12 *mm* trocar. Due to crosstalk in the piezoelectric array, the TactArray sensor array is chosen for the prototype of the Virtual Palpation Gripper. The performance and usefulness of the sensor array is tested and documented through an experiment where 15 surgeons with varying experience participate. The main goal is to compare direct palpation (with gloved fingers

as in open surgery), palpation with a conventional laparoscopic grasper and palpation with a laparoscopic grasper with visually presented tactile information. Results show that direct palpation is superior to both the laparoscopic graspers, but that the grasper with visual feedback of the tactile image seems to be useful for subjects who fully understand how to use it, especially for hardness discrimination (note that the size of the end effector of the conventional grasper and the quality of the grasper differed from that of the laparoscopic grasper with visual feedback of the tactile image, and this may have affected the results).

The tactile shape display consists of small direct-current motors and has a size compatible with conventional laparoscopic instruments. Performance tests of the display are conducted with focus on positioning accuracy, force, bandwidth and stiffness. In addition, an experiment focusing on pin shapes for tactile displays is described. The results show that there is no significant variation in perception with the different pin shapes investigated.

Finally, the communication between the tactile sensor and the tactile display is described, and the full system is evaluated by performance tests and a psychophysical experiment. The display can successfully convey useful information about the size, hardness and shape of objects pressed against the tactile sensor array, although there is a definite potential for improving the bandwidth and resolution such that small scale information about texture and sharp edges can be represented. Ten subjects participate in the psychophysical experiments, where the goal is to compare our full remote palpation instrument with tactile feedback with a conventional laparoscopic grasper. The results show that the remote palpation system seems to work somewhat better than conventional laparoscopic instruments for discriminating between and locating different sizes.

Preface

This thesis is submitted in partial fulfillment of the requirements for the degree philosophiae doctor (PhD) at the Norwegian University of Science and Technology (NTNU). The research has been carried out at the Department of Engineering Cybernetics during the period of September 2002 through March 2006. My supervisor has been Professor Tor Arne Johansen. Postdoctoral Fellow Øyvind Stavdahl and Chief Physician Ronald Mårvik have been my advisors. The research was funded by the Research Council of Norway under grant 147830/V50. The project was initiated by the National Center for Advanced Laparoscopic Surgery (NSALK) at St.Olavs's hospital, Norway, and has been a collaboration between the Department of Engineering Cybernetics, SINTEF and NSALK.

I want to use this preface to thank all the persons who have helped and inspired me on the long journey towards completing this PhD. So many people have contributed, but I only have space to mention a few whom I think deserve special recognition.

My advisor Øyvind Stavdahl and my supervisor Tor Arne Johansen. Øyvind for his passionate interest in my work, his high spirits and his endless range of (usually) brilliant ideas. Tor Arne for always providing advice and motivation when needed, for dealing so efficiently and generously with financial issues and for maintaining an impressive response time on all queries. The interaction with my advisors has been of utmost importance for my work. Professor Robert Howe for giving me the opportunity to visit the Harvard BioRobotics lab and helping and backing me up in every possible way. My advisor Ronald Mårvik, Thomas Langø, Yunus Yavuz and Kirsten Rønning for useful discussions and help related to laparoscopic surgery and equipment.

All my friends and colleagues at the Department of Engineering Cybernetics and SINTEF IKT for providing an inspiring working environment. I would particularly like to thank the following persons: My dear friend

Anne Bjertnes for always backing me up, for asking the right questions when the journey seemed endless and for introducing me to the possibility of taking this PhD degree. My dear Petter Tøndel for your love, encouragement and enjoyable chats on MSN - often the highlight of a day at work. My friend Terje Mugaas (the LabVIEW expert) - your contributions have been invaluable. My friends Einar Idsø, Erik Kyrkjebø, Anne (again), Petter (again) and Bjørnar Bøhagen who always take their time to discuss any topic with me.

My friends and colleagues at the Harvard BioRobotics lab, especially Chris Wagner for his help and inspiration. The test persons who have made my experiments possible. At least 25 persons have willingly spent their spare time in the lab with me. This thesis would not have been a reality without your help.

The capable staff at the Department of Engineering Cybernetics for helping me with mechanical and electronic designs and paper work (Arvid, Terje, Hans, Stefano, John Olav, Rune, Jan, Kjell, Per Inge, Knut, Tove, Eva, Unni, the apprentices..). Life at the department would have been difficult without you. A special thanks goes to Arvid Lervold for his patience, inputs and help when working with my (sometimes bad or nonexistent) designs. Torgrim Gjelsvik for his work on my electronics and Marit Øvstedal for her contributions to the experiments conducted at St. Olav's hospital.

My dear friend Thale C. Holter for guiding me into the world of biomedical engineering and those nearest to me for being so patient about my long working hours.

My friends, my boyfriend and my family without whom my life would have been infinitely poorer (but my thesis might have been finished earlier).

Finally, I would like to dedicate this thesis to my parents and my brother. I thank you for your love, encouragement and interest in my work. My father Jan Helge for always believing in me and for speaking so warmly about the engineers at work - I would never have become an engineer if it was not for this! My mother Inger Lise for the hours spent on the phone trying to convince me that it would all be ok in the end and for keeping me company on my conference trip to Japan. My brother Jonas for being my proofreader, role model and dear friend. I would not and could not have done this without you.

I'm Still Learning (Michelangelo)

Maria Vatshaug Ottermo, June 2006

Contents

Chapter 1

Introduction

1.1 Motivation

Minimally Invasive Surgery (MIS) is an innovative approach in surgery and is one of the methods that make use of advanced technology to raise the standard of surgical procedures. In the case of laparoscopy, minimally invasive surgery to the abdomen, the operation is performed with instruments and viewing equipment inserted into the body through small incisions created by the surgeon. This method has many advantages, including minimization of surgical trauma, less damage to healthy tissue, smaller scars and faster recovery, all of which makes it a winning proposition for patients (Garry, 2005). Despite this, the method also has disadvantages due to reduced dexterity, workspace and sensory input to the surgeon, the latter of which is mainly available through a 2D video image.

The seeds for MIS were planted as far back as Hippocrates (460-377 BCE). His description of anoscopy for diagnosis of fistula and hemorrhoids is the earliest recorded reference to endoscopy (Jones, Wu and Soper, 2004). Over the years, a succession of physicians have searched for new ways to probe the mysterious inner workings of the body, including Albukasimi and Bozzini, who used endoscopic instruments to examine body orifices (Cueto-García, Jacobs and Gagner, 2003).

Minimally invasive techniques have come a long way and are now common in many gynecological, urologic, orthopedic and abdominal procedures. The first laparoscopic cholecystectomy was done in 1987, and in 1996, 70 % of all gall bladder removals were done using laparoscopic techniques (Bicchi, Canepa, Rossi, Iacconi and Scilingo, 1996).

Although post-operative complications are lower in laparoscopic surgery than in traditional surgery, it does not mean that it is risk free or straightforward. Per-operative complications are high, and this is due to several factors. The lack of the tactile sense is maybe the most important disadvantage associated with laparoscopy, because it limits the surgeon's abilities to examine and palpate internal organs. An example is detection of tumors. Since they tend to be harder than the surrounding tissue, tactile feedback can indicate the presence, size and exact location of a tumor, thereby enhancing the chances of performing successful diagnosis and surgery.

Despite the lack of the tactile sense, the use of laparoscopic techniques is ever-increasing, and this, in turn, leads to demands for better surgical tools. The work presented in this thesis aims at bringing research in this field closer to the optimal replacement of the human finger in laparoscopic techniques.

1.2 Contributions

The original scope of this project was to make a device that could compensate for the lost ability to palpate organs, tumors, blood vessels and gall stones in laparoscopic procedures. The idea was to make an endoscopic hand to be inserted through the incisions created by the surgeon, where 2-3 fingers on the instrument's end effector would measure tactile information (pressure distributions) to be sent to the surgeon's fingers. In this way the surgeon would be able to palpate structures (Virtual Palpation) and at the same time use the fingers to hold/move tissue (Gripper). Over time the extensiveness of the project has been reduced to developing a grasper with only one finger instead of an endoscopic hand.

The main contributions of the project are the early prototype of the remote palpation instrument called the Virtual Palpation Gripper (consisting of two main parts; a tactile sensor array and a tactile display), the accompanying driver circuits and the experiments conducted with parts of the system and the full system.

- The design and development of a sensor array based on piezoelectricity is described, as is the development of the amplifier circuit and filters to capture low frequencies. This sensor array was, however, replaced by a custom made system based on a commercially available sensor (TactArray).
- The tactile display has been designed and built from scratch and is one of the smallest available tactile shape arrays as of today.
- The compact driver circuits accompanying the tactile display were designed and developed.

- Communication between the tactile sensor and the tactile display has been implemented in LabVIEW software.
- The first experiment involves only the sensor part of the system, and the aim was to identify if information is lost in laparoscopic surgery compared to open surgery. The experiment provides useful information about the complexity of laparoscopic surgery and helps map the information needed to make surgery more effective.
- The second experiment excludes the tactile sensor array and uses the tactile shape display to investigate the importance of pin shapes used for such devices.
- The usefulness of the full system is investigated with simple performance tests and a psychophysical experiment aiming at comparing conventional laparoscopic instruments to our Virtual Palpation Gripper.

1.3 Publications

The thesis is based on several papers, and the connection between chapters and papers is as follows:

- Chapter 3 is based on (Ottermo, Stavdahl and Johansen, 2004)
- Chapter 4 is based on the paper (Ottermo, Øvstedal, Langø, Stavdahl, Yavuz, Johansen and Mårvik, 2006)
- Chapter 5 is based on the papers (Ottermo, Stavdahl and Johansen, 2005), (Ottermo, Stavdahl and Johansen, 2006a) and (Mårvik, Nesbakken, Langø, Yavuz, Bjelland, Ottermo and Stavdahl, 2006)
- Chapter 7 is based on the paper (Ottermo, Stavdahl and Johansen, 2006b)

1.4 Outline of the Thesis

PART I presents motivation, background information and earlier work on related devices.

- Chapter 2 gives basic information about laparoscopic surgery and human sensing, in particular touch and palpation. It also focuses on how tactile information can be captured and rendered and presents state of the art in both tactile sensors and displays.

PART II contains information about tactile sensor arrays and related experiments.

- Chapter 3 provides information about a sensor based on piezoelectricity, as well as a short presentation of the TactArray system, which is based on capacitive technology.
- Chapter 4 aims at evaluating the role of tactile feedback in laparoscopic surgery. The focus is put on comparing open surgery to laparoscopic surgery and evaluating if visually presented tactile information can compensate for the loss of tactile information in laparoscopic surgery.

PART III presents the design and performance of the tactile display.

- Chapter 5 gives a detailed description of the tactile display and the driver circuits that were custom made for the display. Additionally, it attempts to provide some implications for future displays.
- Chapter 6 describes an experiment aiming at finding implications for pin shapes to be used in tactile displays.

PART IV contains a description of the full system, called the Virtual Palpation Gripper, as well as evaluation of the performance of the system.

- Chapter 7 describes how the tactile sensor array and the tactile display communicate and experiments for evaluating the performance of the system, both from a technical and a psychophysical point of view.

PART V contains some concluding remarks.

- Chapter 8 discusses the results in the previous chapters and attempts to draw some conclusions. Suggestions for future work are also presented.

Appendix A presents calculations of the torque constant for our DC motors.
Appendix B contains details on the statistics used in Chapters 4 and 7.

Part I

Remote Palpation Systems

Chapter 2

Laparoscopic Surgery and Tactile Feedback

2.1 Introduction

Minimally invasive techniques were developed to reduce trauma (Bicchi et al., 1996) and have in many ways revolutionized surgical procedures. Not many years ago, removal of the gallbladder (cholecystectomy) was considered a major surgery, often followed by a one week hospital stay and a relatively high probability for postoperative complications. In recent years, minimally invasive techniques have brought laparoscopic cholecystectomy to a new level and is now performed as day surgery in many hospitals (Darzi and Munz, 2004, Begos and Modlin, 1994, Buanes, Mjaaland, Waage, Solheim and Færden, 1995). Despite this, there are drawbacks with laparoscopic surgery that need to be overcome to make it safer for the patient and easier to perform for the surgeon. One of the most important improvements could be to integrate some kind of tactile feedback on the instruments, such that the surgeon is able to examine and palpate internal organs in a way similar to open surgery. To achieve this, it has been proposed to make an instrument containing a tactile sensor and a tactile display (see Figure 2.1).

This chapter seeks to illuminate some of the advantages and problems related to laparoscopic surgery, as well as giving an overview of human tactile sensation. It also explains some of the challenges and requirements related to tactile feedback and how a remote palpation instrument can capture and display tactile information. Additionally, existing devices are discussed.

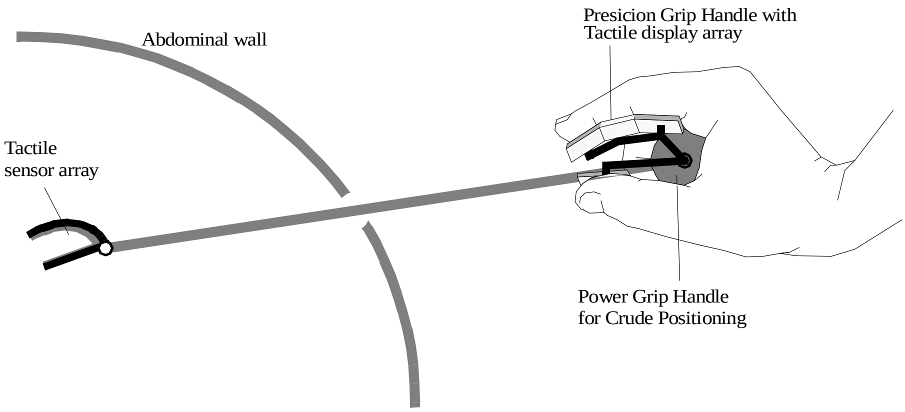

Figure 2.1: A sketch of the instrument with tactile sensor and display.

2.2 Laparoscopic Surgery

As mentioned in Chapter 1, laparoscopic surgery involves inserting a series of tubes through incisions (trocars) created by the surgeon. Through these trocars, camera and instruments can be inserted to the abdominal cavity after insufflation of $2 - 4\ l\ CO_2$ for elevation of the abdominal wall (see Figures 2.2 and 2.3).

The incisions made in laparoscopic procedures are only $2 - 12\ mm$, and this results in less damage to surrounding tissue, reduced chance for haemorrhage and infections, reduced post-surgical pain and a better cosmetic result (Broeders and Ruurda, 2002). Consequently, the recovery times decrease, more patients can be treated and waiting lists shrink. In a study of clinical and economic considerations of laparoscopic and open cholecystectomy, Berggren, Zathraeus, Arvidsson, Haglund and Jonsson (1996) found that the costs were reduced with $370 per patient in laparoscopic surgery compared to open procedures. Blomqvist, Lönroth, Dalenbäck and Lundell (1998) found that the total cost was 45% lower in laparoscopic fundoplication than in open fundoplication. In other words, laparoscopic surgery is a winning proposition both for the patient and those who pick up the bill.

Despite the advantages, minimally invasive techniques have drawbacks and often these end up resting on the surgeon's shoulders. Working with instruments through trocars severely restricts the surgeon's dexterity. Most importantly, the trocars limit the workspace and the degrees of freedom to

Figure 2.2: A laparoscopic procedure (printed with permission from NSALK (National Center for Advanced Laparoscopic Surgery)).

four (in/out, left/right, up/down and rotation), meaning that it is difficult to manoeuvre the instruments to an optimal position relative to the tissue. Secondly, a movement outside the abdominal cavity will result in an inverted response on the inside. Another problem is that a small deflection on the outside can result in a major displacement of the instrument's end effector if a large portion of the instrument is inside the abdomen (Broeders and Ruurda, 2002).

In addition to dexterity, the visual perception is degraded. The two-dimensional representation of the three-dimensional reality results in loss of depth, and hence the requirements for resolution, color and contrast are high. When the surgeon looks at the monitor instead of his hands he also looses some of the important hand-eye coordination (Broeders and Ruurda, 2002). Tendick and Cavusoglu (1997) measured movement trajectories under direct and videoscopic conditions. The task was to touch targets (nails) spaced from $30-50$ *mm* apart. Results showed that the initial phase (from initiation of movement to the first minimum in the speed curve) of point-to-point movements were equal under the two viewing conditions, but that the accuracy of the movement was better under direct viewing (10 *mm* for

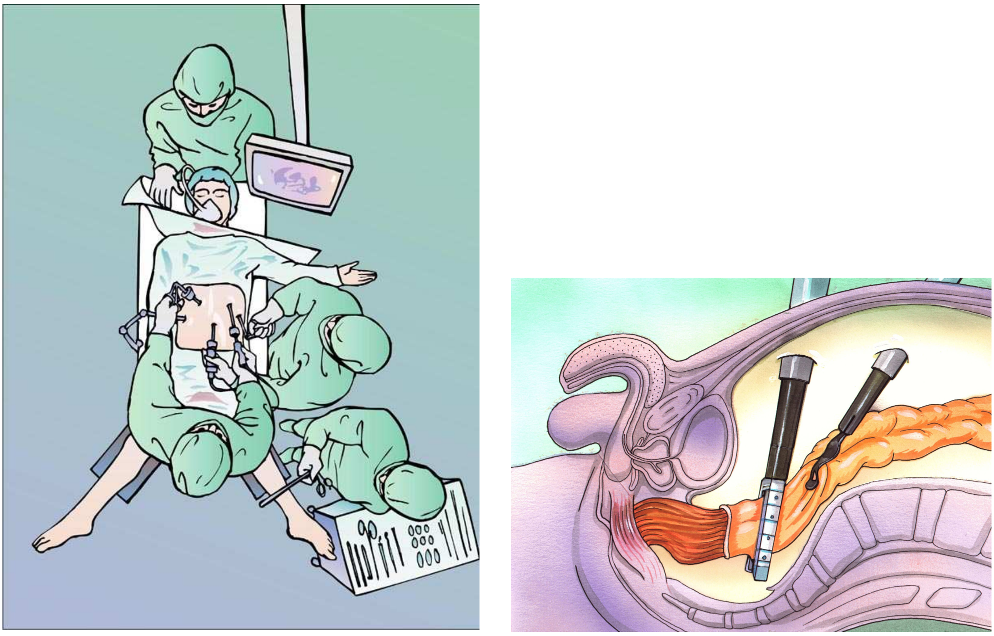

(a) Full setup (b) Inside the abdominal cavity

Figure 2.3: Figures showing the setup in laparoscopic surgery and the instruments inside the abdominal cavity.

direct viewing versus 15 *mm* for laparoscopic). This resulted in a shorter total movement duration (from initiation of movement until the subject lifted the instrument after touching the goal) of around 0.7 *s*. Another problem with the endoscope is that the surgeon is dependent on an assistant to control it. It is important that the assistant has the required training for this, as the surgeon can easily become disoriented (Øvstedal, 2005).

When performing conventional surgery, the surgeons use palpation actively for diagnosing tumors, inflamed tissue, gallstones etc. In laparoscopic surgery, most of this haptic feedback is eliminated. In Wagner, Stylopoulos and Howe (2002) they showed that the absence of force feedback increased the average force magnitude applied to the tissue by at least 50%, and that the number of errors that damage tissue increased by more than a factor of 3. In fact, restoring the haptic capability is considered so important that it is a prime research area in laparoscopy at present (Eltaib and Hewit, 2003). There are, however, disagreements about to what extent haptic feedback is lost in minimally invasive techniques. Bholat, Haluck, Murray, Gorman and Krummel (1999) stated that haptic feedback is altered but not eliminated when using laparoscopic instruments, and then the question arises about whether or not this altered information is useful for the surgeon. Other groups have demonstrated that an operator could easily differentiate between tissue samples of varying stiffness when provided with force feedback, although not as successfully as a gloved hand (Hu, Tholey, Desai and Castellanos, 2004, Tholey, Desai and Castellanos, 2005, MacFarlane, Rosen, Hannaford, Pellegrini and Sinanan, 1999).

As already mentioned, the lack of tactile information in minimally invasive techniques in combination with more complex procedures have resulted in a lot of research in the area. Some robot-assisted systems that allow for better dexterity and 3D view of the surgical field (i.e. the Da Vinci system from Intuitive Surgical, USA) have been developed. The drawbacks mentioned above often result in more time-consuming interventions, especially for complex procedures. This is obviously tiresome for the surgeons, who already work with their hands in awkward positions. This will not be a problem with robot-assisted technology (Broeders and Ruurda, 2002). Robots are also more stable and reliable, but unless the system is specifically designed to avoid it, all haptic feedback will be lost. Studies of how the surgeons work and how they use their fingers are, therefore, important to be able to make a useful system.

2.3 Human Sensing

2.3.1 Haptic and Tactile Feedback

Early in the 20th century David Katz emphasized that the sense of touch is an active, richly informative and highly useful perceptual modality (Klatzky and Lederman, 2004). The word haptic refers to the capability to sense a natural or synthetic mechanical environment through touch. The term haptic can be further divided into two components, where one is concerned with manipulation (such as gripping) and the other collects sensory information from the world around us. Tactile and kinesthetic channels work together to provide humans with means to perceive and act on their environment (Hayward, Astley, Cruz-Hernandez, Grant and Robles-De-La-Torre, 2004).

2.3.2 Touch

Touch is one of the somatic senses, which are the nervous mechanisms that collect sensory information from the body. The mechanoreceptive somatic senses include both tactile and position sensations that are stimulated by mechanical displacement of some tissue of the body. The tactile senses include touch, pressure, vibration and tickle senses, and the position senses include static position and rate of movement. Although touch, pressure and vibration are frequently classified as separate sensations, they are all detected by the same types of receptors (Guyton and Hall, 2000). The skin is the largest sense organ of the body and consists of two major layers: the epidermis (outer) and the dermis (inner) (see Figure 2.4). The figure also shows the location of the four receptor types in the volar part of the hand.

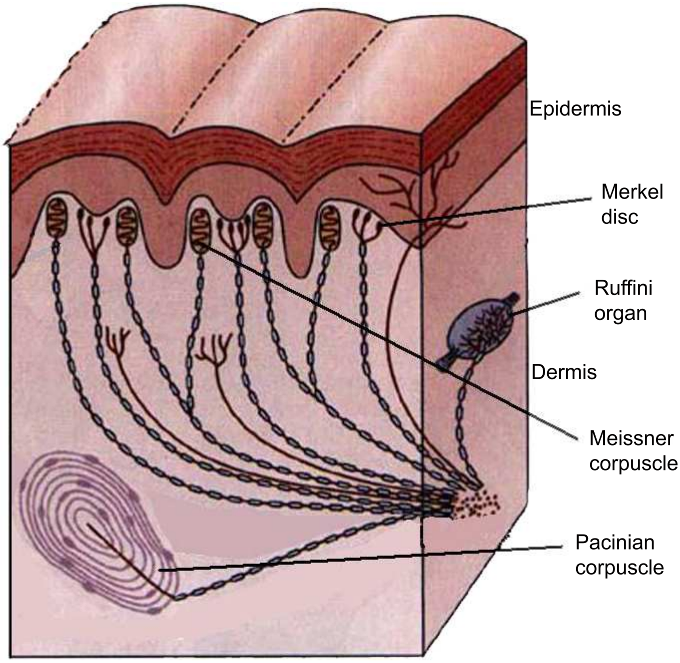

Figure 2.4: The glabrous skin on the human finger pad (modified figure from Kandel et al. (2000)).

A special characteristic of all sensory receptors is that they adapt, either partially or completely, to any constant stimulus after a period of time. This means that when a continuous sensory stimulus is applied, the receptor responds at a high impulse rate at first and then at a progressively slower rate until, finally, the rate of action potentials decreases to very few or often none at all (Guyton and Hall, 2000). The *Meissner's corpuscles* are fast adapting, and they are particularly sensitive to movement of objects over the surface of the skin and low-frequency vibration. *Pacinian corpuscles* are also fast adapting, and they are stimulated by rapid movements. They are particularly important for detecting tissue vibrations or other rapid changes in the mechanical state of tissues. *Merkel's discs* are slowly adapting and responsible for giving steady-state signals that allow one to determine continuous touch of objects against the skin. They are important for localizing touch sensations to surface areas and in determining the texture of objects. Finally, *Ruffini's end organs* adapt very slowly and they are important for signaling continuous states of deformation of the skin and deeper tissues, such as heavy and prolonged touch and pressure signals. They are also present in joint capsules and help signal the degree of joint rotation (Guyton and Hall, 2000).

The finger is one of the most sensitive areas of the human body. The spatial resolution is often determined by using a method called two-point discrimination. Two needles are pressed lightly against the skin at the same time, and the subject determines whether two or one points of stimulus are felt. While the two-point discrimination on the finger is as close as $1 - 2$ mm, it can be as far apart as $30 - 70$ mm on the person's back (Guyton and Hall, 2000). Humans can also detect extremely fine textures. LaMotte and Srinivasan (1991) showed that humans can feel dots as small as 2 μm high when there is tangential relative motion between the object and the finger pad skin.

The temporal resolving capacity has been measured by looking at sensitivity to vibratory frequency, showing that human subjects can detect a wide range of frequencies. Pacinian corpuscles can detect signal vibrations from 30 to 800 cycles per second. Low-frequency vibrations from 2 up to 80 cycles per second stimulate other tactile receptors, especially Meissner's corpuscles (Guyton and Hall, 2000).

Tests of absolute and relative sensitivity to applied force describe people's threshold responses to intensive aspects of mechanical deformation (e.g., the depth of penetration of a probe into the skin). In Boff, Kaufman and Thomas (1986), Sherrick and Cholewiak states that the power needed to excite a response in the skin and kinesthetic senses is about $10 \cdot 10^{-8}$ W.

2.3.3 Palpation

Palpation means to examine or explore by touching (an organ or area of the body), usually as a diagnostic aid. Medical procedures utilize a wide variety of palpation techniques, depending on the task objectives (Peine, 1998).

Some studies have been conducted to classify specific motions and postures during haptic exploration, including Napier (1956), (Lederman and Klatzky, 1987), (Cutkosky and Howe, 1990) and (Peine, 1998).

Napier (1956) divides the movements of the hand into two main groups: prehensile movements and non-prehensile movements. Prehensile movements include movements in which an object is seized and held partly or wholly within the compass of the hand. Non-prehensile movements, on the other hand, are movements in which no grasping or seizing is involved, but by which objects can be manipulated by pushing or lifting motions of the hand. Prehensile movements are further divided into precision and power grips, where a power grip squeezes an object strongly between the pads of the fingers and the palm, while a precision grip includes using the tips of the fingers only. Lederman and Klatzky (1987) suggest a taxonomy for purposive hand movements that achieve object apprehension. Cutkosky and Howe (1990) observed single-handed operations by machinists in working with metal parts and hand tools and developed a systematic arrangement of the space of human grasps. Peine (1998) observed surgeon's palpation and developed a table of typical palpation motions and parameters that can be sensed using these motions. In general, finger motion has two components: normal motion into the tissue and tangential motion caused by sliding or pushing along the surface of the tissue. The amount of normal pressure depends on the type of tactile sensation and if the object is deep into the tissue. The extent of lateral motion, on the other hand, depends mainly on whether the tactile cues are spatially distributed or not.

Palpation is an active and complex process. Any equipment for enhancing the surgeon's understanding of the object he is palpating should, therefore, be designed in such a way that it does not introduce any interference with the surgeon's original task. The design of a remote palpation instrument also depends on the specific surgical application. Our instrument will eventually be mounted on a conventional laparoscopic grasper and should not obstruct the surgeon's movability. Additionally, we focus on using the index finger for sensing the tactile display, because this leaves the thumb and the middle finger free to manipulate the grasper, as is common for many grips.

2.4 Capturing Tactile Information

2.4.1 Challenges and Requirements

A tactile sensor measures the spatially distributed parameters of contact on the surface between the sensor and an object, including vibration, pressure and tickle senses; therefore a tactile sensing array can be considered to be a coordinated group of touch sensors (Krishna and Rajanna, 2004).

One of the main limitations for tactile sensors for remote palpation instruments is that it must fit through a $2 - 12\ mm$ entry port. Since the sensor will be in direct contact with internal tissue, it also has to be disposable or easy to disinfect. The range of forces it should be able to measure is quite broad, from $0\ N$ to around $5 - 15\ N$. At the same time, high sensitivity and resolution is required, where the ideal situation would be to match the sensitivity threshold and two-point discrimination mentioned in Section 2.3.2. The frequency response of the finger should also be considered, but since our tactile sensor array sends the information to a shape displays it is more important to capture low frequencies that help convey information about local shape. It should be kept in mind, though, that since palpation is an active process, the shape rendered on the tactile display will be a function of the hand and finger movements of the surgeon. In other words, the full potential of the system will not be utilized if the bandwidth is too low.

A distributed pressure sensor is preferred over a shape sensor for locating tumors in soft tissue. If a shape sensor was used it would need to have a compliance similar to the tissue. The reason for this is that if the sensor is too hard, the tissue will deform during contact and conversely, if the sensor is too soft, the tissue will not deform (Peine, 1998). The optimal solution would probably be a sensor that replicates the properties of the human finger pad.

In open surgery the surgeon can palpate the tissue directly. The goal of designing our remote palpation system is to capture the tactile sensations that are created when the finger and tissue are in direct contact and present this in a useful way to the surgeon. Ideally, the user should not be able to discriminate between actually touching the object and touching the replica of the object given by the remote palpation system. In other words, the sensitivity of the tactile feedback system should be adjusted to that of the human sense of touch (Peine, 1998). Therefore, it is crucial to understand the mechanical interaction between the surgeon's fingers and the tissue.

Some studies have been conducted to understand how a mechanical stimulus to the finger is interpreted. Srinivasan and LaMotte (1987) studied the responses of monkey cutaneous mechanoreceptive afferents to steps of varying shape. Phillips and Johnson (1981) also used rigid objects pressed against the skin to predict the mechanoreceptor responses. In palpation, however, the objects under investigation are often softer than the finger. This means that both the finger and the object will deform. Srinivasan and LaMotte (1995) showed that the ability to discriminate softness or compliance of objects depends on whether the object has a deformable or rigid surface. When the surface is deformable, the spatial pressure distribution within the contact region is dependent on object compliance, and hence information from cutaneous mechanoreceptors is sufficient for discrimination of subtle differences in compliance. When the surface is rigid, kinesthetic information is necessary, and the discriminability is much poorer than for objects with deformable surfaces. Srinivasan and LaMotte (1995) also found that kinesthetic sensing alone is insufficient to gain accurate information about the compliance of objects in direct manipulation experiments. Peine (1998) did a study to determine the relationship between physical stimulus and detection of a hard ball embedded in a soft rubber ball. He found that the hard ball could only be detected when the change in skin curvature reached a threshold level.

2.4.2 Existing Devices

Although not necessarily designed for use with instruments for laparoscopic surgery, many tactile sensors have been made. Among others, designs based on capacitive (Pawluk, Son, Wellman, Peine and Howe, 1998), piezoelectric (Krishna and Rajanna, 2004, Dargahi and Najarian, 2004, Kolesar, Dyson, Reston, Fitch, Ford and Nelms, 1996), MEMS (Engel, Chen and Liu, 2003), mechanical (Pagh, Heginbotham and Page, 1977), resistive (Sugiyama, Kawahata, Yoneda and Igarashi, 1990, Lowe, King, Lovett and Papakostas, 2004) and magnetoresistive techniques (Tanie, 1986) have been developed. Some sensor arrays have shown good performance, and e.g. Lowe et al. (2004) is commercially available from Tekscan Inc. (USA). However, many designs have limitations due to complexity, low resolution, size, lack of DC response, crosstalk and the magnitude of forces that can be measured (often restricted to a few grams).

Chapter 3 will describe the sensors considered in this project in more detail.

2.5 Displaying Tactile Information

2.5.1 Challenges and Requirements

A tactile display is a device that stimulates the skin to generate a sensation of contact (Howe, n.d.). The Pacinian corpuscles units are the most important receptors for vibratory information above about 60 Hz, and since they do not exhibit a localized response, a single high frequency source can be used. Fine resolution to stimulate the Merkel discs and Meissner corpuscles is needed to simulate effects such as edges, shear effect, localized texture and motion across the finger. For this purpose an array-type display can be used (Caldwell, Tsagarakis and Giesler, 1999).

Several research groups have tried to identify requirements for the ideal tactile display. According to Moy, Wagner and Fearing (2000), the force required is 1 N per tactel (TACTile ELement) when the actuator density is 1 per mm^2, with up to 2 mm indentation and a bandwidth > 50 Hz. Peine, Wellman and Howe (1997) suggest that the indentation should be $2 - 3$ mm with a force up to $1 - 2$ N per tactel. They also suggest that the bandwidth should be set to 30 Hz to match maximum finger speeds during natural haptic exploration. In addition, Wellman, Peine, Favalora and Howe (1997) state that since the human finger pad has a stiffness as high as 3.5 N/mm at 1.2 N indentation force when indented with a flat plate, the pins need to have high stiffness when displaying shape. The results in Peine (1998) indicated that a shape display should control the shape output to a high level of accuracy of at least 0.05 mm. Other parameters to consider are the scaling of information between object and operator and the tolerable magnitude of delays. Depending on the application for the tactile display, the shape of the display itself could be another important design parameter. In the case of remote palpation instruments, it is crucial to be able to attach the display to the surgical instrument without adding unnecessary constraints for the user.

The mechanical interface that the user touches is also important. There are probably several approaches to improve the way information is presented to the user. For instance, in most tactile displays a thin rubber cover is adhered to the top of the actuator pins to provide spatial low pass filtering. Experiments have been conducted to find optimal parameters for this filter, although the results showed no significant change in perception for the different rubber covers (Lee, Wagner, Lederman and Howe, 2003). Other possibilities for improving the displays could be to change the material of the tactel to better match the nature of the object the tactile display is replicating. In Chapter 6 the importance of the shape of the tactel is discussed in more detail.

Pawluk, Peine, Wellman and Howe (1996) considered what is needed to make a display feel like a compliant object. They used a principle where the surgeon imparts the desired contact force to the display. A tactile shape display was mounted on an instrumented linear actuator, where the shape display provided the tactile information, while the linear actuator system provided the kinesthetic information. They also measured the total force exerted by the surgeon's finger. By approximating the quasi-static pressure response of the finger pad to Herzian contact and estimating the deformation profile of the finger pad, they provide the appropriate position command to each of the pins of the shape display and thereby find an estimate of the object's compliance.

2.5.2 Existing Devices

Most tactile displays use an array of pins in contact with the skin to stimulate mechanoreceptors in the finger tip, and previous designs include use of several technologies. Shape memory alloy was tested by for instance Wellman et al. (1997) and Fischer, Trapp, Schuele and Hoffmann (1997). Details concerning array configuration and performance for both displays can be found in Table 5.3. In general, shape memory alloy allows for high force and large displacement, but the response speed can be insufficient due to cooling problems.

Caldwell et al. (1999), Moy et al. (2000) and Makino and Shinoda (2005) all used pneumatics to actuate their tactels. Details for the first two can be found in Table 5.3. Makino and Shinoda (2005) created a suction display based on the assumption that the human cannot distinguish a compression by a pin-like object from a suction pressure stimulation through a hole. The display is made for selective stimulation of superficial mechanoreceptors in the whole palm. The main advantage with pneumatic actuators is that they have good power density, but the problem is that they are nonlinear, and that aerodynamic effects may limit the bandwidth.

Several groups have tested use of piezoelectric actuators. The display made by Kyung, Ahn, Kwon and Srinivasan (2005) is considered in Table 5.3. In Fritschi, Buss, Drewing, Zopf and Ernst (2004), Hayward and Cruz-Hernández (2000) and Pasquero and Hayward (2003) focus is put on lateral skin stretch as opposed to contactors moving orthogonally to the surface of the skin. Piezoelectricity provides the possibility to convey high frequencies, but the displacement will typically be small.

Frisken-Gibson, Bach-y-Rita, Tompkins and Webster (1987) (see Table 5.3) used solenoids in their shape display, and they faced problems with the size of the actuators which limited the resolution of the display. Solenoids are also nonlinear and positioning accuracy is complicated. In comparison, voice coils have bidirectional capabilities (no need for a spring to make the core retract when current is switched off), as well as linearity, but introduce some problems with position control (Fritschi et al., 2004).

Use of electrical stimulation has also been attempted, and Kajimoto, Kawakami, Tachi and Inami (2004) made a display for selective stimulation of the mechanoreceptors. Electrical stimulation is simple, but perceptual effects are hard to analyze (Moy et al., 2000).

Iwamoto and Shinoda (2005) have designed a display based on ultrasound actuation, and this technology provides high frequencies and high spatial resolution, but the devices are quite large.

Finally, Sarakoglou, Tsagarakis and Caldwell (2005) and Wagner, Lederman and Howe (2004) have demonstrated the use of servomotors in tactile displays, and both are considered in Table 5.3. Servomotors have good positioning accuracy, but often additional friction is introduced when transforming the rotational motion to linear motion. Due to tradeoffs between display bandwidth and actuator density, and also size and weight of the system, no completely satisfactory solution has emerged.

2.6 Devices for Tactile and Haptic Feedback

The idea of remote palpation instruments is not new. Peine (1998) at Harvard University designed a prototype which was able to locate lumps in rubber models. The sensor array on this instrument was based on capacity (Pawluk et al., 1998), and had limitations due to lack of sensitivity, the number of rows in the array which was restricted to one and stress concentrations induced by edge effects. The tactile shape display was based on shape memory alloy technology, and was restricted by the configuration of the pins, fidelity in pin motion control and size and weight of the device (Peine, 1998).

Yao, Hayward and Ellis (2005) developed a probe that could enhance the tactile sensations experienced while probing objects during minimally invasive arthroscopy, and found that for tactile reproduction, the prototype could amplify signals by 10 dB on average. Results from statistical methods showed significant improvements of performance in the case of tactile and auditory feedback, and the system could measurably improve the ability to detect small cuts in cartilage-like elastic surfaces.

Bicchi et al. (1996) modified a commercial laparoscopic tool and was able to measure the force applied from the tool and the angular displacement of the tool jaws. They found it useful for identifying elastic properties. From observations in the operating room they also observed that the surgeon's movements are quite slow, and this simplifies the task of making useful actuation tools.

van Hemert tot Dingshof, Lazeroms, van der Ham, Jongkind and Honderd (1996) developed a telemanipulated master-slave system based on feedback of force. A laparoscopic instrument driven by a DC motor was used as the slave device. The system was controlled by a force reflection scheme, and they concluded that it is hard to feed back the small forces in soft tissue, but that proper testing should speed up surgical procedures.

Rosen, Hannaford, MacFarlane and Sinanan (1999) developed a force feedback endoscopic grasper (FREG) based on measurements of positioning errors, ant they were able to incorporate the system on a conventional laparoscopic instrument. Their testing showed significant improvements in performance in ranking of stiffness compared to a standard endoscopic grasper. Hu et al. (2004) and Tholey et al. (2005) developed a prototype of a laparoscopic grasper with force feedback and demonstrated that an operator could easily differentiate between tissue samples of varying stiffness. Jackman, Jarzemski, Listopadzki, Lee, Stoianovici, Demaree, Jarret and Kavoussi (1999) made a device called the EndoHand, a laparoscopic three-fingered hand, with standard laparoscopic instrumentation and found a significant promise in the ability to perform certain manipulation tasks.

Part II

Tactile Sensing

Chapter 3

Tactile Sensor

The results in this chapter were in part presented in Ottermo et al. (2004). The design and development of the electronics for the piezoelectric sensor array presented in Sections 3.2.3 and 3.2.4 was done in close cooperation with Øystein Eliassen. These contributions are acknowledged by the author.

3.1 Introduction

A key element in a remote palpation instrument is the tactile sensor array, which is attached to the end effector of the grasper, where it measures the magnitude and location of the forces between the device and some internal tissue of the body (Ottermo et al., 2004). This information is in turn sent to the surgeon's fingers via a tactile display to provide a feeling of the shape and hardness of the tissue. Our sensor array is designed to fit on the end effector of a laparoscopic grasper, hence size is an important parameter. As is resolution, price, crosstalk and the ability for a point-to-point mapping between the elements on the sensor array and the corresponding tactile display. We also focus on the opportunity to represent both AC and DC response, and therefore have a specially designed amplifier circuit for this purpose. A low price is ensured by using PZT-material, which is relatively cheap. Crosstalk is reduced, and a point-to-point mapping is ensured by using distinct coaxial cables for each element in the array. A commercially available sensor array (TactArray) is also described in this chapter.

3.2 Principle and Design

3.2.1 Principle

The sensor array is based on piezoelectricity, which is the ability of certain materials to produce a voltage when subjected to mechanical stress. To obtain a spatial resolution close to that of the human finger, the choice of element size is based on theories on two-point discrimination, while the shape of the array is chosen with a view to imitate the human finger tip. A thin protective layer of silicone rubber is adhered to the surface of the sensor to provide low pass filtering (Lee et al., 2003) and enhance mechanical robustness.

For this sensor, the Pz27 material was used (Ferroperm Piezoceramics A/S). This is an all-round soft PZT material suitable for medical instrumentations because of its high coupling factors, high charge coefficients, high Curie temperature, low mechanical quality factor and low temperature coefficients. As the forces exerted to the sensor array will be large, typically around $5 - 15\ N$, the requirements for mechanical stability are high.

Piezoelectric crystals have a nonuniform charge distribution within the unit cell of the crystal. When it is exposed to an electric field, this charge distribution shifts and the crystal will change its shape. The capacitance of the material is:

$$C = \frac{K_{33}\epsilon_0 LW}{t} \tag{3.1}$$

where K_{33} is the dielectric constant, $\epsilon_0 = 8.854 \cdot 10^{-12}$ is the permittivity of vacuum, L and W is the length and the width of the piezoelectric element, respectively and t is the thickness of the material. The static voltage is given by (for thickness):

$$U = \frac{gF}{LW} \tag{3.2}$$

where g is the piezoelectric voltage coefficient and F is applied force.

3.2.2 Design

The sensor array has an overall dimension of $40\ mm \times 12\ mm \times 2.5\ mm$ and consists of 4-by-8 square piezoelectric elements. Spacing is $0.3\ mm$ between the rows and $0.7\ mm$ between the columns. The elements are connected to a flexible circuit board, and the hot point and ground for each element is connected from the printed circuit with $2\ m$ long coaxial cables ($0.6\ mm$ in diameter) (see Figure 3.1). To stabilize the design, the flexible circuit board is attached to a hard substrate, and a soft polymer is used as filling material between the elements. Finally, the array is coated with a 1 *mm* protective silicone layer, which also provides spatial low pass filtering. The array is watertight and can be disinfected with alcohol.

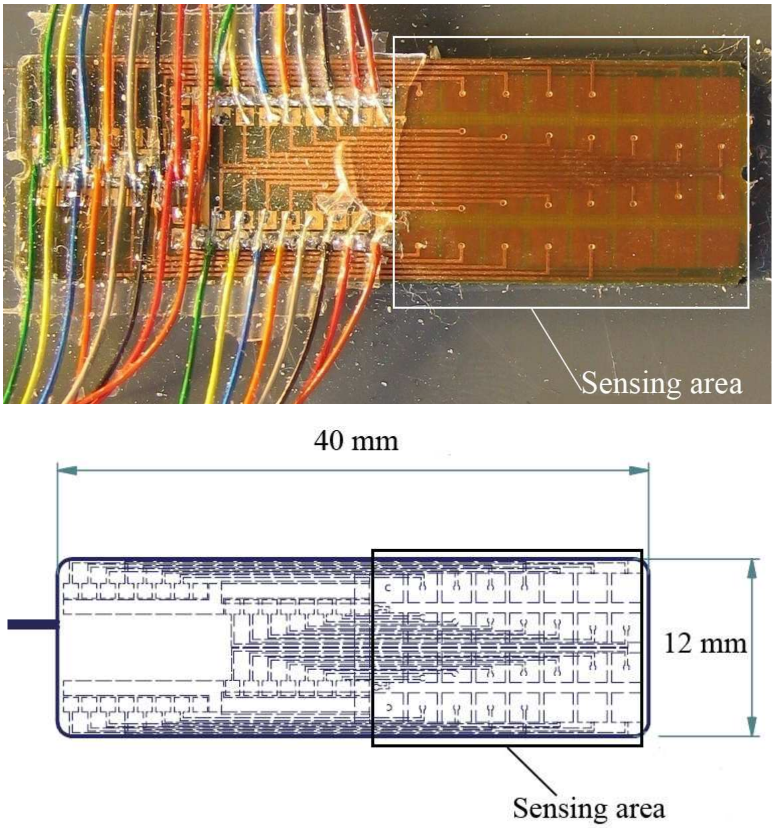

Figure 3.1: The piezoelectric sensor array.

The coaxial cables from the array are connected to the amplifier circuit, which in turn is connected to a dSPACE DS2002 Multi-channel ADC board. MATLAB is used for filtering, calibration and presentation of the data.

3.2.3 Amplifier Circuit

Due to the capacitance of the piezoelectric element, it will act as a high pass RC filter in combination with a resistive load R. A high impedance in the amplifier circuit gives a large RC and a correspondingly small $\frac{1}{RC}$. Since the signal range we are interested in is below the high pass cross frequency,

$w_{cH} = \frac{1}{RC}$, we need a high impedance amplifier to avoid total depression of the low frequency components and a first order low pass filter to counter the sensor characteristics.

The amplifier circuit is constructed using AD623 instrumentation amplifiers with first order low pass filters (see Figure 3.2).

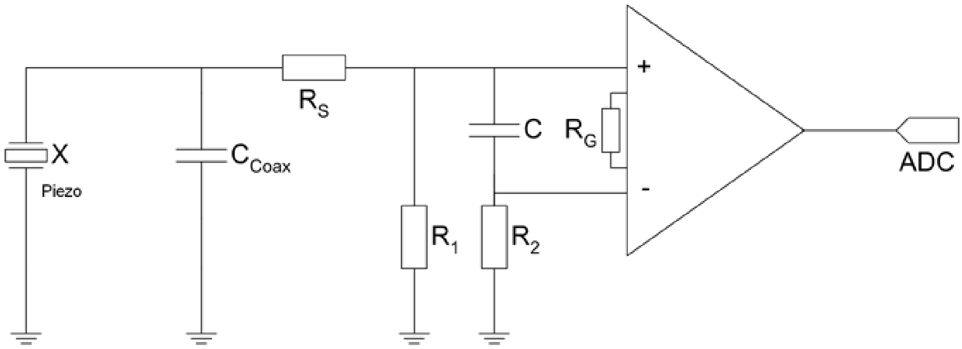

Figure 3.2: Basic schematic of the amplifier circuit. X is the piezoelectric element, C_{Coax} is the capacitance of the coaxial cables, R_G is the amplifier gain selection resistor and R_s is a shunt resistor for stability.

The AC coupled high impedance nature of the piezoelectric element will make the coaxial cable act like a floating wire seen from the amplifier. It is therefore necessary to bias the inputs with the resistors $R_1 = R_2 = 33\ M\Omega$. These should be high precision to minimize DC offset on the output. C and R_2 acts as a high pass filter on the negative input, resulting in a total low pass effect. For $w_{cL} = 2\pi f = 0.628\ Hz$, the capacitor is chosen as $C = \frac{1}{2\pi 0.1\ Hz \cdot 33 M\Omega} = 33\ nF$.

The capacitance of the 2 meter coaxial cable is assumed to be $C_{Coax} = 100\ pF$. This lowers the high pass cross frequency, w_{cH}, of the sensor only slightly and is thus not a problem. Additionally, it will lower the amplitude of the signal since the produced charge will be divided between the two capacitors. The shunt resistor, $R_s = 1\ k\Omega$, is put in for stability. The gain resistor, R_G, was chosen through trial and error as a trade-off between output signal strength and output DC offset originating from difference in R_1 and R_2. Although the signal does not have a DC response, a large offset will result in saturation of the amplifier, which will distort the signal. $R_G = 1.8\ k\Omega$ results in a gain of approximately 60, an output signal of $1Vp - p$ and a DC offset of no more than 1.5 V with 1% tolerance resistors. AC response of the circuit is shown in the Bode plot in Figure 3.3.

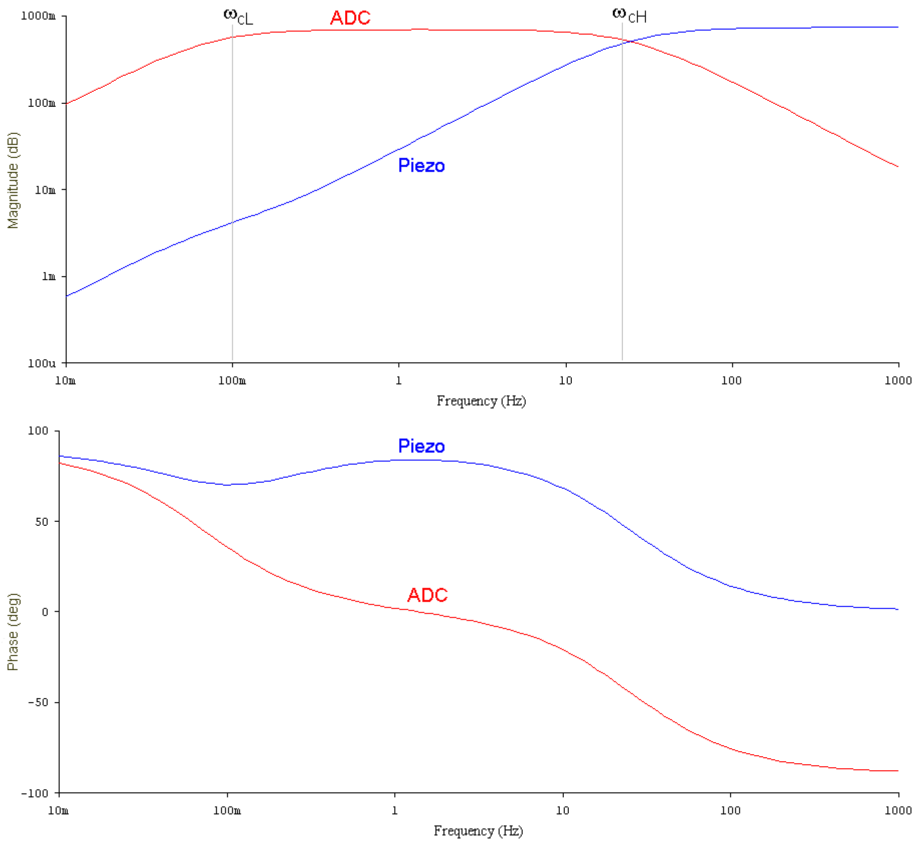

Figure 3.3: Simulated circuit characteristics, where Piezo is the output from the piezoelectric element (X), and ADC is the output of the amplifier circuit (see Figure 3.2)

3.2.4 Frequency Shaping

To find an estimate for the sensor's time constant, the step response was found by putting a weight on the array and recording the signal data. The data was then analyzed using MATLAB's System Identification Toolbox. From this, the estimated transfer function of the sensor (from input of sensor to output) is:

$$h_s(s) = \frac{T_{sensor}s}{1 + T_{sensor}s} \tag{3.3}$$

with $T_{sensor} = 0.21\ s$. Some signal processing was implemented in software to suppress some of the high frequency noise. A sampling frequency of 1 kHz was chosen. The noise was analyzed with the Fast fourier transform, which showed that the sensor has some noise at $55 - 60\ Hz$ (probably caused by the computer screen or the communication bus in the computer). These frequencies were removed by adding a low pass filter:

$$h_n(s) = \frac{1}{1 + T_n s} \tag{3.4}$$

with $T_n = 0.02\ s$. We also shifted the sensor's time constant with a filter, such that frequencies close to DC response are amplified. This provides us with additional information about slow changes in the array. With reference to the sensor's time constant T_{sensor}, a new time constant T_1 a decade below was chosen, and the following filter was added:

$$h_1(s) = \frac{1 + T_{sensor}}{1 + T_1 s} \tag{3.5}$$

As some DC offset was present, a cutoff filter was included (where T_c is the time constant for the cutoff filter chosen 1 decade below T_1.:

$$h_c(s) = \frac{T_c}{1 + T_c s} \tag{3.6}$$

The response of the software filters are shown in Figure 3.4.

The flexible circuit board on top of the sensors results in high mechanical crosstalk between the elements. The optimal solution to this problem would be to remove the flexible circuit board, but this will make the implementation of the sensor array complex since both sides of the piezoelectric element must be connected to be able to measure the voltage change. For this version of the sensor, the crosstalk is reduced by displaying major changes between samples only. This was implemented using a dead zone. The dead zone will suppress the insignificant amplitudes, such that only major differences in amplitude from one time step to the next will be visible. This, however, should be compensated for, and in order to do this, a model of the system is needed. Typically one could base the model on the element with the greatest recorded force and scale this and the surrounding elements appropriately. This filter would then act similarly to a rank filter for image processing (for instance a median filter).

3.3 Performance

Some technical data for the array is shown in Table 3.1.

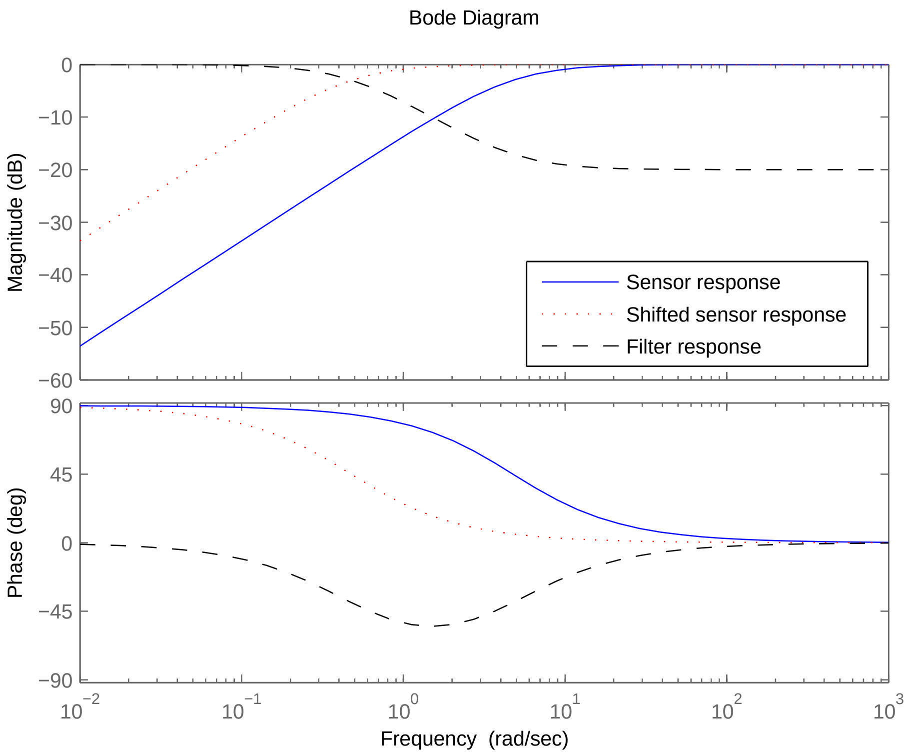

Figure 3.4: Bode plots showing the sensor response, the shifted sensor response, and the low pass filter response.

Table 3.1: Technical data for the sensor array.

Property	Value
Force range	$5 - 15\ N$
Output signal	$1\ Vp - p$
Resolution of ADC converters	16 bits
Size	$40 \times 12 \times 2.5\ mm^3$

Figure 3.5 shows the response of the array when a silicone ball with a diameter of approximately 1.3 cm is pressed against it.

The sensor works well for most frequencies, but as mentioned before, frequencies above $55 - 60\ Hz$ are deliberately attenuated. The sensor array has trouble with crosstalk, and this makes it hard to discriminate between

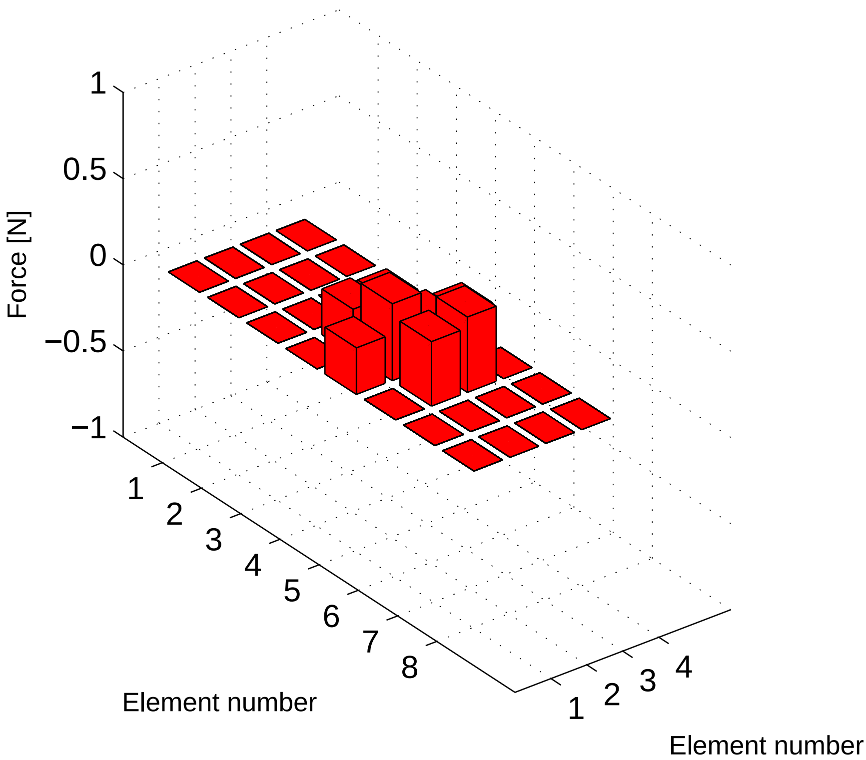

Figure 3.5: Graphical presentation of sensor response when a silicone ball is pressed against it.

objects with different sizes. The poor low frequency response of the piezoelectric array also makes it less suitable for our application.

3.4 TactArray

An alternative tactile sensor array is the commercially available PPS TactArray (Pressure Profile Systems Inc.) developed for measuring the tactile pressure distribution between objects in direct physical contact. It consists of a two-dimensional array (15×4) of pressure sensing capacitive elements in a thin, continuous sheet, and the total size of the array is $3.5\ cm \times 1\ cm$. Our system has been custom made to fit on to a reusable laparoscopic grasper (see Figure 3.6). Included with the system is software for acquiring, visualizing and storing data (see Figure 3.7).

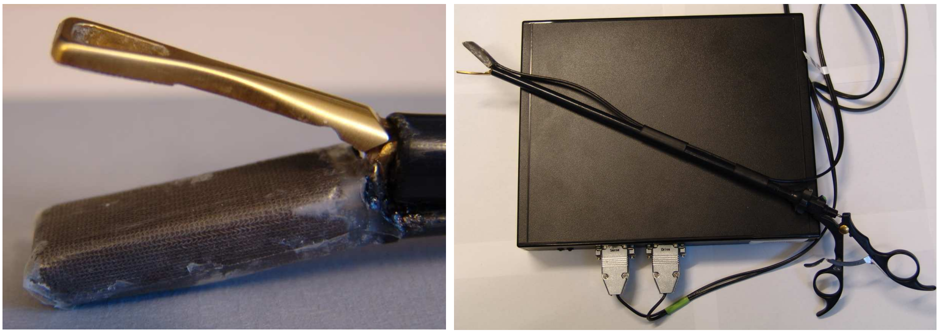

(a) End effector (b) Full system.

Figure 3.6: The figures show the laparoscopic grasper with the TactArray attached and the full TactArray system.

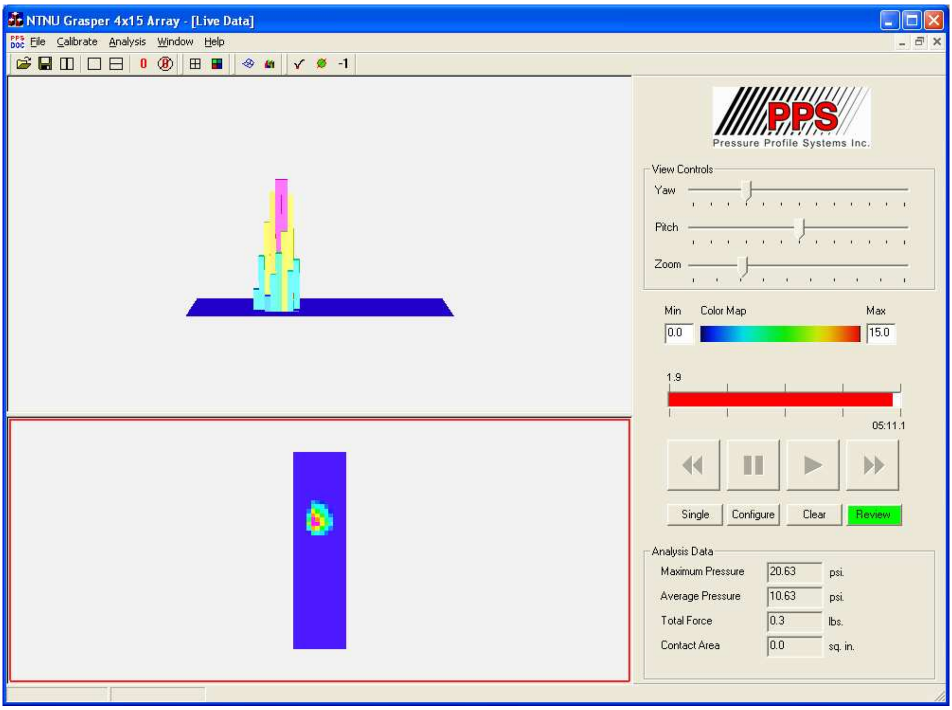

Figure 3.7: Visually presented tactile information (pressure distribution).

The maximum pressure range of the sensor array is $0 - 7\ N/cm^2$. The problem with lack of DC-response addressed for the piezoelectric array is not present for this array, and the electronics provide continuous throughput at a bandwidth of over 1 kHz.

3.5 Discussion

The design and implementation of a tactile sensor array based on piezoelectricity has been described. Additionally, the commercially available TactArray system was briefly presented. The final choice of sensor for our system fell on the TactArray, and this was custom made to fit on a conventional reusable laparoscopic grasper from Olympus. The decisive parameter for this choice was the problems related to crosstalk and the limited DC-response of the piezoelectric array. The spatial resolution of the TactArray sensor is also slightly better than that of the piezoelectric sensor. Despite these advantages, separating between objects with small variations in size is not trivial. The system is also quite expensive, and the electronics (cables and hardware) that come with the system could preferably have been made smaller.

Chapter 4

The Role of Tactile Feedback in Laparoscopic Surgery

The results in this chapter were presented in the paper Ottermo, Øvstedal, Langø, Stavdahl, Yavuz, Johansen and Mårvik (2006).

4.1 Introduction

The lack of the tactile feedback in laparoscopic surgery limits the surgeon's abilities to palpate internal organs, a technique actively used for locating tumors, gallstones and abnormalities in the tissue during open surgery. Combining the lack of tactile feedback with poor visual feedback also results in reduced positioning and manipulation control of the instruments. Based on this problem, it is important to identify which information is lost in laparoscopic surgery compared to open surgery. In Chapter 3, tactile sensor arrays for capturing tactile information are presented, and in Chapter 7 a full surgical instrument, which serves as an extension of the surgeon's fingers, is described. In this study the tactile information is presented visually on a monitor.

Some previous studies describing haptic feedback in laparoscopic surgery have been done. Bholat et al. (1999) conducted a single-blinded study where subjects were asked to identify objects by direct palpation, conventional (surgical) instruments and laparoscopic instruments. From this study, they stated that haptic feedback is altered but not eliminated when using laparoscopic instruments. Bicchi et al. (1996) used a position sensor and a force sensor attached to a conventional instrument to measure the force acting on the tissue from the instrument and the angle deflection of the end effector. They used these measurements to find the viscous elasticity of objects, and this information was presented graphically (position versus force) to the user. Experiments showed that subjects could discriminate between objects of different materials using this instrument. den Boer, Herder, Sjoerdsma, Meijer, Gouma and Stassen (1999) examined the sensitivity of laparoscopic dissectors when touching a simulated arterial pulse. The results showed that feedback quality was significantly better with reusable dissectors than with disposable dissectors, but that the overall sensitivity of instruments was low compared to bare fingers. Hu et al. (2004) and Tholey et al. (2005) developed a prototype of a laparoscopic grasper with force feedback (using a PHANToM) and demonstrated that an operator could easily differentiate between tissue samples of varying stiffness. The same results were found in MacFarlane et al. (1999) and indicated that a force feedback device is significantly better than a standard Babcock grasper at rating tissue compliance but not as successful as a gloved hand. Wagner et al. (2002) showed that the absence of force feedback increased the average force magnitude applied to the tissue by at least 50%, and that the number of errors that damage tissue increased by more than a factor of 3. Other attempts of providing tactile feedback have also been made. Jackman et al. (1999) compared the EndoHand, a laparoscopic three-fingered hand, with standard laparoscopic instrumentation. They found a significant benefit in the ability to perform sophisticated manipulation of objects, although it fell short in both dexterity and tactile feedback. The experiments described in this chapter aim at comparing the sensitivity of a laparoscopic grasper and gloved fingers, and at investigating whether additional information about the contact forces between the instrument and the internal tissue contributes to a better understanding of the properties of the tissue. The main difference from earlier experiments is that the tests are done in a more realistic environment, known to the laparoscopic surgeon. Instead of manipulating the objects directly, they are hidden in pig's intestine. In this way, we simulate a situation with resemblance to real surgery. In addition, the equipment used differs from that used for force feedback in e.g. Tholey et al. (2005) and MacFarlane et al. (1999) in that our system measures and displays spatially distributed parameters of contact (not single point, as in the mentioned force feedback devices).

4.2 Materials and Method

4.2.1 Tactile Sensor Array

The tactile sensor array we use is the PPS TactArray (Pressure Profile Systems Inc.) described in Chapter 3.4. The system has been custom made to fit on to a reusable laparoscopic grasper (see Figure 3.6), and when sensory information is available it is presented visually to the surgeon on a screen (see Figure 3.7).

4.2.2 Silicone Rubber Balls

Palpation is used actively for many discrimination tasks, but we chose to focus on identification of tumors. We made several artificial tumor samples using silicone rubber. We used a two-component silicone rubber, where the amount of component B determines how soft the rubber becomes. The recommended compositions are 9:1, 9:2, 9:3 and 9:4, where the hardest (9:1) is 25 shore A (close to the hardness of a rubber band). For the hardness tests we used the 9:2, 9:3, and 9:4 compositions. Additionally, we used a glass ball (marble) and a foam rubber ball to provide extreme points. The choice of tumor samples was based on a pilot where experienced surgeons were asked to distinguish between the samples with their fingers. The soft silicone (9:4) has a hardness that resembles a lymph node or the intestine wall, i.e. it is not as hard as a tumor. The medium silicone (9:3) has a hardness close to that of a benign tumor, for instance in prostate or lymph node and lipoma. The hard silicone (9:2) resembles a malign tumor, while the glass ball is as hard as bone, gallstones etc. All balls used in the hardness experiment had a diameter of 1.5 cm. For size we used the following 5 diameters: 0.5 cm, 0.9 cm, 1.3 cm, 1.8 cm and 2.4 cm. All had the same silicone rubber composition (9:2).

4.2.3 Experimental Design

We were interested in evaluating the information needed, the information present and the information lost during laparoscopic surgery. In addition, we wanted to evaluate the new instrument with sensor array attached to see if the technology complicates the tasks. To do this the following points of interest were listed:

- How well can the surgeon discriminate size and hardness using his fingers (F), state of the art laparoscopic instruments (LI) and a laparoscopic instrument with tactile sensor (LIS), respectively?
- Is the attention drawn from the original task when LIS is used, and does the visually presented tactile information introduce any additional benefits or problems to the surgeon?

As our target goal was to evaluate the loss of information in laparoscopic surgery, we chose to reproduce this environment as closely as possible. Therefore, all objects to be identified were hidden in pig's intestine and placed in a simulator for laparoscopic training (Figure 4.1).

Figure 4.1: Simulator for laparoscopic training.

To avoid the problem of the surgeon not being able to locate the objects at all, we separated the intestine into pockets, where each pocket contained one ball (see Figure 4.2).

The subjects were given visual feedback on a video screen by use of standard endoscopic viewing equipment (Olympus A5294A) inside the simulator (see Figures 4.3 and 4.4).

For the first experiment, the subject was presented with 5 silicone balls, all with varying hardness. The subject was asked to rank the 5 balls from softest to hardest, using either his fingers, conventional laparoscopic instruments, or the laparoscopic instrument with sensor (the order of which instrument to use first, second and last was randomized between subjects). The subjects were allowed to feel the different objects as many times as necessary.

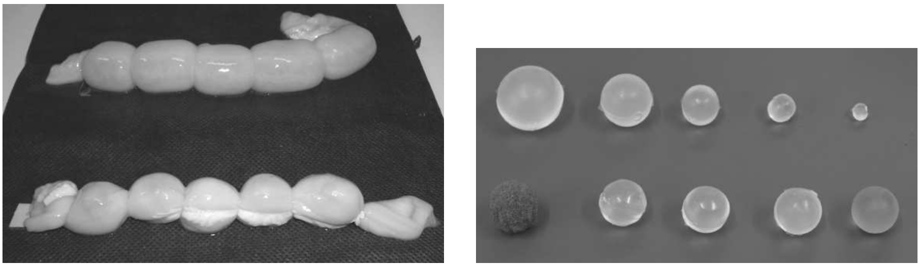

Figure 4.2: The picture to the left shows two intestines divided into pockets, where the intestine at the back is filled with water to avoid visual exposure of the sizes. The balls are shown to the right.

Figure 4.3: Experiment setup showing all three laparoscopic simulators, one for each instrument (F, LI and LIS).

The second experiment used the same method as the first, but here the task was to rank 5 silicone balls from smallest to largest. To restrict the subjects from discriminating by using only their eyes, we filled the intestines with water so that the balls were completely hidden (see Figure 4.2).

Figure 4.4: Experiment setup when laparoscopic instrument with sensor was used (the laptop behind the surgical simulation trainer presents the pressure distribution visually).

Although we conducted two separate experiments, one with focus on hardness and one with focus on size, the subjects performed both at the same time, meaning that they performed all trials for either hardness or size first and after a short break proceeded directly to the next. The order of the two experiments was randomized between subjects. The subjects were encouraged to talk during all trials and tell what they felt and saw, and all trials were video recorded. This was done to ensure that no information was lost and to double check the results. All subjects were given a short presentation of all instruments prior to the experiments. They were also informed about the scope of the experiments, how the tests would be conducted and asked to complete two questionnaires. The subjects were not allowed to see the silicone balls before or during the experiments.

4.2.4 Test Persons

Nine surgeons with varying surgical experience and 6 medical students and doctors participated in the experiments. The subjects were from 23 to 53 years old, with an average of 35.2 years. Of the 15 subjects, 9 were male and 6 female. Five of the subjects had performed more than 200 surgical interventions and were classified as experienced surgeons, while 4 of the subjects (with 15-200 interventions) were classified as surgeons with some experience. The remaining 6 subjects were described as unexperienced. Surgeons familiar with laparoscopic surgery were preferred since using laparoscopic equipment is rather complicated, and special training is needed to feel comfortable using it. Surgeons are also the target group for the device, and feedback from them is of utmost importance. We included 6 completely unexperienced subjects to see if the differences were noticeable.

4.2.5 Data Collection

Altogether, each subject had 18 different tasks to complete, 3 trials for F, LI and LIS with respect to both hardness and size. In each trial, the subject ranked the objects from 1 to 5, with 1 being the softest or smallest and 5 being the hardest or biggest. The data was not characterized as "true" or "false". Instead, we recorded the ranking the subject gave and compared this value with the true value. This was done because we wanted to characterize it as a bigger mistake if the subject exchanged a 1 and a 5, than if he exchanged a 3 and a 4. If a subject could not discriminate between two balls, for instance with hardness 3 and 4, he was told to rate them with the same number (the choice which rating to give (3 or 4) was done by comparing with a softer and a harder ball and determining which one they were closer to, e.g. a 2 or a 5). Since we cannot assume that such a small data set has a normal (Gaussian) distribution, we analyzed the data with nonparametric statistics. Therefore, we used a Friedman test, which is two-way analysis of variance by ranks (Sheskin, 2000). Details about Friedman's test are discussed in Appendix B. For pairwise comparison we based our analysis on the Wilcoxon two-sample test, and the procedure for this analysis is also described in Appendix B. The calculations were done using MATLAB's Statistics Toolbox (The MathWorks Inc.).

4.3 Results

Figure 4.5 shows the average error and the standard deviation of the error for each instrument for both hardness and size. Here the magnitude of the error in each case is taken into account, meaning that if a subject ranked a value 4 silicone rubber ball as a 2, the error has the absolute value 2. As the figure shows, the fingers are superior to laparoscopic instruments for discrimination both in the hardness and the size case. For hardness the laparoscopic instrument with sensor resulted in average error per trial of 1.38, while the conventional laparoscopic instrument led to an average error of 1.98. The difference is not as pronounced in the size case, where LIS has an average error of 1.69 versus 1.96 for LI.

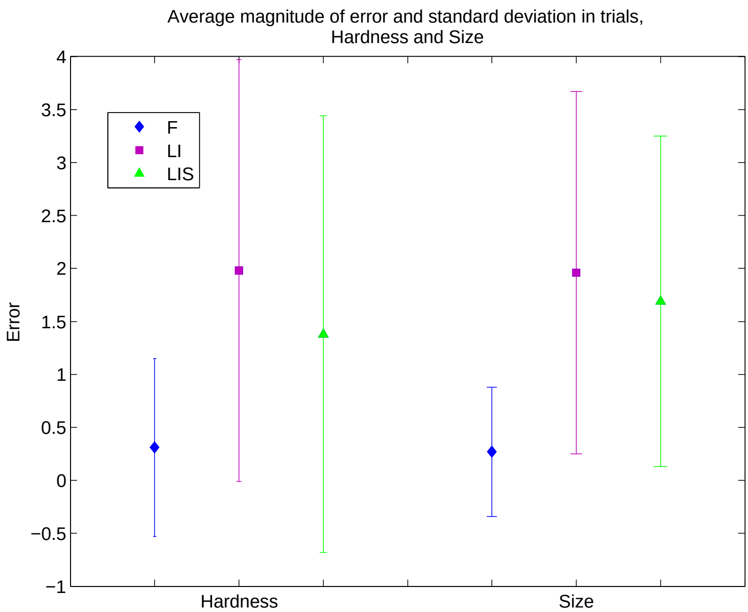

Figure 4.5: Plot showing average magnitude of the error and standard deviation for each instrument (F, LI and LIS) for both hardness and size, respectively.

The subjects were given a post test questionnaire, were they were asked to rate their own performance and to answer some questions about the test and the equipment. We also wanted their subjective opinion about the necessity of including tactile feedback on laparoscopic instruments. Therefore we asked the surgeons whether they missed tactile feedback when performing laparoscopic interventions. They had spilt opinions on this question, but 53% meant that tactile feedback could be somewhat useful, while 33.3% did not know. The remaining felt that it would not be helpful.

The subjects were also asked what they thought of the tasks they had to perform since it is always important to know if the difficulty of the task has the right level. None of the subjects felt it was too easy. In fact, 11 of the subjects thought the tasks had the right level of difficulty, while the remaining 4 meant it could have been easier.

Most of the subjects felt that the experiments were somewhat comparable with real surgery, and only 1 of the 15 subjects felt that the extra source of information (visually presented tactile data as in Figure 3.7) was confusing.

4.3.1 Hardness Discrimination

Hypothesis H_0: When discriminating between balls with varying hardness, a conventional laparoscopic instrument and a laparoscopic instrument with visually presented tactile information perform equally well as gloved fingers, i.e. F=LI=LIS. The alternate hypothesis is H_1: not H_0.

A Friedman test, with a critical p-value=0.05, was conducted to test the above hypothesis against the alternate hypothesis H_1 (see Appendix B for details on the computations). Since we compare k=3 different instruments we have 2 degrees of freedom, and this results in $\chi^2_\alpha = 5.99$. The Friedman test gave $\chi^2_r = 17.43 > 5.99$ ($p = 7.42 \cdot 10^{-5}$), meaning that H_0 is rejected.

When the value of χ^2_r is significant it does not say anything about the pairwise comparison of the 3 instruments. Therefore, we performed an analysis based on the Wilcoxon two-sample test (see Appendix B), and the following cases were tested:

H_0: $WHF = WHLI$ versus H_1: $WHF < WHLI$
H_0: $WHF = WHLIS$ versus H_1: $WHF < WHLIS$
H_0: $WHLI = WHLIS$ versus H_1: $WHLIS < WHLI$

When comparing F and LI, we found that $z_{WHLI} = 1.86 > 1.65 = z_{0.05}$ (with a 0.05 level of significance), meaning that we can reject H_0 and conclude that F is significantly better than LI for hardness. From the table of the area under the normal curve we can find $P_{WHLI} = P(z > 1.86) = 0.0307$. In other words, we can reject H_0 at a level of significance of approximately 0.03.

Performing the same analysis for F versus LIS resulted in $z_{WHLIS} = 1.15 < 1.65 = z_{0.05}$. Hence we cannot reject H_0, and we conclude that F is not significantly better than LIS for hardness.

When comparing LI and LIS, we found $z_{WHLI} = 0.46 < 1.65 = z_{0.05}$ and we cannot reject H_0. In other words, we can conclude that LIS is not significantly better than LI for hardness.

Figure 4.6 shows the errors made by each individual subject in the hardness case. As can be seen from the plot, subject 2 did a lot of errors with all instruments. Except for subject 1, 4, 12, 13 and 15, all performed better with LIS than LI. Gloved fingers were better or as good as both LI and LIS for all subjects.

Figure 4.7 shows how the error percentage varies with the amount of experience with laparoscopic surgery. This plot does not take the magnitude of the error into consideration. As can be seen from the figure, the overall error percentage was 5.8% for F, 32% for LI and 21.3% for LIS. The error rate when using gloved fingers is low for all groups, and the experienced surgeons have better performance using conventional laparoscopic instruments than the other two groups. For the laparoscopic instrument with sensor, it is interesting to notice that the unexperienced subjects have better performance than both the other groups.

The balls used in the experiment ranged in hardness from foam rubber to glass. Between these extreme points, three silicone rubber balls with different hardness were used. As Figure 4.8 shows, the softest ball (foam rubber) stands out as the easiest to distinguish for all instruments. The glass ball was easy to identify with the fingers but harder with the other two instruments (LI and LIS). Compared to laparoscopic instruments, the instrument with sensor seemed to improve the subjects' performance for identification of hardness 2, 3 and 5 (where 5 is the hardest (marble) ball).

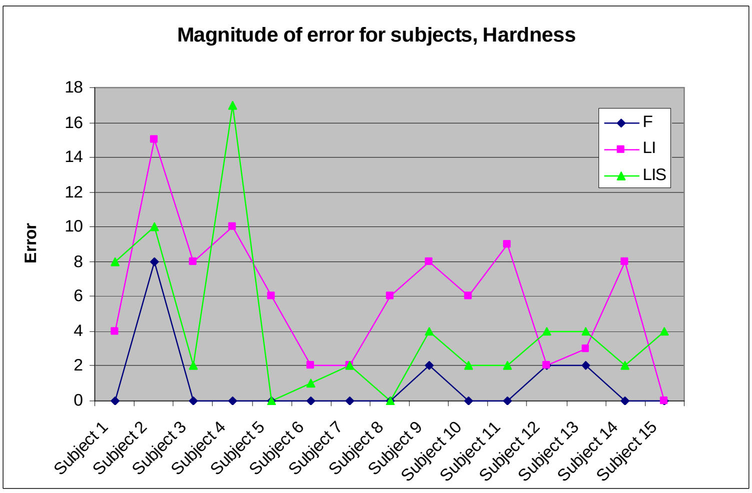

Figure 4.6: Magnitude of total error for each subject in the hardness case.

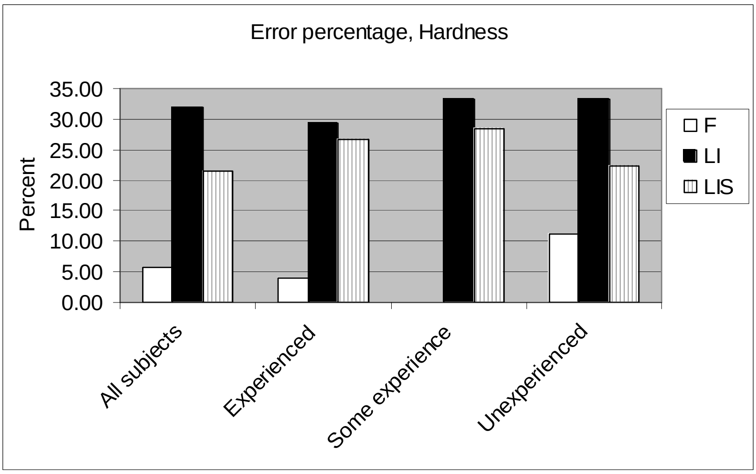

Figure 4.7: Plot showing how often a wrong ranking was given for each instrument in the hardness case.

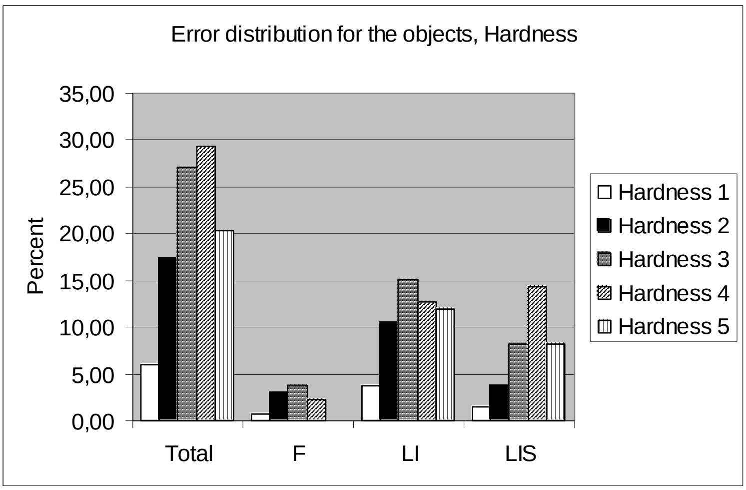

Figure 4.8: Plot showing the distribution of errors for each hardness.

As previously mentioned, we did not characterize errors as ”true” or ”false” but by the magnitude of the error. Of the total 133 errors (out of 675 possible) made for hardness, 108 of them had magnitude 1, meaning that the subjects had characterized for instance a hardness 1 as a hardness

Table 4.1: Average time consumption for hardness.

Instrument	Average [s]	Experienced	Some experience	Unexperienced
F	34.7	27.4	36.8	39.4
LI	134.1	136.3	136.3	130.6
LIS	164	124.1	210.8	166.1

2. Eighteen errors had a magnitude of 2, and the remaining 7 were of magnitude 3.

The time elapsed for each trial was recorded (the time consumed to rank 5 objects). Table 4.1 and Figure 4.9 show the average time for ranking with each instrument in the hardness case. The table and the figure also show how the time varies with experience. Notice that the experienced subjects are somewhat faster with LIS than LI, as opposed to the other two groups which are faster with LI than LIS.

When rating their own performance, only 3 of the subjects felt they performed better with LI than LIS. Four of the subjects thought they performed equally well with LI and LIS, and the remaining 8 felt they performed better with LIS than LI. All meant that they had performed best with the fingers.

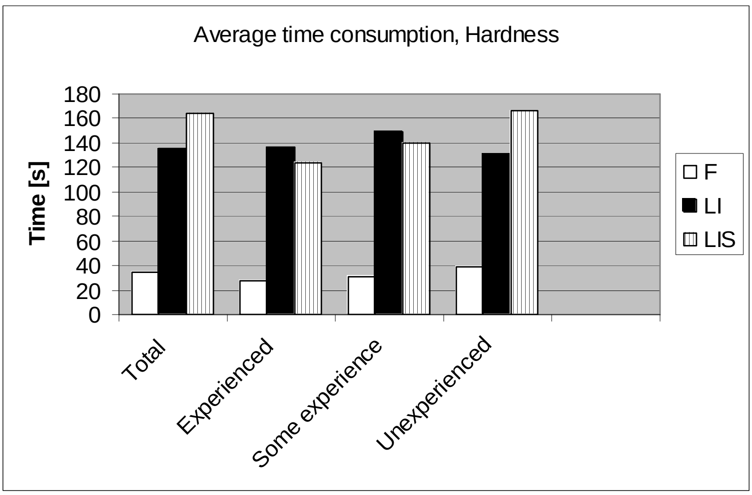

Figure 4.9: Plot showing the average time consumption for hardness.

4.3.2 Size Discrimination

Hypothesis H_0: When discriminating between balls with different size, a conventional laparoscopic instrument and a laparoscopic instrument with visually presented tactile information perform equally well as gloved fingers, i.e. $F = LI = LIS$. The alternate hypothesis is H_1: not H_0.

The Friedman test for size gives $\chi_r^2 = 19.23 > 5.99$ ($p = 4.78 \cdot 10^{-5}$), and H_0 is rejected. We performed the same paired comparisons for size as for hardness, and the following cases were tested:

H_0: $WSF = WSLI$ versus H_1: $WSF < WSLI$
H_0: $WSF = WSLIS$ versus H_1: $WSF < WSLIS$
H_0: $WSLI = WHLIS$ versus H_1: $WSLIS < WSLI$

When comparing F and LI, we found that $z_{WSLI} = 2.01 > 1.65 = z_{0.05}$. We can reject H_0 and conclude that F is significantly better than LI for size. From the table showing the area under the normal curve, we find $P_{WSLI} = P(z > 2.01) = 0.0222$. In other words, we can reject H_0 at a level of significance of approximately 0.02.

For the comparison of F and LIS, the calculations resulted in $z_{WSLI} = 1.86 > 1.65 = z_{0.05}$, hence we can reject H_0 and conclude that F is significantly better than LIS for size.

When comparing LI and LIS we found $z_{WSLI} = 0.39 < 1.65 = z_{0.05}$, meaning that we cannot reject H_0. Therefore, we conclude that LIS is not significantly better than LI for size.

The errors made by the individual subjects in the size case are shown in Figure 4.10. As we can see, gloved fingers are superior for all subjects, except for subject 11 and 15, where LIS is slightly better or equally good. The difference between LI and LIS is not as noticeable for the ranking of size.

Figure 4.11 shows how many times the subjects ranked an object's size incorrectly. For all subjects, the error percentage was 5.3% for the fingers, 29.8% for conventional laparoscopic instruments and 28.9% for the laparoscopic instrument with sensor. As opposed to the hardness case, the experienced surgeons performed better than the other two groups with LIS.

In the same way as in the ranking of hardness, the subjects made more errors with some of the objects (see Figure 4.12). The smallest ball (0.5 *mm* in diameter) was responsible for 45% of the errors. Note that out of the 65 times the subjects made an error with the smallest ball, 46 of them were due to the fact that they could not identify a ball at all (although there was always an object present). The subjects also had some trouble finding the

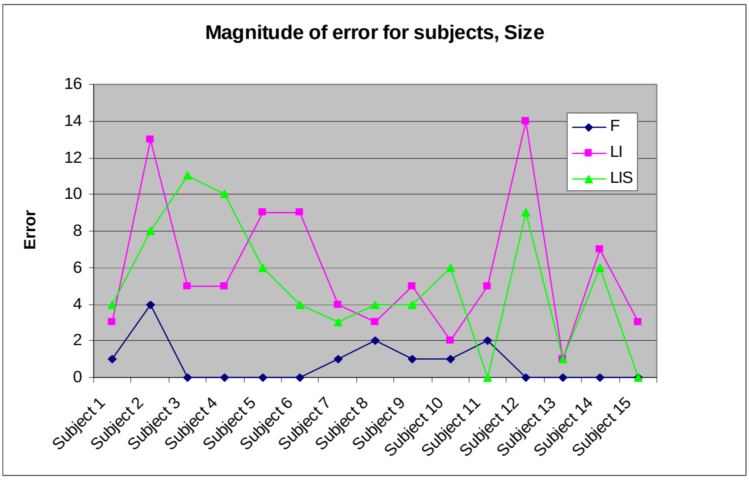

Figure 4.10: Magnitude of total error for each subject in the size case.

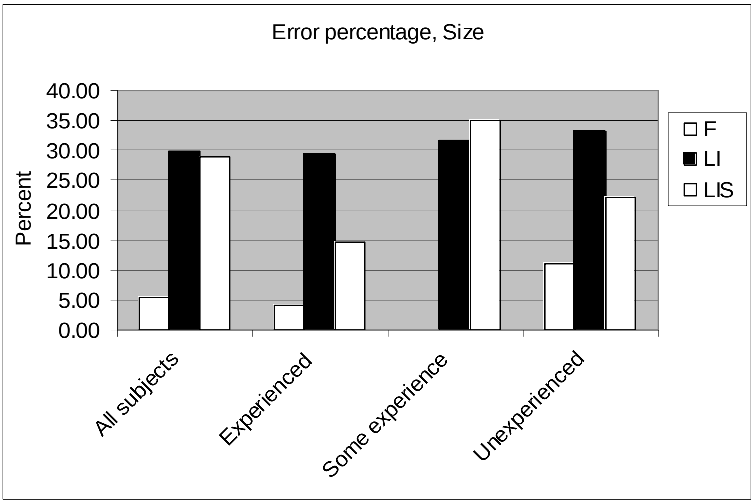

Figure 4.11: Plot showing how often a wrong ranking was given for each instrument in the size case.

second smallest ball using LI and LIS, and in some cases they exchanged sizes 3 and 4. The easiest ball to discriminate was the largest.

Of the 144 errors done in the size case, 116 of them had magnitude 1, 24 had magnitude 2 and 4 had magnitude 3.

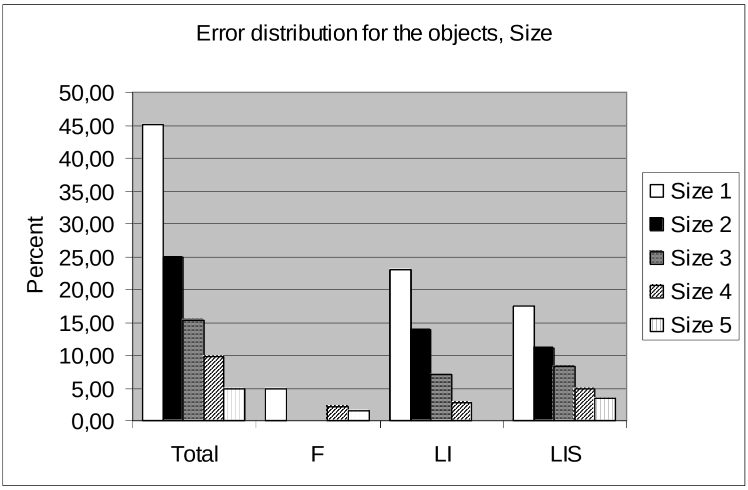

Figure 4.12: Plot showing the distribution of errors for each size.

Table 4.2: Average time consumption for size.

Instrument	Average [s]	Experienced	Some experience	Unexperienced
F	45.3	32.9	57.9	47.2
LI	174.3	150.5	175.5	193.8
LIS	192.3	177.5	197.2	202.0

The average time consumed per trial in the size experiment is shown in Table 4.2 and Figure 4.13. As we can see, the experienced surgeons were slightly faster than the other groups with all instruments.

In the rating of themselves, 6 of the 15 subject thought that they performed better with LI than LIS when ranking sizes. Three of the subjects thought they performed equally well with LI and LIS, and the remaining 6 felt they performed better with LIS than LI. All subjects rated the fingers higher than the other two instruments.

4.4 Discussion

Our experiments show that the fingers are superior for palpation, both compared to conventional laparoscopic instruments and our laparoscopic instrument with visual feedback of the tactile image. This is not surprising, and it indicates that there is a definite potential for improving today's la-

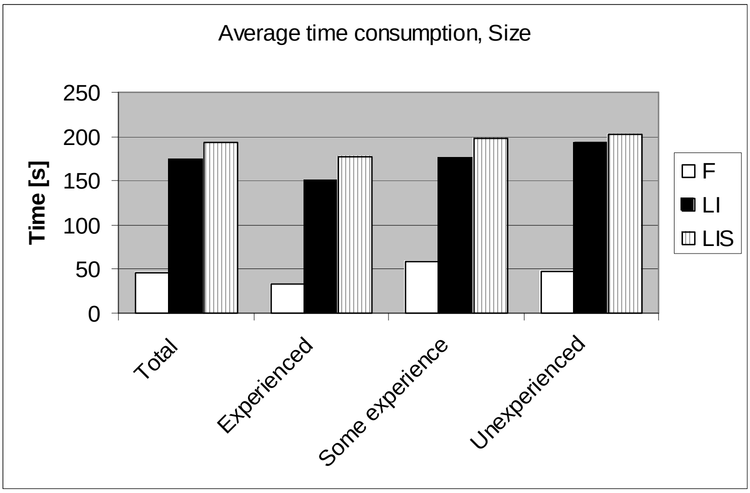

Figure 4.13: Plot showing the average time consumption for size.

paroscopic instruments. Our laparoscopic instrument with sensor did not prove to be significantly better than conventional laparoscopic instruments (LI), neither for hardness nor size, but a positive trend could be noted in the results for hardness, where F (fingers) did not prove to be significantly better (with a 95% confidence interval) than LIS (laparoscopic instrument with sensor).

For hardness the unexperienced subjects seemed to find the sensor most helpful. There can be many reasons for this, one of them being that they are not familiar with the conventional laparoscopic instruments and do not have the necessary techniques to utilize them as well as an experienced surgeon. Therefore, any extra information to help them discriminate between the objects could be useful. The experienced surgeons, on the other hand, have the advantage that they are used to both the instruments and the 2D view of the objects, and thus it is easier for them to analyze the compliance of the objects without help from the sensor. The experienced surgeon also has the advantage of knowing that intestines are quite strong and robust; therefore they use more force when investigating the balls. In a couple of cases, the experienced surgeons used too much force, resulting in damage to the intestine.

In contrast to the hardness case, the experienced surgeons actually performed better with the sensor in the size experiment. It is likely that the reason for this is, again, technique. While the experienced surgeons slid the grasper along the intestine or used a poking technique, the less experienced and unexperienced subjects used grasping. In this way, the experienced surgeon was able to ensure that the object under investigation did not slip, and he could corner it and use visual feedback to tell the size (often by comparing with the length of the grasper). In some cases when the objects were too small, and the subjects were not able to corner them, sliding the grasper with tactile feedback over the intestine helped them identify the object. When using LIS, the poking technique was not as useful as with LI, due to the bigger size of the grasper. Some subjects reported that the size of the grasper in LIS compared with LI made it harder to distinguish between the objects, while some reported that it was easier. As opposed to conventional graspers, the grasping surface of the laparoscopic instrument with sensor was smooth. This seemed to be a bigger problem for the unexperienced subjects than the experienced ones. Some research has been conducted to make the sensor surface similar to a grasper surface (Dargahi, Parameswaran and Payandeh, 2000, Sedaghati, Dargahi and Singh, 2005), and depending on the application, it is an important parameter to consider for future instruments.

In the experiments the subjects made more errors with some of the balls. In Figure 4.8 we see that the instrument with sensor seemed to improve the subjects' performance for identification of hardness 3 and 5 but not for hardness 4. This is a strange result since the improved performance when identifying hardness 3 and 5 should have affected hardness 4 as well. It is probable that this is a coincidence and a mere result of the underlying stochastic process, rather than an indication of that hardness 4 is more difficult to identify than hardness 3 and 5.

As mentioned before, we recorded the time spent on each trial. The experienced surgeons were, in general, faster than the other two groups, and this is not surprising owing to their experience with laparoscopic surgery. All groups performed faster with gloved fingers than both LI and LIS, and ranking with LIS was most time consuming in both experiments. A probable reason for this is that it takes time to get used to the extra source of information. Therefore, a longer training period with the new equipment could have been useful. The experienced surgeons have many years of training using the conventional instruments but very little training with the new equipment. A follow-up study where some subjects went through a training program over several weeks could be interesting.

Most of the subjects did not find the extra source of information confusing, although it was suggested that the information should be placed on the same screen as the endoscopic video, and that information about the pressure (numbers) should be more visible. It should be noted that the visually presented tactile information competes with the endoscopic video for the surgeon's attention. In addition, it is debatable if the brain is able to translate visual images into meaningful tactile impressions fast enough for it to contribute to the surgeon's tactile understanding of the object under investigation (Simpson, 1973). In Chapter 7, presenting the information with a tactile display is considered, and in this case the graphically presented data will probably be redundant. Conducting the same experiments with a tactile display could also give different results.

In conclusion, gloved fingers proved to be better than both LI and LIS for palpation. Despite this, a visual feedback of the tactile image seemed to be useful for the subjects who fully understood how to use it, especially for hardness discrimination. This, however, is just a small step in the right direction, as the overall goal should be to make the instrument as good as the human finger.

Part III

Tactile Display

Chapter 5

Design and Performance of a Tactile Display

This chapter is based on the papers Ottermo et al. (2005), Ottermo, Stavdahl and Johansen (2006a) and Mårvik et al. (2006).

5.1 Introduction

Tactile feedback is critical for dexterous motor control. Without it, we drop objects and have trouble using different tools. Moreover, when spatial tactile information is unavailable, substantial decrements in performance are observed for most sensory and perceptual tasks (Lederman and Klatzky, 1999).

Tactile displays are devices built to convey small scale spatial information about objects that cannot be directly manipulated by the user. These devices are believed to have a wide variety of applications, including computer interaction, laparoscopic surgery and exploration tasks in general. The complexity of the tactile sense, and the fact that there are still many unanswered questions about human perception have put restrictions on the research on tactile displays, and a satisfactory solution has yet to be found.

Size, weight and fidelity in pin motion control are often the main limitations for tactile shape displays (Peine, 1998). Here we describe the design of a display that consists of 32 micro motors in an array (Ottermo et al., 2005), and the main advantage with our design will be the small size. The tactile display described in Wagner et al. (2004) is also based on small motors and is highly effective, but it will be too big to attach to a laparoscopic grasper. Compared to some displays that include tendons in the actuation mechanism, for instance Sarakoglou et al. (2005), our compact design provides high stiffness. We also have a relatively high resolution of the actuator pins, and the positioning of the pins is more accurate than in many other displays.

5.2 Principle and Design

The motors we use are of type designation SLB-06H1PG79 by Namiki Precision Jewels. Table 5.1 shows some key data for the motor, while Figures 5.1 and 5.2 show the size of the motor (including gear head and shaft).

Table 5.1: Technical data for the SLB-06H1PG79 DC motor.

Property	Value
Diameter	2.4 mm
Total length	10 mm
Gear head ratio	79 : 1
No-load speed	650 rpm
Stall torque	0.2 mNm
Torque constant	13 mNm/A

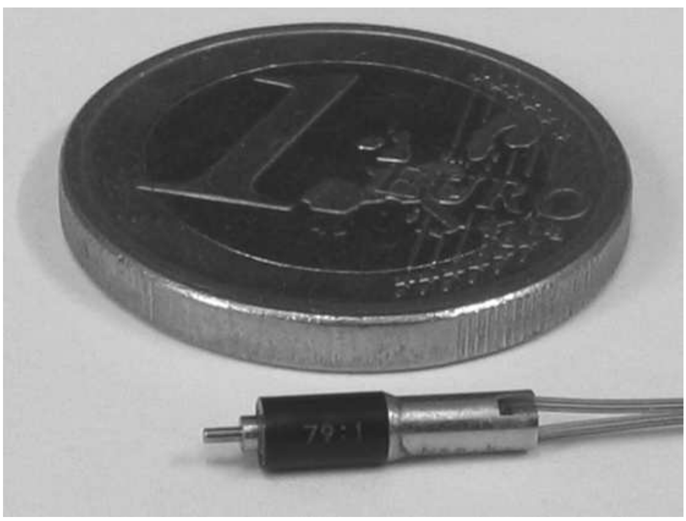

Figure 5.1: Motor of type designation SLB-06H1PG79 by Namiki Precision Jewels.

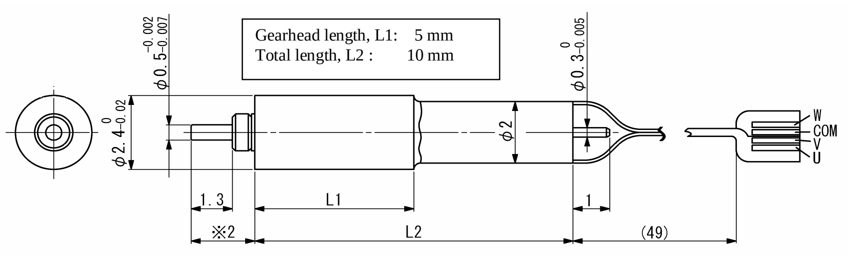

Figure 5.2: A sketch of the motor (courtesy of Namiki Precision Jewels CO.LTD)

For this version of the display the finger is indented vertically, and the principle is to attach a screw to the gear head shaft which screws a tactel up and down when the shaft rotates (see Figure 5.3).

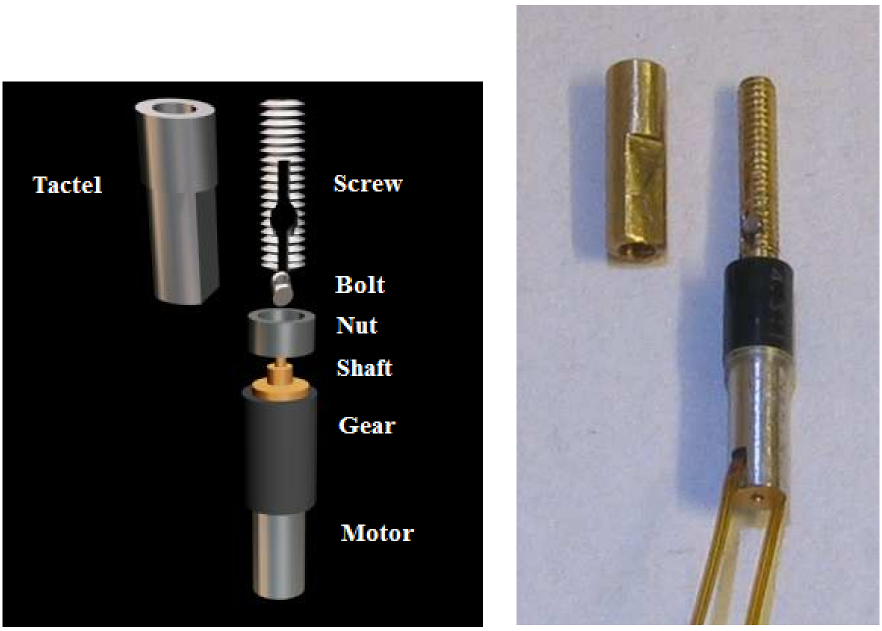

Figure 5.3: Figures showing the integration of tactel and motor.

The position setpoint of each tactel is determined by an electric signal and will be a function of the force exerted on the tactile sensor array, which is attached to the grasper's end effector.

5.2.1 Tactel Mechanism

The mechanism used to attach the screw to the shaft is shown in Figure 5.3. It consists of a small cylindrical bolt that has a diameter of 0.8 *mm* and a length of 1 *mm*, and a screw with a diameter of 1.4 *mm*. Through the bolt we drill a hole such that it can be threaded onto the motor's shaft. The screws have a split running about halfway through them in the vertical direction and a hole with a diameter of 0.9 *mm* in the horizontal direction. In this way, the screw fits around the bolt attached to the shaft. Finally, a small nut around the screw helps strengthen the connection. The advantage of using this mechanism over glue, is that it is more flexible and will prevent damaging the motor if it is exposed to excessive vertical forces. In addition, it is more modular than glue, because it is easier to replace either the motor or the screw mechanism if any of them should break.

To the left in each of the images in Figure 5.3 the tactel top is shown. The upper part of this top has a cylindrical shape, but on the lower part we grind off some of the material on two opposite sides to obtain two flat sections. These flat sections are the keys to translating the rotational movement of the motor into the linear movement of the tactel. The inner working of the tactel has threads to match those of the screw attached to the motor's shaft. Since the tactels are threaded all the way through, different tops can be screwed onto the tactel, allowing for testing with different effector shapes.

5.2.2 Display Housing

The overall design of the display housing is shown in Figure 5.4, while the current version of it is shown in Figure 5.5.

Each hole in the display housing shown in Figure 5.5 corresponds to a cylinder, that is designed to house the tactel mechanism described in Section 5.2.1. One of the major challenges of designing the display is to make it mechanically stable without damaging the gear heads, which are encapsulated in plastic. In other words, we need a design that will prevent external forces from acting on the gear head, in either direction, because this might destroy the gears. An additional problem is that the motor is only loosely attached to the gear head. Our design consists of several blocks stacked together, where each block is carefully fitted to the different parts of the motor and screw mechanism. Another reason for using several blocks in the design, is that it makes it easy to replace one of them in case we want to change parts of the mechanism.

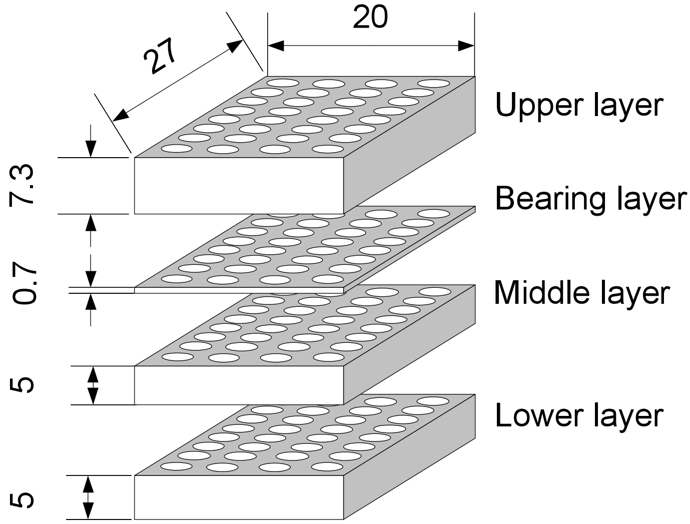

Figure 5.4: Overall design and measures of display (all measures in mm).

The different layers are shown in Figure 5.4. The lower layer's hole dimensions match those of the motors, while the middle layer's hole dimensions match those of the gear heads. The bearing layer is intended for the nut in the screw mechanism to rest upon, such that pressure from the finger will be absorbed by the bearing layer instead of the gear heads. The upper layer's inner workings have splits in the lower part and cylinders in the upper part. The splits fit the flat sections of the tactel top and ensure the linear movement needed to indent the finger vertically.

All top layers are made of an acetal resin engineering plastic, while the lower one is made of iron or μ-metal (in our case a Permimphy material, which is a Fe-Ni soft magnetic alloy) in order to prevent magnetic crosstalk between the motors. When using μ-metal, which has a permeability close to 100 times higher than iron, we expect a slight increase in the torque, as the high permeability adds a positive component to the motor's magnetic field. Therefore, both these materials are tested in the torque performance test.

A thin protective layer of silicone rubber is adhered to the top surface of the display to provide spatial low pass filtering (Lee et al., 2003).

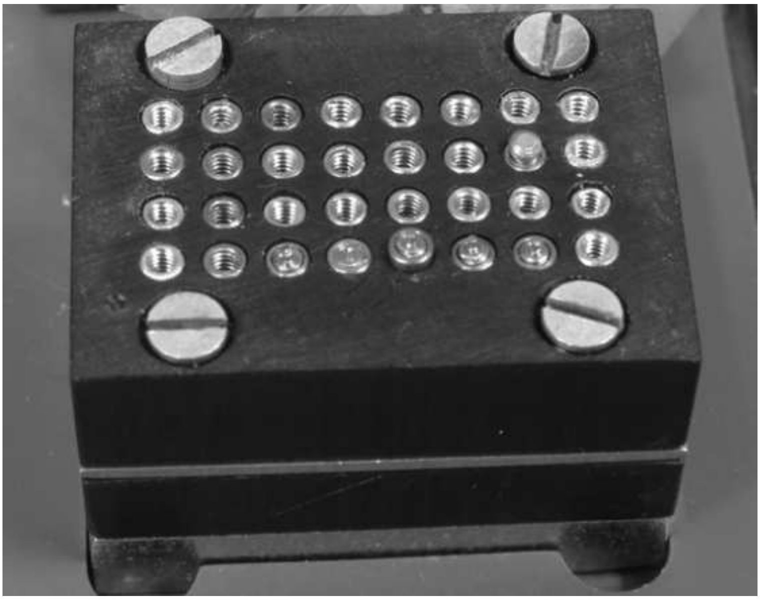

Figure 5.5: Figure showing the display housing. Five of the tactels in the front row have a pointed pin shape, while one of the tactels in the third row has a round pin shape.

5.2.3 Integration on Handle

Figure 5.6 illustrates how the display can be attached to a laparoscopic handle. The laparoscopic handle is custom made to be able to integrate both the display and the driver circuits into the handle (Nesbakken, 2004, Mårvik et al., 2006), although it is also a possibility to attach the driver circuits at the bottom of the handle if this proves to be more convenient.

5.2.4 Driver Circuits

Principle and Design

The original driver circuit designed to operate the motors is a SSD04 3-phase sensorless driver circuit from Namiki, which is shown to the right in Figure 5.7. Since we need 32 of these driver circuits, they are too big. Therefore, we have made a control unit that integrates the 32 driver circuits in one block (see left part of Figure 5.7). The block consists of 5 cards stacked together, including the card for connection to computer/power, and the total size is 34 $mm \times 34$ $mm \times 45$ mm.

(a) Handle with tactile display. (b) Handle.

Figure 5.6: The above figure illustrates how the display can be integrated into a custom made laparoscopic handle. The full grasper handle is shown to the right.

Each card controls 8 motors and contains an FPGA together with driver circuits, circuits for programming of the FPGA, RS485 transceiver and connectors for the motors. When stacking the cards, the FPGAs are automatically cascaded such that each card can be addressed directly. Although only 4 cards are used for controlling the 32 motors, it can be expanded to as much as 8 cards, and each card has dedicated addresses in the address space of 256. In addition, the cards have a common address space, which addresses all cards simultaneously.

Serial communication with a computer is done with Universal Asynchronous Receiver/Transmitter (UART). A 4-wire RS485 enables communication at as much as 1 *Mbaud* over a few meters. Each data message is assigned a register, and all functions are implemented as accesses to internal registers in the FPGA. Messages are 2 bytes, with register address in the first byte and data in the second. Register FFh is reserved for resynchronization of the message flow. LEDs on the cards indicate traffic to all cards and unique access to a specific card, respectively.

Setpoints for position and acceleration are easily set by the user. The original SSD04 driver circuit uses two phases to control the motor and the third phase as a rotation sensor. The custom made circuit commutates the motor as a stepper motor (dividing one revolution of the motor shaft into 6 discrete steps) and uses all phases for control. The major advantage of using this stepper motor approach is that it gives us the opportunity to accurately dictate the position without having to verify the position with a shaft encoder (Hambley, 2002). The drawback is that the precise and repeatable positioning of the motor shaft comes at the sacrifice of speed capacity. Since the commutation with our circuit is done without feedback, we do not know when it is optimal to commutate again, and hence we need to limit the commutation frequency in order to avoid slippage. Our circuit is approximately 49% slower than the original circuit at no load speed. This difference is probably smaller under load, as we have more torque available to drive the load when using our commutation scheme (since we get a higher torque constant). Due to inertia in the motors, commutation is done using a speed ramp. This is implemented as a table of 20 elements, where each element determines how many periods of 16 *MHz* will pass between commutations.

Commutation of the motors is controlled by a state machine that compares the position state with a reference position. New setpoints can be set at any time, and if the motor is already running it will be adjusted according to the new setpoint. Check bits to reset the counters and change direction are also available such that the motors can be run to end points in both directions. In this way we can also re-calibrate the motors if necessary.

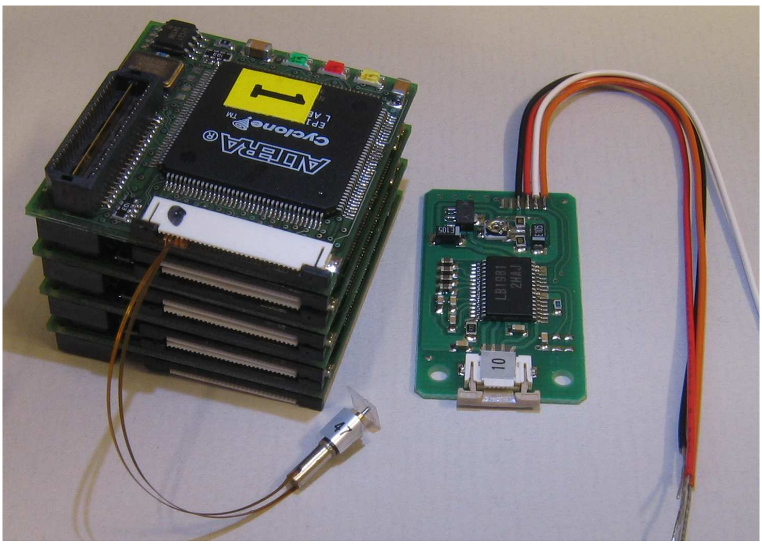

Figure 5.7: The specially designed driver circuit for 32 motors to the left and the original SSD04 driver circuit to the right.

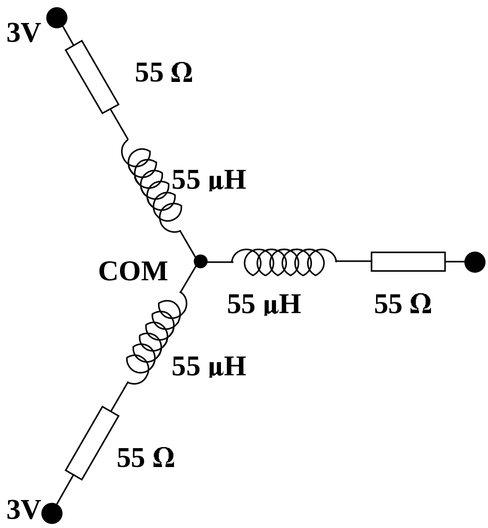

Figure 5.8: Stator winding configuration and impedances.

Calculations

With the custom made driver circuit, the motor is run by applying voltage to all three terminals simultaneously, with their common point being ground. +3 V or -3 V is applied to each terminal depending on where the motor is in the commutation cycle (see Figure 5.8 and Table 5.2). At stall (motor is forced to a stop), there is no back-emf and the inductance is irrelevant. Each resistance now sees a voltage of 3 V, differing only in direction, causing all phase currents, I_p, to have the same theoretical absolute value:

$$I_p = \frac{U}{R} = \frac{3\ V}{55\ \Omega} = 54.5\ mA \tag{5.1}$$

To find the actual input current, a 1.2 Ω resistor was connected in series with one of the motor inputs and the voltage drop measured. The mean voltage drop at stall was approximately 0.061 V, corresponding to 51 mA.

The nominal torque constant given by the data sheet is based on normal operation where only two phases are used for the commutation. Since we use three phases we need to calculate a new torque constant where the new geometry is taken into account (see Appendix A for calculations). The two cases are compared in Figure 5.9. With the new estimated torque constant,

$K_t = 15\ mNm/A$ and the measured input current, I_m, we get the torque, T_m, available for driving the load:

$$\begin{aligned} T_m &= T_d - T_{fm} = I_m K_t - T_{fm} \\ &= (15\ \frac{mNm}{A} \cdot 51\ mA) - 0.156\ mNm \\ &= 0.609\ mNm \end{aligned} \tag{5.2}$$

where T_d is the torque developed and T_{fm} is the friction torque given by the motor's data sheet.

Table 5.2: Commutation sequence.

Rotor position	Phase C	Phase B	Phase A
0°	$-3\ V$	$+3\ V$	$-3\ V$
60°	$-3\ V$	$+3\ V$	$+3\ V$
120°	$-3\ V$	$-3\ V$	$+3\ V$
180°	$+3\ V$	$-3\ V$	$+3\ V$
240°	$+3\ V$	$-3\ V$	$-3\ V$
300°	$+3\ V$	$+3\ V$	$-3\ V$

5.3 Performance

To evaluate the performance of the tactile display, we used the setup shown in Figure 5.10. It includes a high resolution potentiometer from which a voltage proportional to the displacement can be read. We also used our display to gain knowledge about friction. Estimating the friction is always challenging and almost impossible without the actual device, although Richard, Cutkosky and MacLean (1999) looked at methods for identifying friction for an aluminum block sliding on brass, Teflon and rubber.

5.3.1 Positioning Accuracy

Each tactel can be given 150 different position setpoints distributed along the maximum height of 3 mm. This implies a theoretical positioning resolution of 20 μm. To verify this, a typical tactel was given 25 incremental steps from 0 to 149. The results for three trials are shown in Figure 5.11. The maximum error between true linear value and pin height was 0.1517 mm, and the standard deviation was 0.0382 mm. This corresponds to a positioning accuracy of approximately 40 μm.

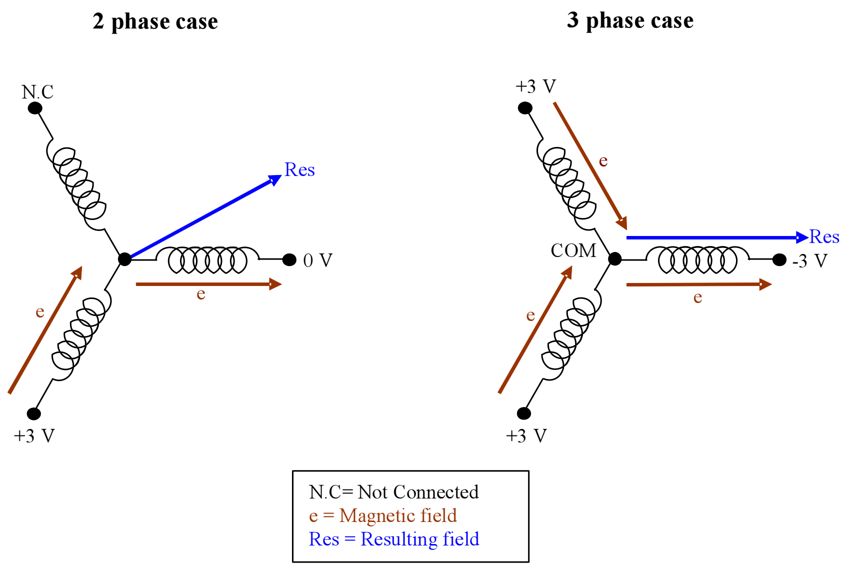

Figure 5.9: Resulting field when using 2 and 3 active phases, respectively.

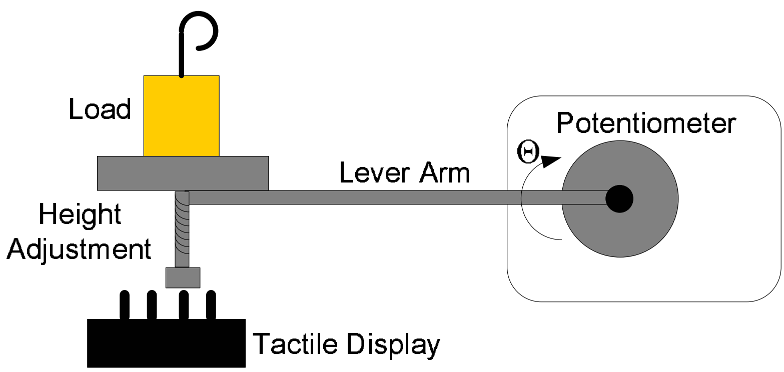

Figure 5.10: Figure showing the experimental setup.

5.3.2 Force and Bandwidth

To specify the force and bandwidth the display can provide, two typical tactels were stepped from 0 to max excursion (3 *mm*) and from max excursion to 0, at our maximum speed. With 6 commutations per revolution, a

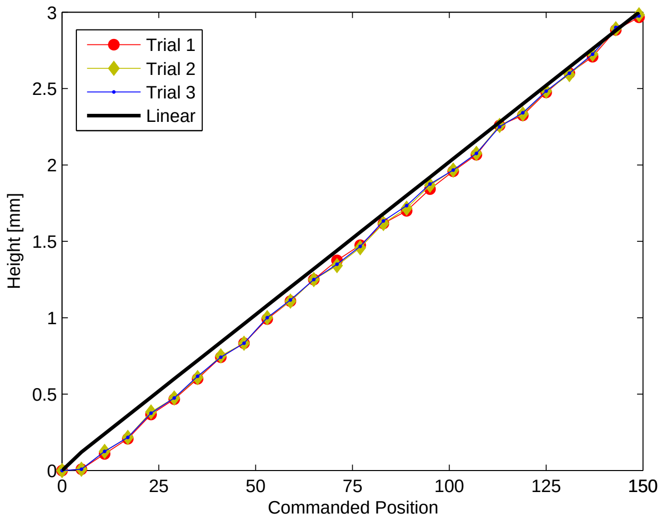

Figure 5.11: Plot showing commanded position versus height [mm].

gear head reduction, n, of 79:1 and a minimum of 10 periods of 16 MHz between commutations, we have a maximum speed, $v_{rps} = 1041 rps$, which with a thread pitch, $p = 0.3\ mm/round$, corresponds to:

$$v = \frac{v_{rps}p}{n} = \frac{1041\ rps}{79} \cdot 0.3\ \frac{mm}{round} = 4\ \frac{mm}{s} \tag{5.3}$$

The results showed that the fall time was 0.7 s and the rise time 0.76 s, which gives us a bandwidth of approximately 0.68 Hz. This corresponds well with theory:

$$f = \frac{v}{(2h_{max})} = \frac{4\ \frac{mm}{s}}{(2 \cdot 3\ mm)} = 0.67\ Hz \tag{5.4}$$

where h_{max} is maximum excursion and v is maximum speed. As mentioned before, we experimented with encapsulating the motors in both iron and μ-metal to provide extra shielding. Because μ-metal has a considerably higher permeability than iron, we wanted to check if this would affect the torque exerted by the motors. In both cases, the tactels were run under different loads starting with 0 load and ending with the weight at which the motors ceased to respond consistently. The mean values for the iron case under different loads are shown in Figure 5.12.

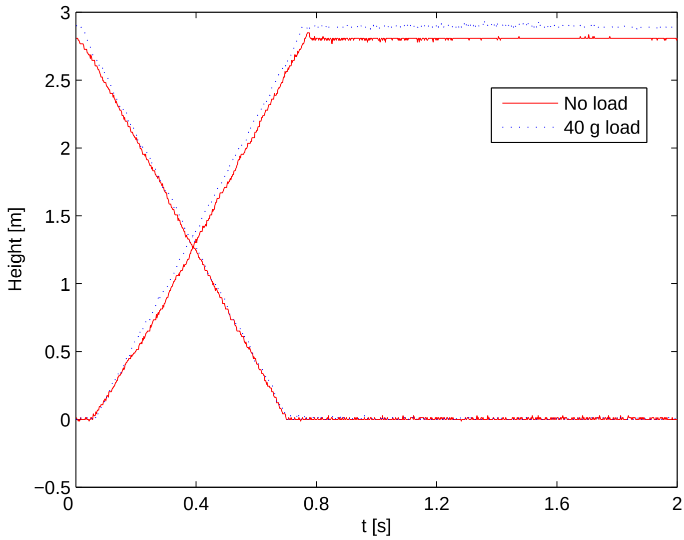

Figure 5.12: Plot showing step response under different loads when motors were encapsulated in iron.

For iron we concluded that the maximum load a tactel could lift at maximum speed was 40 grams, corresponding to approximately 0.4 N. μ-metal showed the same step response, but the maximum load at maximum speed increased to 50 grams. This indicates that using μ-metal shielding does indeed increase the torque. The μ-metal did also prove to be very effective as far as shielding is concerned. Note that at very low speeds we were able to lift up to 1 N when the motors were encapsulated in μ-metal.

A 6 ms delay between command and pin movement was observed in performance trials.

5.3.3 Stiffness

To test the stiffness, which we expected to be relatively high due to our compact design, we loaded a tactel with successive weights ranging from 100 grams to 1000 grams, again using the setup of Figure 5.10. The result is shown in Figure 5.13.

As the figure shows, the yield was only 0.21 mm with a load close to 10 N, and hence we have a stiffness of close to 50 N/mm.

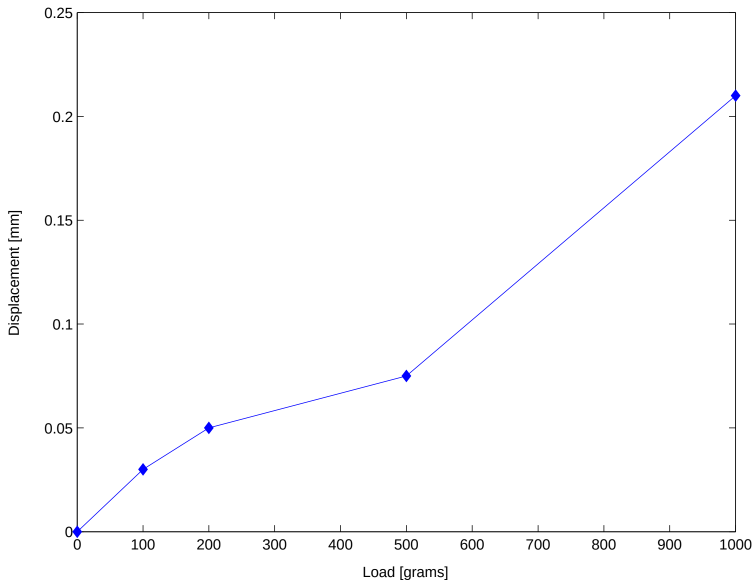

Figure 5.13: Plot showing stiffness of display.

5.3.4 Friction

We have based our friction estimates on the classic Coulomb friction model, where friction force is proportional to load (Egeland and Gravdahl, 2002).

$$F_f = \mu F_l \tag{5.5}$$

Here μ is the coefficient of friction and F_l is the normal force. There is also an initial static friction (stiction), $F_s = C$, that must be overcome for the motor to start rotating:

$$F_n = F_l + F_f + F_s = F_l + \mu F_l + C \tag{5.6}$$

Here F_n is the total force available for driving the mechanism, F_l is the load the tactel is actually able to lift and F_f the friction force (see Figure 5.14). We know that

$$T_m \omega = F_n v \tag{5.7}$$

and

$$p\omega = v \tag{5.8}$$

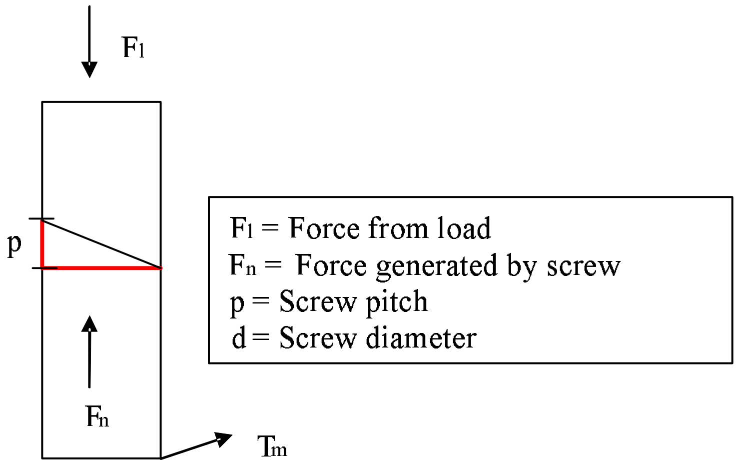

Figure 5.14: Forces and torques in the screw mechanism.

where p is the screw pitch, ω is the motor's angular velocity, and v is the linear velocity of the tactel. Hence we can estimate the friction constant for the screw mechanism from the following equation:

$$T_m = I_m K_t - T_{fm} = T_l + T_f + T_s = p[F_l(1 + \mu) + C] \tag{5.9}$$

Here F_l is assumed to be the maximum load we can put on the tactel before the motor stalls. From experimental data we find a relationship between the voltage input to the motor and the maximum load a tactel can lift. Then we use these data to find a relationship between the torque and the load $[N]$. To estimate the friction we find how F_f varies with maximum load and use equation (5.9) to determine values for C and μ. This result is shown in Figure 5.15. Using linear regression we finally find that $C = 0.46$ and $\mu = 12.81$.

5.4 Discussion

Table 5.3 shows a comparison of different tactile displays (Wagner et al., 2004), including our display.

Our display is small and has a size compatible with both the finger tip and the handle of a laparoscopic grasper. The number of pins can easily be increased, but this will result in a corresponding increase in size. The resolution would preferably have to be improved, but in our case it is restricted

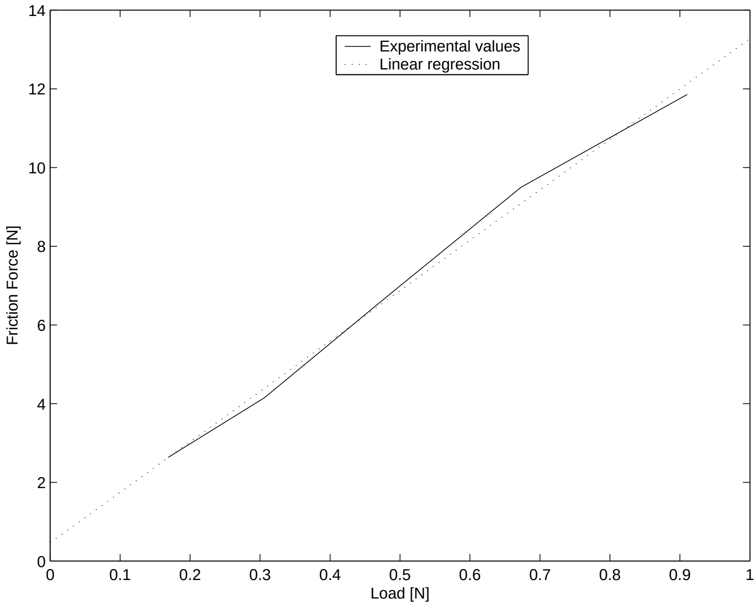

Figure 5.15: Load vs. friction, experimental values and the linear curve (found by minimum square error).

by the size of the motors. Both using smaller motors and a two-layer approach (where the top layer has shorter screws than the bottom layer, such that the motors can be stacked closer to each other) will increase the resolution significantly. The latter will, however, introduce other problems, such as different screw lengths or sluggishness. Changing the mechanism and introducing some sort of reorientation in the direction of applied force is also a possible option.

Theory corresponds well with reality for the bandwidth in that it follows the commanded velocity as long as the commutation is not too fast. If the motors cannot follow the input velocity, they slip and do not move at all. Despite this, the bandwidth of the display is well below the requirements introduced by Moy et al. (2000). There are several ways to increase the velocity, the most important being changing the gear head reduction and increasing the screws' thread pitch. The motors we are currently using are not available with a suitable gear head reduction to increase the bandwidth and still provide a significant force on the finger tip. The same is the case when changing the screw pitch, as the forces will decrease both due to friction caused by the increased angle of attack between screw and nut and

Table 5.3: Comparison of tactile shape displays (n.s = not stated).

Reference	Goal: [a]	Ours	[b]	[c]	[d]	[e]	[f]	[g]	[h]	[i]
Actuator	n.s.	Servos			Pneumatic		SMA		Solenoid	Piezo
Array Size	10x10	4x8	6x6	4x4	4x4	5x5	1x10	8x8	8x8	6x5
Tactel Spacing $[mm]$	1	2.7	2	2	1.75	2.5	2	3.2	5	1.8
Temp. Bandw. $[Hz]$	≥ 50	0.67	7.5/25	15	11	5	30	0.1	n.s.	360
Max Pin Force $[N]$	0.5-1.0	0.5 (1.0)	2	3	3	0.2	1.5	2.5	n.s.	0.06
Pin Disp. $[mm]$	3	3	2	2.5	5	0.6-0.7	3	3.5	1	0.7
Height Res. $[mm]$	0.4	0.04	0.1	n.s.	n.s.	n.s.	0.1	n.s.	0.25	n.s.
Size $[mm]$	n.s.	27x20x18	76x119	12x15x20	15x15x10	12x12	78x35x57	n.s.	40x40	40x20x23

[a] (Moy et al., 2000)
[b] (Wagner et al., 2004)
[c] (Sarakoglou et al., 2005)
[d] (Caldwell et al., 1999)
[e] (Moy et al., 2000)
[f] (Wellman et al., 1997)
[g] (Fischer et al., 1997)
[h] (Frisken-Gibson et al., 1987)
[i] (Kyung et al., 2005)

the gear-up from increasing the thread pitch.

The maximum pin force at maximum speed is 0.5 *N* for our display, as opposed to the proposed 1 *N* in an ideal display. However, this is not as big a problem as the bandwidth limitations, so in later versions, maintaining this torque while increasing the bandwidth should be a priority.

The performance tests showed that the accuracy in the positioning resolution was around 40 μm. As can be seen in Figure 5.11, there is a dead zone in all trials in the first few position steps. A probable reason for this can be given in Figure 5.3, where the split in the screw is shown. As the hole that the bolt fits into is not circular, but slightly oval, this can result in commutations of the motor that do not cause any vertical motion. The dead zone is noticeable in all trials, and if this had been accounted for when comparing with the linear case (by shifting the linear case to start at the point where vertical movement actually starts in the trials), it would have resulted in a higher positioning accuracy. Another reason for the dead zone can be inaccuracies in the commutation scheme at start up. It was important to verify the positioning accuracy and repeatability, because the display does not provide position feedback. Introducing position sensors would require additional space but would have been necessary if the tactels had been less repeatable. Despite this, putting too much load on the tactel could still introduce problems, since the control system can lose track of the motor's position. In such cases the motor must be re-calibrated.

The high stiffness of the display, which is an intrinsic property of the screw-based design, should be kept in later versions.

Since as much as 90% of the torque is lost due to friction (see Figure 5.15), better lubrication, polished screws, or using more optimal materials such as Teflon, would probably improve the performance considerably.

5.4.1 Implications for Future Displays

Although the bandwidth and force the reported display can provide are well below the ideal criteria posted by Moy et al. (2000), we think that the design of this display is promising since it provides the opportunity of making small displays. Small stepper motors have the positioning resolution tactile displays require, and as we have seen we obtain very high stiffness using our design. Since the major limitations are the bandwidth and the force, the following section attempts to estimate requirements for motors to be used in later versions. Ideally, we want to feed our screw parameters, as well as our requirements for bandwidth, positioning resolution and force into a "black box" and end up with torque and velocity requirements for the motor (see Figure 5.16).

Figure 5.16: "Black box" parameters for finding required torque and velocity.

We start off with the parameters provided by the motor's data sheet and use the estimates for velocity and torque obtained for our commutations scheme, as well as our friction calculations to design a calculator which will be helpful for future designs.

We know that there is usually a $30 - 50$ Hz requirement for tactile displays. However, with reference to Wagner et al. (2004), where they made a similar, but larger display, a 7.5 Hz bandwidth was found to be adequate, especially for lump detection, which usually requires small palpation speeds. With a 3 mm excursion, a 7.5 Hz bandwidth corresponds to a speed of 45 mm/s (11850 rps). Generalizing the velocity requirement we get:

$$v_r \geq \frac{45 \ \frac{mm}{s}}{p \ \frac{mm}{round}} \tag{5.10}$$

where v_r is the required velocity out of the gear head and p is the screw pitch. We want a positioning accuracy (r) of at least:

$$r \leq 0.1 \ mm \tag{5.11}$$

From before, we know that a typical tactel can lift 0.5 N (using μ-metal as shielding), and that we want to double this to able to lift 1 N at high velocities. If there was no friction in the screw mechanism, the torque measured would have been adequate to provide more than 1 N. With the estimates for friction, one can use any motor's torque-velocity curve to find if it is strong and fast enough to be used in a future display.

The resulting calculator, see Figure 5.17, makes it easy to verify motor specifications for new motors.

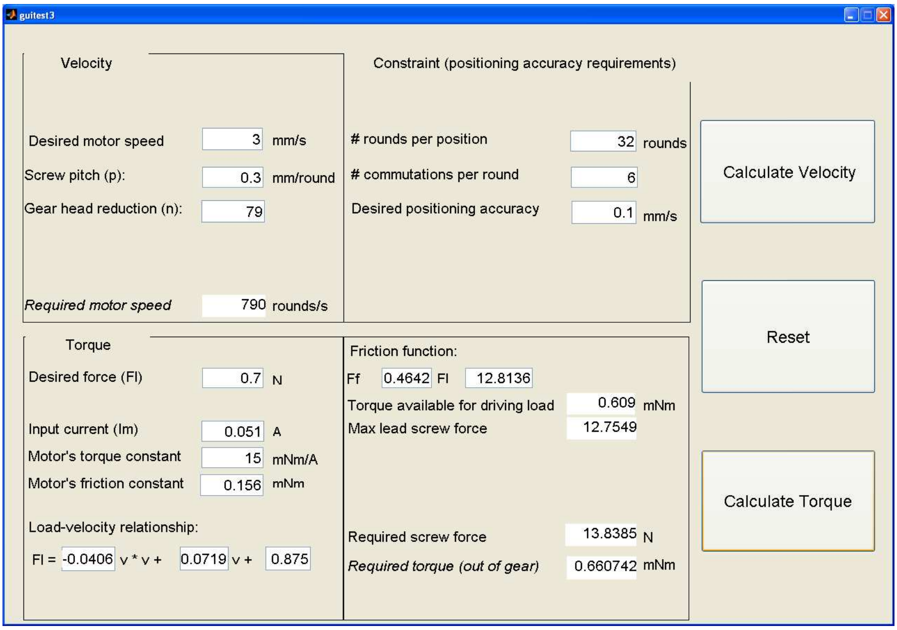

Figure 5.17: Calculator.

The design and performance of a tactile shape display has been described. Although we found that our display does not meet the requirements for bandwidth and force, we think that the design is promising. Therefore, we found an estimate for friction such that it will be easier to find specifications for motors to be used in future versions.

Chapter 6

Pin Shapes for Tactile Displays

6.1 Introduction

Ideally, the user should not be able to discriminate between actually touching the object and touching the replica of the object given by a tactile display. This, however, is not the case with today's existing displays, due to many factors. The most important is the lack of technology to provide a satisfactory resolution for the actuator pins yet maintaining the necessary bandwidth and force. In addition, there are probably several ways to improve the way information is presented to the user. For instance, a thin rubber cover on top of the pins can provide spatial low pass filtering (smoothing). Other possibilities for improving the displays could be to change the material of the tactel to better match the nature of the object the tactile display is replicating.

In addition to these possible improvements, we hypothesize that the shape of the pin makes a difference for how well a shape can be represented on a tactile display. In particular, based on literature on edge detection (Srinivasan and LaMotte, 1987), we assume that it is easier to convey many different shapes using a pointed shape, rather than using a blunt shape, although the blunt shape can be better in certain cases, such as representing square waves.

To examine these ideas, we conducted a psychophysical experiment where we investigated the relationship between the perception of a line signal and pin shape. The experiment attempted to discover whether the subjects could recognize a given signal represented on the display for each pin shape.

6.2 Materials and Method

6.2.1 Equipment

The display discussed in Chapter 5 was used in the experiment (see Figure 6.1). To eliminate errors resulting from subjects pressing their finger pad with different forces against the display, the display was mounted on a spring-loaded plate, as shown in Figure 6.2. Participants were asked not to press harder than a red line indicated on the ruler on the side of the mounting (see Figure 6.2).

Figure 6.1: Tactile display with 23 tactels mounted. The left column shows pointed pins. In the front row the adaptive shape is shown. The rest are blunt pins.

6.2.2 Pin Shapes

The 3 different pin shapes investigated in this experiment are illustrated in Figure 6.3. The pointed shape to the left is the sharpest and is 0.5 *mm* in diameter. This shape is also shown in the leftmost column of the display in Figure 6.1. The second, circular, flat shape (diameter = 2 *mm*) is

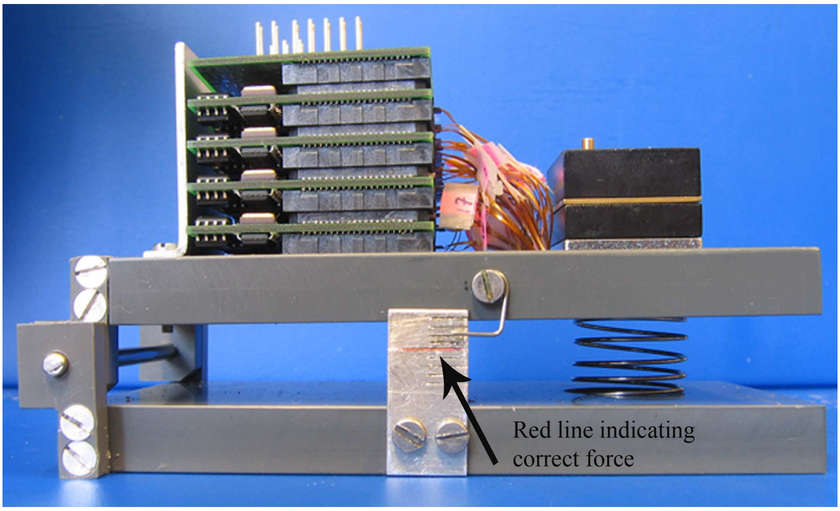

Figure 6.2: Display mounted on spring-loaded plate.

also shown in Figure 6.1. The last shape in Figure 6.3, called ”adaptive”, is a semi-elliptical mounted on a ball joint, which allows for the shape to change angle depending on how the finger rests on the pin. The radius of the semi-elliptical is 1 *mm*, and the radius of curvature is approximately 0.5 *mm* (see Figure 6.4). In a simple pilot study done prior to this experiment, a hemisphere shape as well as a triangle shape were also considered as possible options for the pins, but they indicated a close resemblance to the flat and pointed shape, respectively.

6.2.3 Signal Shapes

The signal shapes used in this experiment were sine, square and sawtooth waves. Figures 6.5 to 6.7 show examples of one cycle of each of these signals (where cycle is the number of complete periods of the signal shape distributed over the column of 6 pins). It also indicates how each pin corresponds to a sample in the discrete case. Based on these examples, we hypothesize that the pin shape that minimizes the difference between the actual signal shape and the shape represented on the tactile display would be the optimal. This means that for the square wave we anticipate that it will be rendered more realistically with the flat pin than with the pointed one. We also expected that the ”adaptive” pin would render a sine and a sawtooth wave better than the blunt pin shape, because of the possibility to adjust to different angles depending on pin height.

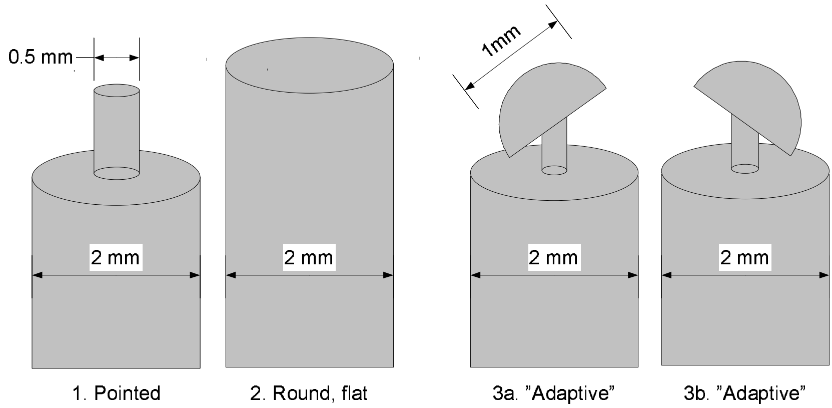

Figure 6.3: The 3 pin shapes.

Figure 6.4: The adaptive pin shape, where the right part shows the screw with a ball joint, and the left part is the actual tactel top.

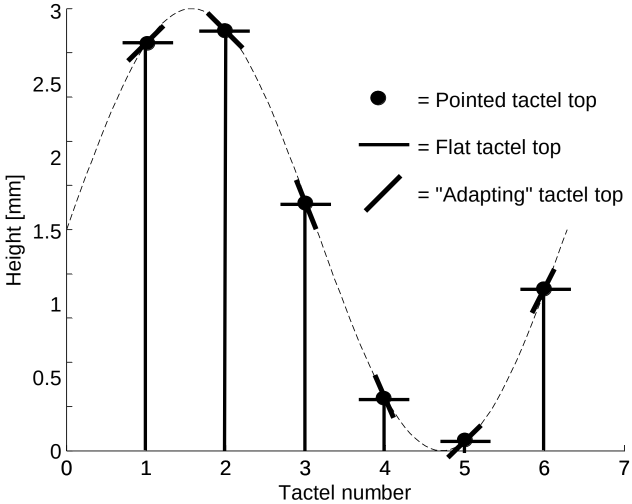

Figure 6.5: Sine wave, with one cycle distributed over 6 pins..

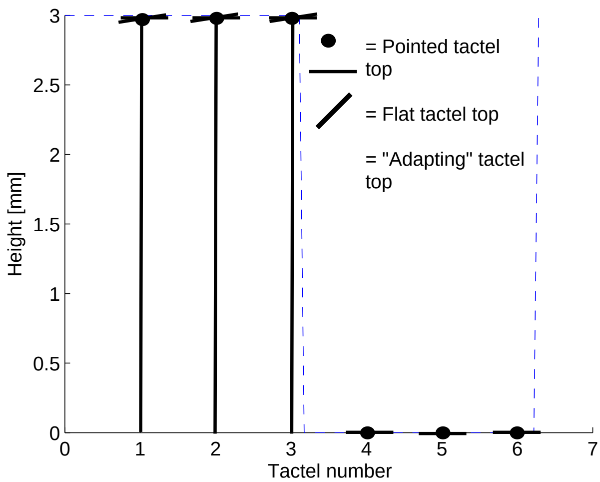

Figure 6.6: Square wave, with one cycle distributed over 6 pins.

Because of the spacing of the pins, the same waveform can be displayed differently depending on if it is centered between two pins or directly on a pin (Lee et al., 2003). To try to eliminate this effect, we changed the wave-

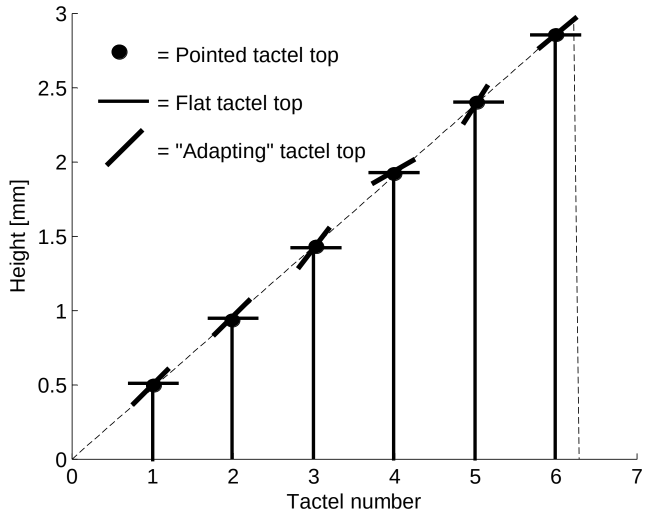

Figure 6.7: Sawtooth wave, with one cycle distributed over 6 pins.

length in all trials by varying the number of cycles displayed by the 6 pins between 1, 1.5 and 2. Choosing smaller wavelengths would result in aliasing. We did not try larger wavelengths, mostly because we wanted to keep the number of trials at a minimum for each subject.

6.2.4 Experimental Design

The experiment attempted to discriminate between 3 different pin shapes by presenting known signal shapes propagating over a column of 6 pins to the subjects. The subjects tested the different pin shapes twice, before and after being presented with information about pin shapes and signal wavelengths. They were presented alternating wavelengths randomized between trials. In addition, the order of the pin shapes was counterbalanced across subjects.

6.2.5 Test Persons

A total of 6 subjects, 4 male and 2 female, volunteered to participate in the experiment. They were between 25 and 32 years and had no prior experience with tactile displays. Two of the subjects were left handed. None of the subjects had any known abnormalities in either hand.

6.2.6 Procedure

First, the subjects were given some background information on tactile displays and told that they would be asked to do several discrimination tasks during the session. They were also told that they would feel a simulation of either a sine, sawtooth, or square wave propagating over the display. The direction of the stimulus was from the hinder part of the finger pad towards the front, and the speed of the tactels was kept constant at approximately 1.3 mm/s.

All subjects were familiar with the signal shapes from before. Participants were not given time to gain familiarity with the tactile display, but halfway through the trials they were showed drawings of the three different tactel shapes, and the signal shapes and their possible wavelengths.

The subjects put their index finger of their dominant hand on top of the display through a hole in a case covering the display. They were not given any visual feedback during the experiment. The subjects did not control the display themselves (see Figure 6.8), but they could always ask for lower or higher signal amplitude if they found it necessary.

They were not given any time limits to complete each task, so the successful completion criteria was to tell the test monitor which signal shape they felt in each case. They were asked not to guess but rather respond with "do not know" if necessary. After that, a new task was immediately presented to them. Each subject completed a total of 54 trials, with breaks every ninth trial. Normal completion time for each task was between 10 and 20 seconds.

6.3 Results

Recognizing the different signal shapes proved to be difficult for all pin shapes. Therefore, the ability to classify the signals became more important than finding threshold amplitudes in each case (which would have been a good measure for how well each pin shape conveyed the signal). This was not surprising after the initial pilot study, although it was believed that learning effect would be more significant than it actually was. It was surprising, however, that the average rate of recognition was as low as 29.3%. The highest rate of recognition was 42.6%, while the lowest was only 15%. In 18% of the trials, the subjects answered "do not know", meaning that they could not classify the signal. Note that these numbers are based on all answers, including the cases when the subjects said they did not know. (If the cases when the subjects answered "do not know" were excluded, the average rate of recognition was 35.8%.)

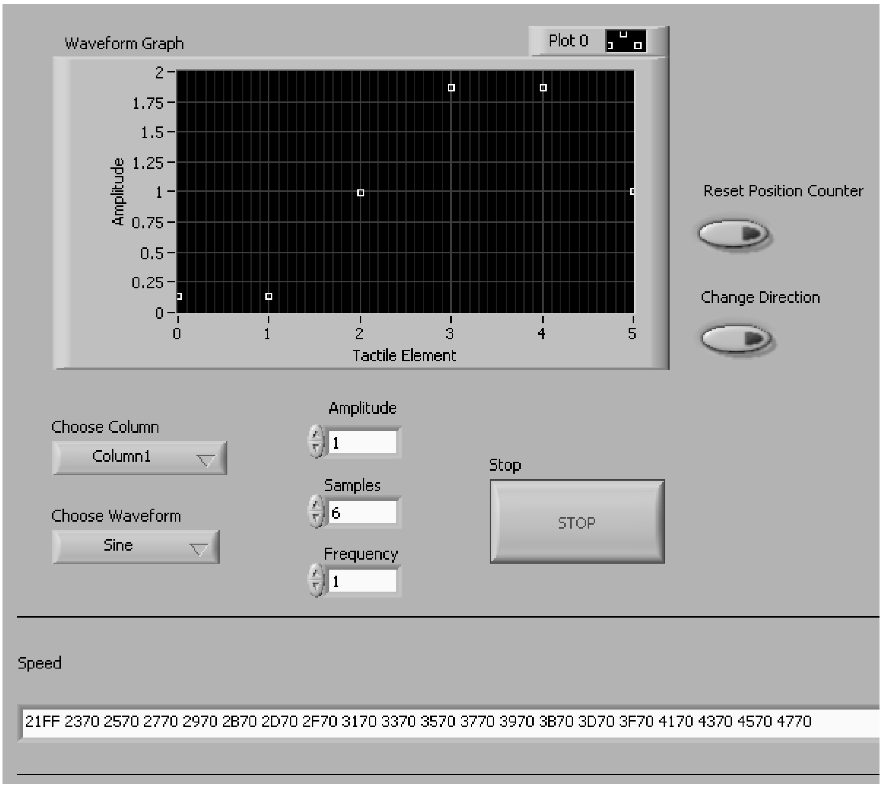

Figure 6.8: The interface controlled by the operator (not viewed by subjects).

The overall difference in recognition rate for the 3 pin shapes was not significant. Of the total 95 correct classifications, 35.8 % were done with the ″adaptive″ shape, 31.6 % with the pointed shape and 32.6 % with the flat, circular shape. Despite this, Figure 6.9 shows that the flat shape often has the worst performance (5 of 9 cases). As mentioned before, we anticipated that the different tactel shapes would convey particular signal shapes better than others, but the experiment did not support this hypothesis. In the sine wave case, 12 out of 38 correct classifications were done with the ″adaptive″ shape, 14 with the pointed shape, and 12 with the flat shape. The subjects had a lot of difficulties classifying the sine wave with the shortest wavelength (2 cycles), which was not surprising due to the close resemblance with a sawtooth wave with the same wavelength. For square waves, the ″adaptive″ shape accounted for 14 of the 39 correct answers, the pointed for 9 and the flat for 6. It should be noted that for the square wave with the longest wavelength (1 cycle), the subjects thought it was a sine wave in 60.5% of the cases, because it felt smooth. For the sawtooth waves, both the ”adaptive” and pointed shape accounted for 28.6% of the correct answers and the flat shape for 42.8%. These figures are summarized in Figure 6.9. Subjects commented that they felt their sensitivity was reduced after several trials, but results showed that the ability to recognize signals was not reduced after several trials. This could, however, be due to some learning effects.

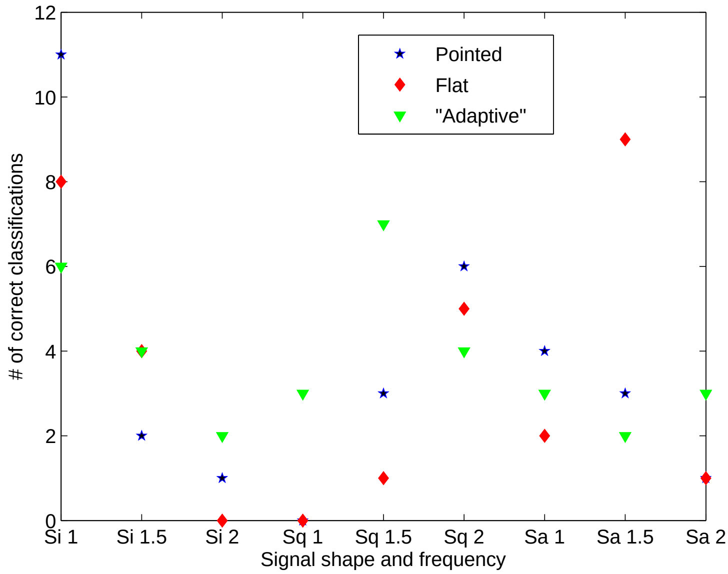

Figure 6.9: Plot showing number of correct classifications for each signal shape and pin shape. Si=Sine, Sq=Square, Sa= Sawtooth. 1, 1.5 and 2 are the number of cycles.

6.4 Discussion

In this experiment we attempted to examine the importance of pin shape in tactile shape displays. Based on this, we expected to find guidelines for how to choose the most appropriate pin shape for tactile displays, depending on the application and stimulus type we want to represent with the display. In the experiment, subjects were asked to discriminate between 3 known signal types, and we hypothesized that the shape of the pin did matter for how easy it is to classify the different signals. In particular, we anticipated that it would be easier to convey a broader range of shapes using a pointed shape, rather than a blunt shape.

As mentioned before, the subjects had trouble recognizing the signal shapes, and there was no significant difference in how easy the signals were to recognize when the different pin shapes were used. Despite this, all subjects believed that they performed better with the pointed and "adaptive" pin shapes than with the flat, circular shape. In general, subjects also asked for more amplitude to be able to classify the signals when the blunt shape was used.

It was surprising that the learning effect was not significant, especially after informing the subjects about how the signals propagated over the display.

We chose to use the same slow propagation speed in all trials, and this might have affected the results, especially in the square wave case, since the steps probably felt smoother than they should. It is also possible that the tasks given were too specific and difficult, meaning that a different classification task could have been investigated, for instance specifying the direction of a wave. Some of the subjects also reported that they would have preferred to be able to press their finger harder against the display, because they wanted a more active exploration.

Despite the fact that the subjects could not recognize the signal shapes very accurately, they reported many distinct sensations for the different signal shapes. For instance some felt it like a wheel was rolling over their finger pad or that they were touching something pulsating (for instance a blood vessel). This indicates that it is not necessarily important to reproduce the exact shape we want to convey, but rather focus on how we can give the user the illusion that he is feeling this shape.

Although this experiment suggests that designers of tactile displays do not need to concern themselves too much about the actual shape of the tactel, it would be interesting to investigate the results in more detail by changing the classification task and also adding more than 1 column of tactels. Another interesting experiment would be to use the "dual task paradigm", where the amount of concentration needed for a task is evaluated by making the subjects perform a second unrelated task simultaneously with the classification task. By performing one of the tasks faster or changing the level of difficulty, one can find out when a specific task becomes too difficult. Adding the traditional spatial low pass filter on the tactile display (Lee et al., 2003) could also be of interest in future work.

Part IV

Tactile Feedback

Chapter 7

Virtual Palpation Gripper

The results in this chapter is presented in the paper Ottermo, Stavdahl and Johansen (2006b).

7.1 Introduction

The previous chapters have described a tactile sensor and a tactile display, as well as experiments related to each of these components. A remote palpation instrument incorporates both components and the communication between them. The goal is to make an instrument that can give tactile feedback and thereby provide the surgeon with additional information about the tissue under investigation, for instance the presence of a tumor. This chapter will focus on the communication between the sensor and the display and how the tactile display can be attached to the grasper with the tactile sensor array. This will result in what we call a Virtual Palpation Gripper. This does not refer to the use of virtual reality, but rather on the fact that we are trying to provide the surgeon with a sensation that he could not have obtained without this instrument. Further, the chapter describes some simple experiments related to the performance of the instrument. The main advantage with our system compared to some of the other systems described in Section 2.6, is the ability to measure and display the spatially distributed parameters of contact on the surface between the sensor and an object and not only single point contact. Another advantage is the size of the system, which is small and light enough to fit onto a conventional laparoscopic grasper.

7.2 Communication between Tactile Sensor Array and Tactile Display

The TactArray communicates to host PC using an Application Program Interface (API) contained with a Windows Dynamically-Linked Library (dll). Since we use LabVIEW (National Instruments Inc.) software to run and control the motors in the tactile display, we chose to program against the API using the same software. Figure 7.1 shows a block diagram of the full system.

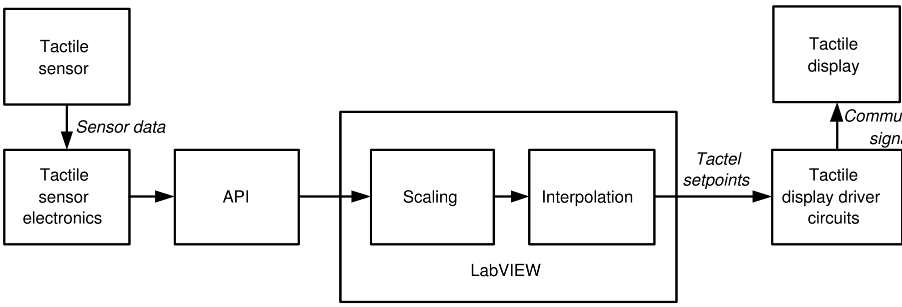

Figure 7.1: A block diagram showing the different parts of the Virtual Palpation Gripper system.

With LabVIEW we can easily visualize real-time data from the sensor (see Figure 7.2). As mentioned in Chapter 3.4, the TactArray sensor has 15×4 sensing elements, and the total area of the sensing surface is $3.5\ cm \times 1\ cm$. The display, on the other hand, has 8×4 tactels, but due to trouble with the motors, only 7×4 were used in the final system. The total area covered by the 7×4 tactels is approximately $1.8\ cm \times 1\ cm$. To match the sensor area with the display area we decided to use only 9 rows of the sensor (which corresponds to the length covered by the tactels ($1.8\ cm$)). The 9 elements in each column were interpolated to match the 7 tactels in a column on the display. The fitting was done using a general polynomial fit function in LabVIEW. The polynomial fit function finds the polynomial curve values and the set of polynomial fit coefficients, which describe the polynomial curve that best represents the input data set. The following equation gives the general form of the polynomial fit:

$$f_i = \sum_{j=0}^{m} a_j x_i^j \tag{7.1}$$

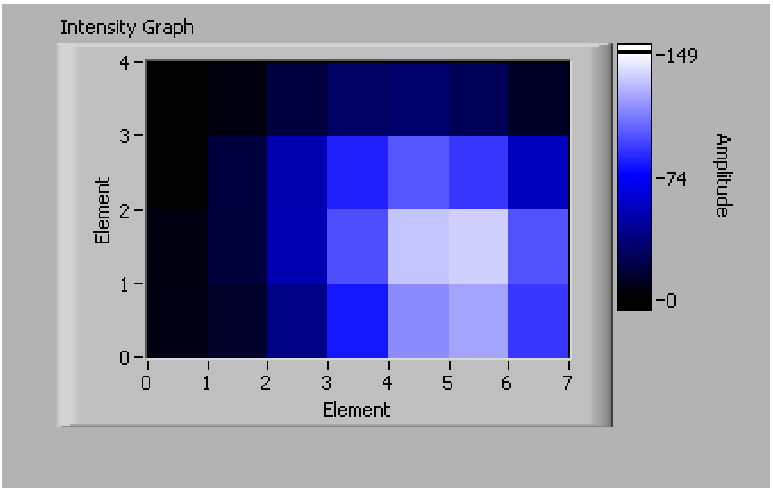

Figure 7.2: Real-time visualization of pressure distribution captured by the TactArray.

where F represents the output sequence best polynomial fit, X represents the input sequence, a represents the polynomial fit coefficients, and m is the polynomial order. The result of the polynomial fit (with order $m = 9$) is shown in Figure 7.3.

7.3 Integrating the System on a Laparoscopic Grasper

When the first ideas for the remote palpation system started to emerge, we decided to focus on making the components small enough to fit onto a conventional laparoscopic grasper. Some might claim that it would be better to make a working prototype first and then go on with the process of making this device smaller. Our decision put many restrictions on our choice of technology, but it also solved some problems since we did not have to concern ourselves with making a prototype of a new grasper. If we were to make our own instrument, we could have faced problems like how to transmit finger motion to sensor motion in a proper way. Additionally, a grasper will provide us with rigid support for the tissue under investigation and ensure full contact between the sensor and the tissue. Another advantage of using a conventional grasper is that if we do not add a significant weight or obstructions to it, we do not introduce additional ergonomic problems. It should be noted that ergonomics is an important research field, because the instruments are not considered to be optimal in their present form, and

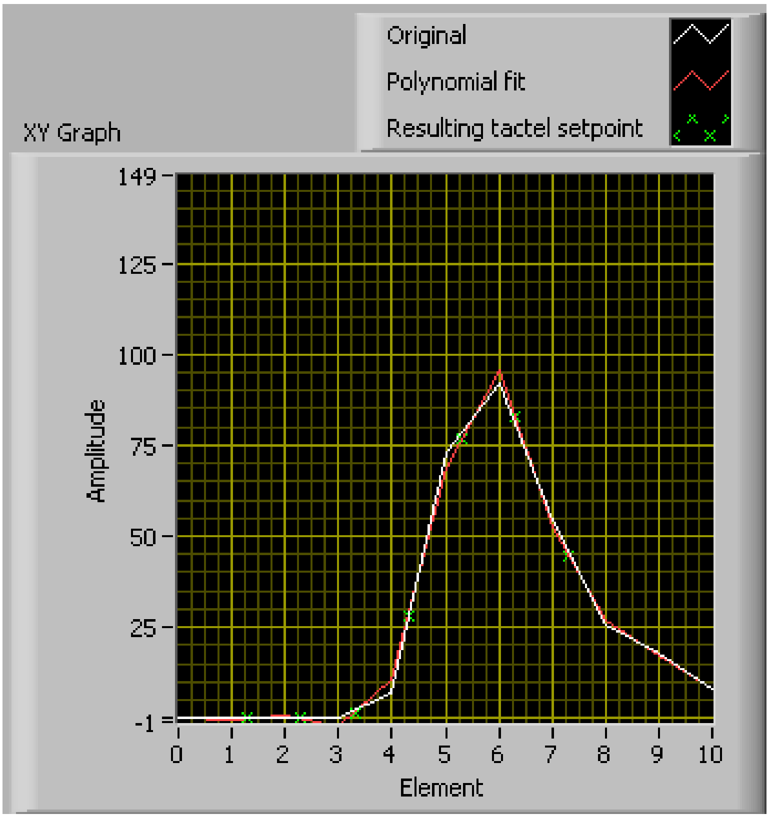

Figure 7.3: Polynomial fit for one column. The original curve shows the output from the 9 sensor elements, while the polynomial fit shows the corresponding interpolated curve rendered by the tactile display.

this is discussed in more detail in (Mårvik et al., 2006). When the choice of using a conventional grasper was made, we also eliminated the possibility for arm-based control of the sensor (for instance probing instead of grasping).

Some of the design parameters, such as spatial resolution, bandwidth and positioning accuracy were discussed in Sections 2.4.1 and 2.5.1. Here some of the challenges related to attaching the components onto a grasper are considered. When designing the sensor array, the two main restrictions were that the sensor area should be equal to the area of one side of the grasper jaws, and that the cabling should not result in a need for making the incisions (trocars) wider (usually $2 - 12$ mm in laparoscopic surgery).

The thickness of the sensor was also important, and we limited this to 2 *mm*. The TactArray system was custom made to an Olympus A6998 grasper and covers the area of the grasper jaw in an optimal way. It is also very thin and does not obstruct grasping. The extra weight of the sensor is barely noticeable when using the grasper. The cables from the sensor are approximately 2 *mm* thick, so when adding this to the shaft, which has a diameter of 10 *mm*, it fits into the largest trocars. The cables are 1.5 *m* long, meaning that the electronics can be placed close to a PC but well away from the surgical area. For the tactile display, the most important design criteria was that it should fit onto the grasper handle, and preferably in a way such that the index finger was used to touch the display. In the handle made by Nesbakken (2004), the thumb is in contact with the display. Since the handle described in Nesbakken (2004) did not contain a working grasper, we chose to attach the custom made TactArray system on a conventional reusable grasper. For this reason, we also attached our display on the same instrument. It would be interesting, however, to test if there is a noticeable difference between the two approaches, both with respect to ergonomics and the fact that the index finger is more frequently used for point-to-point contact with objects than the other fingers are. The measures for the display are described in more detail in Chapter 5.2. The cables from the motors are short (5 *cm*); therefore the motors must be placed close to the driver circuits. The cables are also quite fragile and do not have any chord anchorage, so the driver circuits and display are at present attached on the same rigid surface (see for instance Figure 6.2). Because of this, we also focused on making the driver circuits as light and small as possible (see Chapter 5.2.4 for details). The display and driver circuits mounted on the plate have a total weight of 240 grams (including the plate). The cables from the driver circuit can be made fairly long, so that both the power source and interface to PC can be separated from the surgical area.

7.4 Performance

7.4.1 Shape, Hardness and Size

The easiest way to evaluate the system is to press a known object against the sensor array and look at the response on the display. Since we had a spare sensor mounted on a plate with the same specifications as the one attached to the grasper available, we used this to make the evaluation more straightforward.

The first thing we did was to look at shape. In Figure 7.4 we can see the response of the display when a relatively hard silicone ball, a relatively

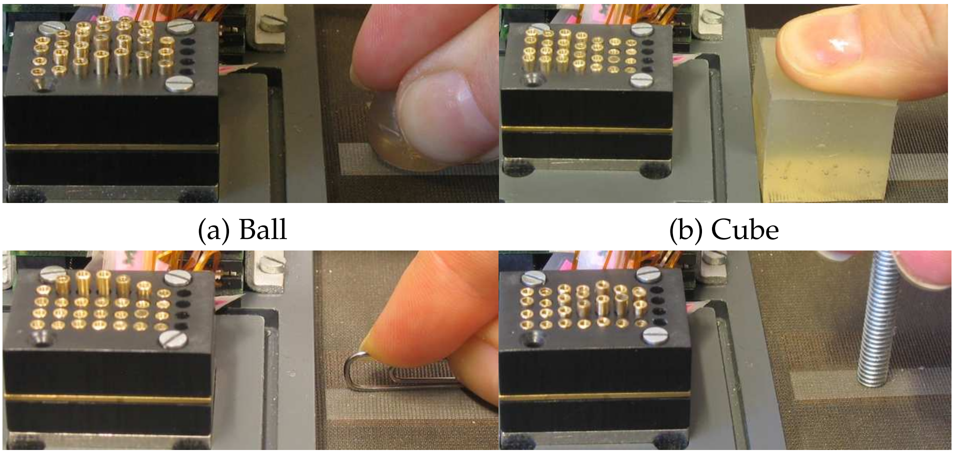

(a) Ball (b) Cube

(c) Paper clip (d) Screw

Figure 7.4: Figure showing the response of the the display when objects with different shapes are pressed against the sensor array.

hard silicone cube, a paper clip and a screw (flat, circular surface), respectively is pressed against the sensor surface.

Figure 7.5 shows how the display conveys information about the hardness of an object. The response for a soft ball is a more flat than for a hard ball, although the forces used were in the same range and the size of the balls (1.5 *cm* in diameter) was the same.

Figure 7.6 shows the response when balls with different sizes are pressed against the sensor array. Note that a small, soft ball has the same signature as a larger hard one, so it is important to keep track of the amount of force the operator applies.

7.4.2 Dynamic Response

To evaluate the dynamic response of the system, we made a setup where a lever arm attached to the shaft of a DC motor pushed on a single sensor element, while a linear potentiometer measured the response of the corresponding tactel on the tactile display. The setup is shown in Figure 7.7.

The DC motor is controlled by using a motor driver and a function generator, such that a signal with known amplitude and frequency can be sent to the motor. This causes the lever arm to push against the sensor, which then generates a position setpoint for one of the tactels. The magnitude of the tactel response can be adjusted in software by changing the gain. As the arm of the potentiometer changes position, the voltage output

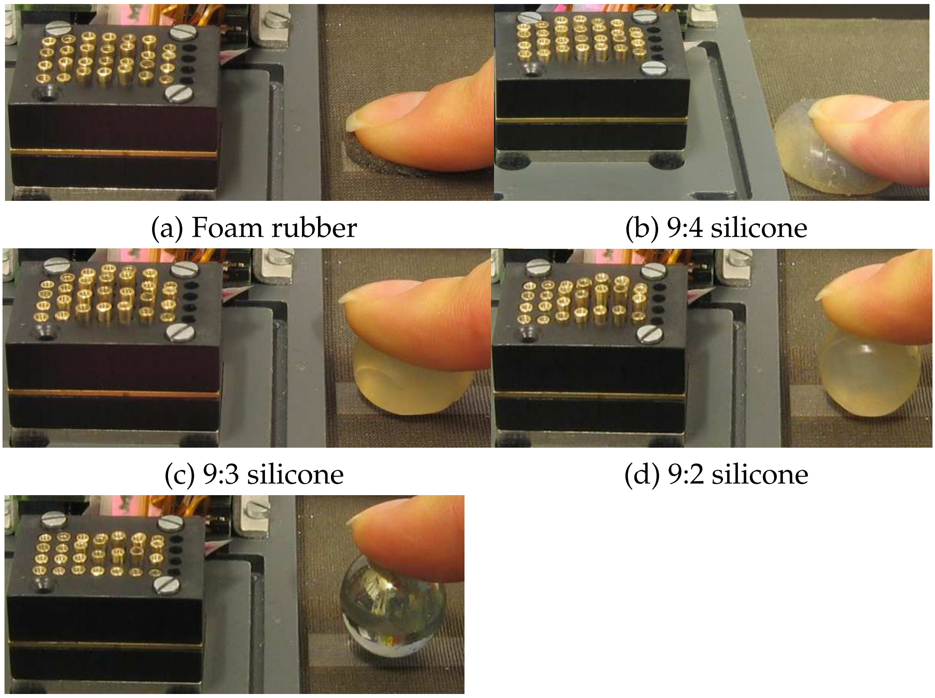

(a) Foam rubber (b) 9:4 silicone

(c) 9:3 silicone (d) 9:2 silicone

(e) Marble

Figure 7.5: Figure showing the response of the the display when silicone balls with varying hardness are pressed against the sensor array. The size, diameter = 1.5 cm, is the same for all balls.

changes proportionally. Figure 7.8 shows the response of both the sensor and the display as the frequency varies from $0.2 - 5$ Hz. Since we had trouble making all tactels run at velocities as high as 4 mm/s, we chose to use a velocity of approximately 3.3 mm/s. Figure 7.9 shows the frequency response with the sensor data as input and the potentiometer data as output (identified with a spectral model and an ARX-model in MATLAB's System Identification Toolbox). As the figure shows, the display follows the desired trajectory for low velocities, but as the frequency is increased towards 1 Hz, the tactel is not able to keep up, and the response is not meaningful.

The sequence of pictures in Figure 7.10 shows the dynamic response of the display when a silicone ball is rolled over the sensor.

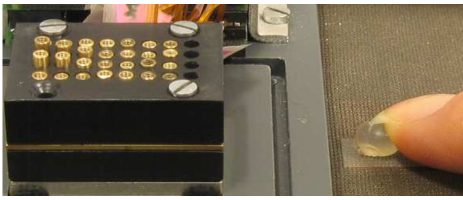

(a) Diameter = 0.5 *cm*

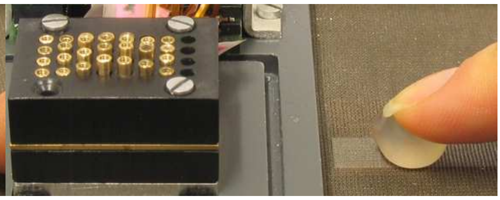

(b) Diameter = 0.9 *cm*

(c) Diameter = 1.3 *cm*

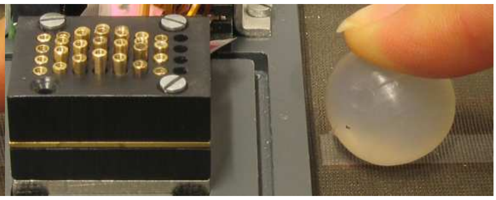

(d) Diameter = 2.4 *cm*

Figure 7.6: Figure showing the response of the the display when silicone balls with varying size are pressed against the sensor array. The hardness is the same for all balls.

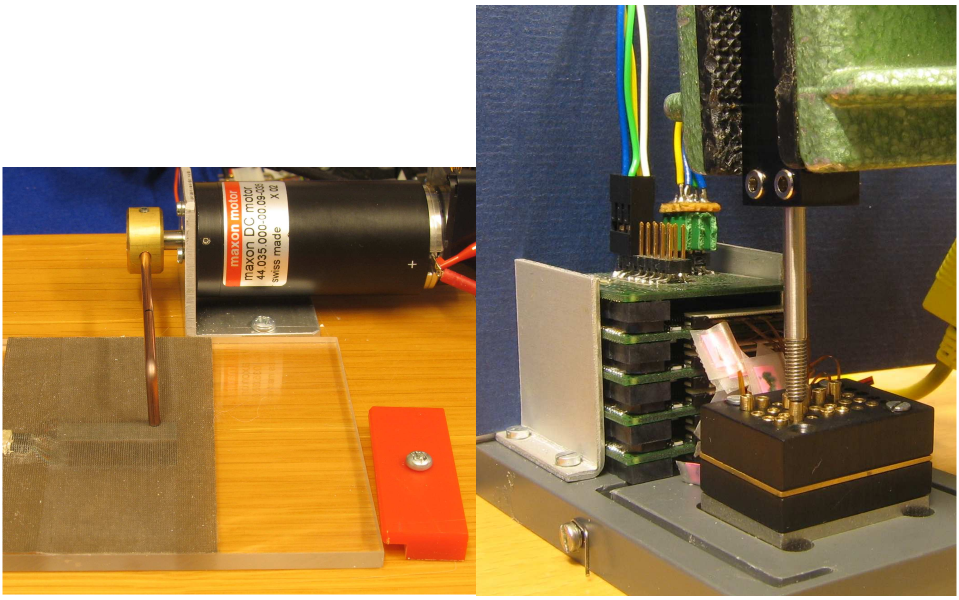

Figure 7.7: Figure showing the setup for dynamic evaluation of the system. The figure on the left shows the DC motor with lever arm pushing on the sensor, while the figure on the right shows the linear potentiometer mounted over the tactile display.

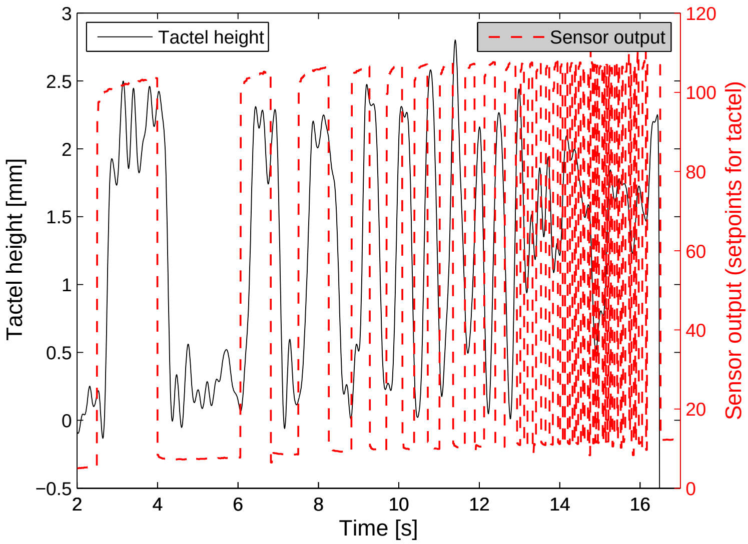

Figure 7.8: Sensor and potentiometer output.

7.5 Psychophysical Evaluation

The experiment described in this section aims at giving a psychophysical evaluation of the remote palpation instrument, and in particular, investigating if the additional information the system provides can contribute to a better understanding of the properties of an object under investigation. Some of the basic ideas from the experiments described in Chapter 4 are used, although the setup is slightly different. The main differences will be the number of test persons, which is reduced to 10, and that experienced surgeons are not used in the experiment. The reason for this is mainly the robustness of the equipment, which needs to be improved before it can be tested extensively. The robustness of the equipment is also why we choose to do the experiments with the tactile display detached from the laparoscopic grasper. If this affects the results, can be investigated in later experiments, but in Peine (1998) it was reported that using two hands did not cause any deterioration in the ability to detect lumps in rubber models. Another difference compared to the experiments in Chapter 4 is that gloved fingers are not considered. The reason for this is that gloved fingers have already proven to be the gold standard for palpation. It is also more interesting for us to see how the remote palpation instrument performs compared to a conventional laparoscopic instrument.

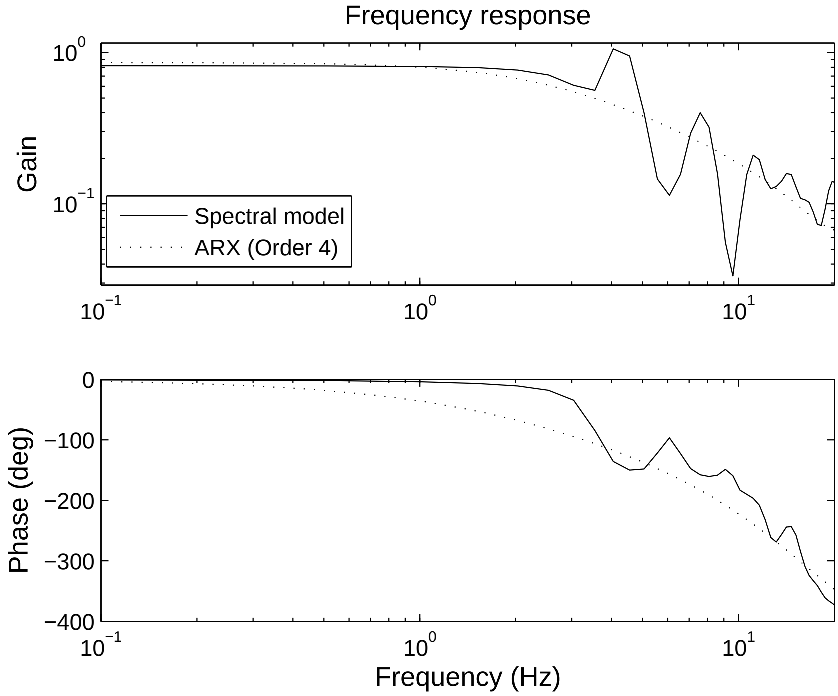

Figure 7.9: Frequency response for sensor input and potentiometer output.

7.5.1 Materials and Method

Equipment

The remote different parts of the palpation instrument used in the experiment is described in detail in Chapters 3.4, 5 and 7.2. As mentioned earlier, the display is not attached to the laparoscopic grasper. The grasper is controlled by the right hand, while the response on the display can be sensed on the left index finger. Note that this prevents the subjects from using a second tool to hold the object under investigation steady, as was often done by the experienced surgeons in the experiment described in Chapter 4. The objects used were the same as those described in Section 4.2.2.

Experimental Design

We are interested in evaluating if the information from a remote palpation instrument is useful for discriminating between objects with varying hard-

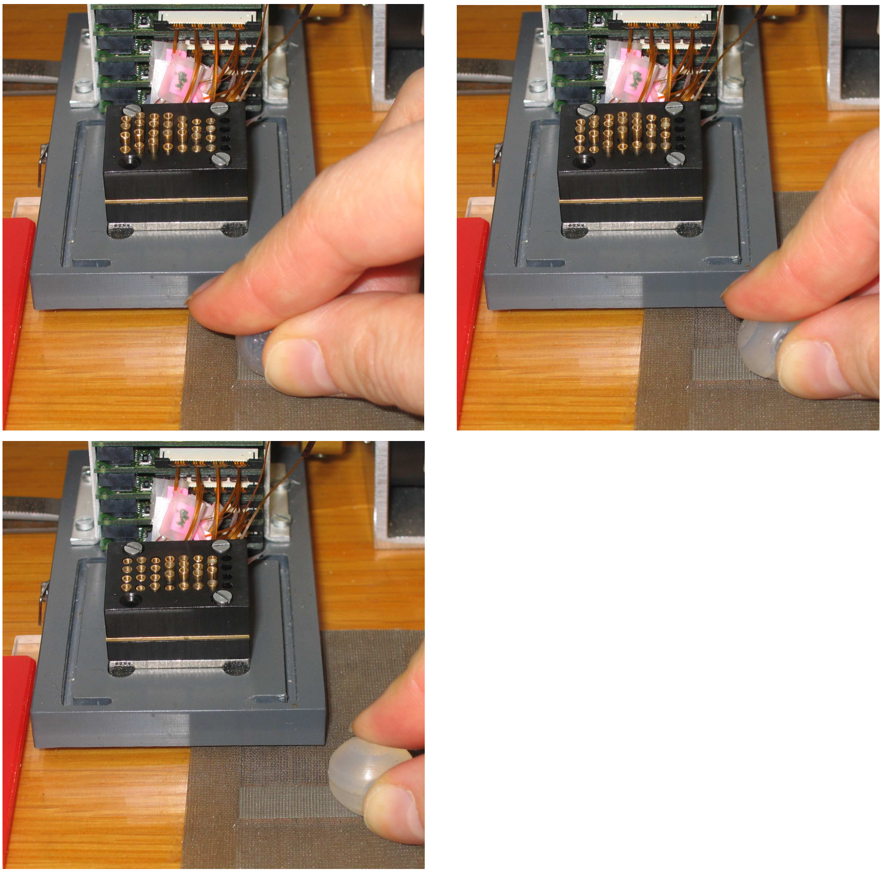

Figure 7.10: Figure showing the response of the the display when a silicone ball with a diameter of 0.9 *cm* is rolled slowly over the display.

ness and size. It is also interesting to find out whether or not the additional technology complicates the tasks.

We chose to reproduce the simulator environment used for minimal invasive training as simply as possible. Figure 7.11 shows the setup. A cardboard box steadily attached to a table was used as a simulator. On top of the box holes were cut. These functioned as trocars and were covered with rubber to make them more flexible. The objects to be identified were hidden in latex finger cots and placed in the cardboard box (Figure 7.12). The latex cots were filled with water and ultrasound gel to replicate the slippery inner workings of intestines and to make sure the objects were completely hidden.

The subjects were given visual feedback by using a digital video cam-

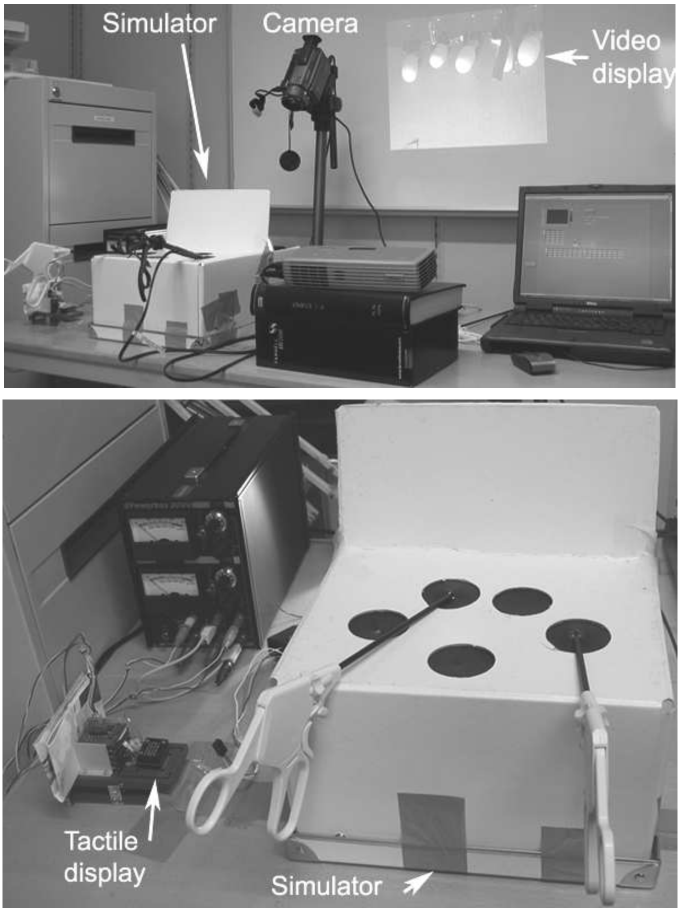

Figure 7.11: The figure shows the full setup of the experiment and a close up view of the laparoscopic simulator.

era placed behind the cardboard box. The back of the box was cut open and illuminated. In this way, the live video from inside the box could be sent to a projector. As the video was taken from behind, the projector was turned upside down to provide the subjects with the right view of the objects. Note that for the first 3 subjects, the image from the projector was mirrored instead of upside down, and this complicated the handling of the instruments slightly.

For the first experiment, 5 objects with different hardness were presented to the subject. The subject was asked to rank the 5 balls from softest to hardest using the laparoscopic instrument with tactile feedback (LIT) or

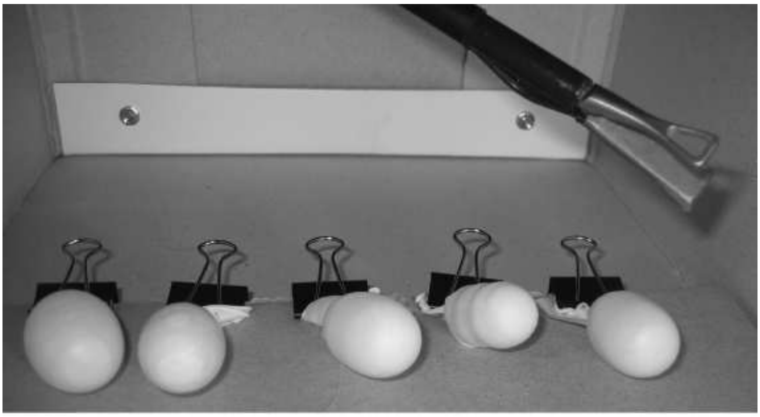

Figure 7.12: Objects hidden in latex finger cots inside the laparoscopic simulator. The objects inside the cots are the same as in Figure 4.2.

a conventional laparoscopic grasper (LI). The conventional laparoscopic instrument was an Endo clinh II (5 *mm*). The subjects were allowed to feel the different samples as many times as necessary. After ranking the 5 samples, the process was repeated (with the same instrument) for a total of 5 trials. In order to prevent memorization, each trial was repeated with random ordering of the samples. After completion of the 5 trials with the given instrument, the subject moved on to the second instrument and repeated the ranking procedure described above.

The second experiment used the same method as the first, but here the task was to rank 5 silicone balls from smallest to largest. Which instrument to start with was randomized.

Although we conducted two separate experiments, one with focus on hardness and one with focus on size, the subjects performed both at the same time, meaning that they performed all trials for either hardness or size first and after a short break proceeded directly to the next. The order of the two experiments was randomized between subjects.

The subjects were encouraged to talk during all trials and tell what they felt and saw. All subjects were given a short presentation of both instruments prior to the experiments. They were also informed about the scope of the experiments, how the tests would be conducted and asked to complete two questionnaires. The subjects were not allowed to see the objects before or during the experiments.

Test persons

Ten persons, 4 females and 6 males, participated in the study. The subjects were from 27 to 51 years old, with an average of 31.1 years. All subjects had dominant right hand, and none of the subjects had any previous experience with laparoscopic surgery. Surgeons familiar with laparoscopic surgery were not used in the study, since this would mean moving the equipment to a hospital, where the possibilities for fixing possible breakdowns would be limited. As mentioned earlier, a study with experienced surgeons will be useful when the equipment is more robust and attached to the grasper handle. In this way the working procedure of the surgeon will not be considerably altered.

Data Collection

Altogether each subject had 20 different tasks to complete, 10 trials with respect to both hardness and size. In each trial the subject ranked the balls from 1 to 5 using the remote palpation instrument or the conventional laparoscopic grasper, with 1 being the softest or smallest and 5 being the hardest or biggest. In the same way as in Chapter 4, the data was not characterized as "true" or "false" but by the size of the error. We used only 10 subjects, but since the experiments involved repeated trials (5 for each instrument), we had a total of 100 trials for both hardness and size. On such a small data set we cannot assume normality, so nonparametric statistics, and more specifically a method based on Wilcoxon two-sample test, was used to analyze the data (see Appendix B).

7.5.2 Results

In Figure 7.13 the average and standard deviation of the error for each instrument for both hardness and size is shown. The magnitude of the error in each case is considered, so a value 4 silicone ball ranked as a value 2, results in an error with an absolute value of 2. As can be seen in the figure, the laparoscopic instrument with sensor resulted in an average error per trial of 0.3, while the conventional laparoscopic instrument led to an average error of 0.5. The difference is more pronounced in the size case, where LIT has an average error of 0.96 versus 2.14 for LI.

In a post test questionnaire, the subjects were asked to rate their own performance and comment on the setup. All subjects felt that the level of difficulty of the tasks was quite right, although they struggled more with discriminating size than hardness. Only 2 of the subjects found the extra source of information provided by the tactile display distracting. In

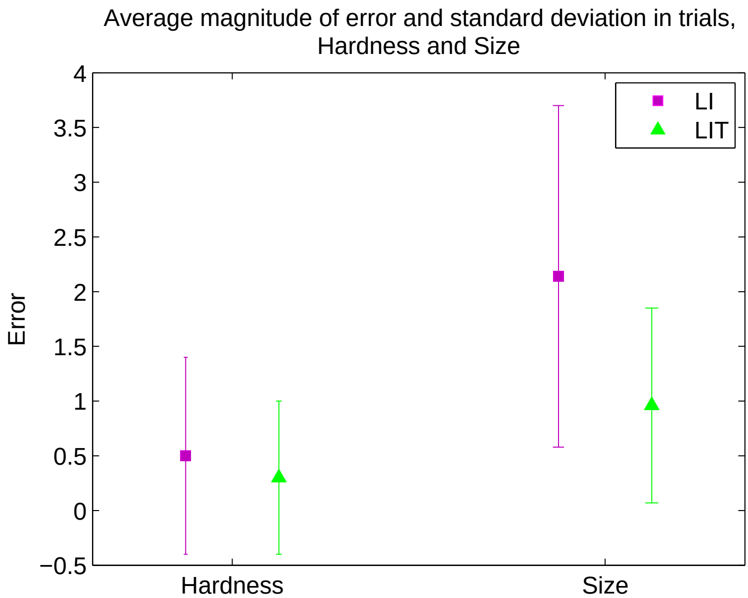

Figure 7.13: Plot showing average magnitude and standard deviation of the error for each instrument (LI and LIT) for both hardness and size, respectively.

fact, some of the subjects who started the experiment with LIT instinctively touched the tactile display when using LI as well because they missed the extra sense. Four of the subjects did not think that there was any difference in the amount of forces they applied to the grasper for the two instruments (LI and LIT), while 5 of the subject thought they used more force when using LIT.

After the first 6 subjects, we realized that the difference between the instruments was quite noticeable in the size case, and we wanted to assess if this could have anything to do with the size of the end effector or the quality of the instrument (the conventional grasper was disposable, while the grasper used for the remote palpation instrument is reusable). Figure 7.14 shows a comparison of the end effectors of LI and LIT, respectively. The reason why we chose different instruments was that we wanted to compare our equipment (LIT) with the conventional grasper the surgeons use most frequently. To check if our concerns about the size and quality of the end effector had influence on our results, we decided to have the last 4 subjects perform the tasks with the same grasper (LIT), but with and without the sensor array/tactile display running. The analysis in the size case takes this into consideration.

Figure 7.14: Figure showing the end effectors of LIT at the top and a conventional laparoscopic grasper (LI) at the bottom.

Hardness Discrimination

Hypothesis H_0: When discriminating between balls with varying hardness, a conventional laparoscopic instrument and a laparoscopic instrument with tactile feedback perform equally well, i.e. LI=LIT.

In Appendix B, the details on testing H_0: $WHLI = WHLIT$ against the alternative that $WHLI > WHLIT$ (where WHLI and WHLIT are the rank sums for LI and LIT, respectively) are presented. The test results showed that (with a 0.05 level of significance) $z_{WHLI} = 0.41 < 1.65 = z_{0.05}$, meaning that we do not reject H_0 and conclude that LIT is not significantly better than LI for hardness.

Figure 7.15 shows the errors done by each individual subject in the hardness case. As can be seen from the figure, the error for LIT is larger than LI for only one of the subjects. In all other cases, LIT performs better or equally well. Subject 8 did a lot of errors with LI compared to the others, and 3 subjects made no errors with neither of the instruments.

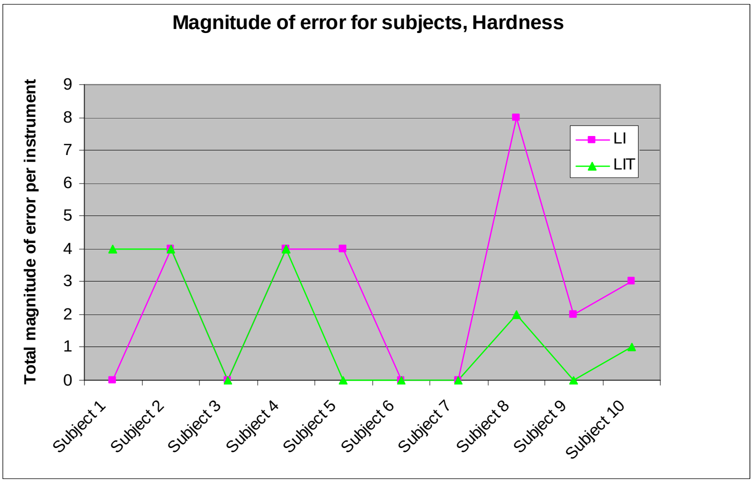

Figure 7.15: Magnitude of total error for each subject in the hardness case.

Since the balls used in the experiment ranged in hardness from glass to foam rubber, we tried to identify if some of the balls were easier to rank than others. This was done by recording how often an incorrect ranking was given for each object (1-5) for the different instruments. Figure 7.16 shows that very few errors were done with the softest ball and that LIT seemed to be useful for identifying the hardest and second hardest ball compared to LI. The second softest ball seemed to be easier to identify with LI than LIT.

Forty errors out of 500 possible were made in the hardness case, and all of them had magnitude 1, meaning that the subjects characterized for instance a hardness 1 as a hardness 2.

Table 7.1 shows the average time consumed to rank 5 objects for each instrument in the hardness case.

When rating their own performance for the hardness discrimination, 4 of the subjects felt they performed better with LIT than LI, while 4 subjects thought they performed equally well with the two instruments.

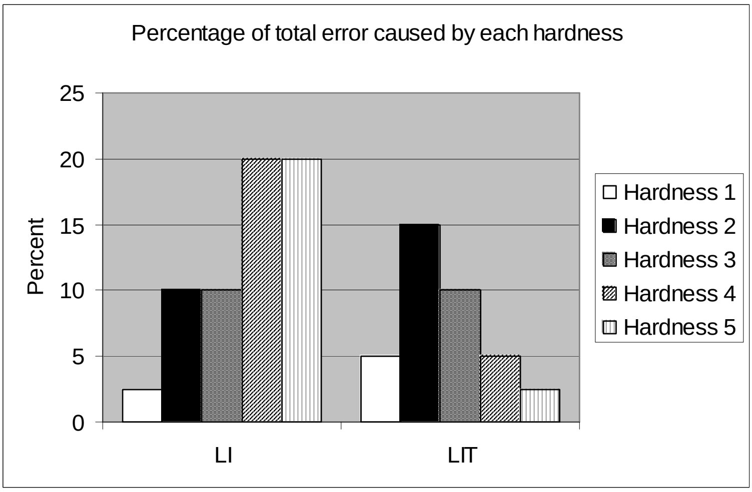

Figure 7.16: Plot showing the distribution of errors for each hardness.

Table 7.1: Average time consumption, hardness.

Instrument	Average time [s]
LI	130
LIT	181

Size Discrimination

Hypothesis H_0: When discriminating between balls with varying size, a conventional laparoscopic instrument and a laparoscopic instrument with tactile feedback perform equally well, i.e. LI=LIT.

In the same way as for hardness, we tested H_0: $WSLI = WSLIT$ against the alternative that $WSLI > WSLIT$. The results showed that $z_{WSLI} = 1.86 > 1.65 = z_{0.05}$, meaning that we can reject H_0 and conclude that LIT is significantly better than LI for size discrimination. In fact $P_{WSLI} = P(z > 1.86) = 0.0307$, which means that we can reject H_0 at a level of significance of approximately 0.03.

When considering only the last 4 persons (with a total of 20 trials), the analysis showed that $z_{WSLI4} = 0.66 < 1.65 = z_{0.05}$, meaning that we cannot reject H_0 in this case (see Appendix B for details on the calculations).

The errors done by the individual subjects in the size case are shown in Figure 7.17. The first 6 subjects made more errors than the last 4, indicating that the size of the end effector or the quality of the grasper seem to affect the results. Despite this, all subjects except number 7 performed better with LIT than LI.

In the same way as for hardness, the subjects made more mistakes with some of the objects. This is summarized in Figure 7.18, and we can see that 57% of the errors were made when trying to identify size 1. LIT seemed to improve the performance when identifying sizes 2, 3 and 4. Note that of the 75 errors done with the smallest ball (size 1), 81% were caused by the fact that the subjects could not find the ball at all.

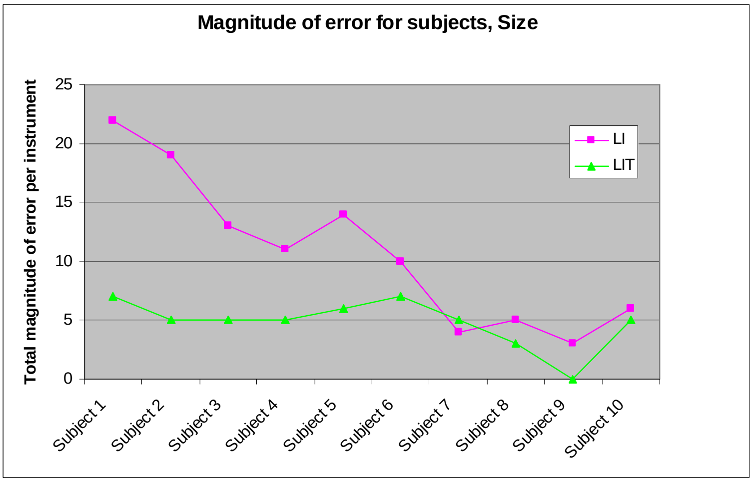

Figure 7.17: Magnitude of total error for each subject in the size case.

Of the 131 errors done in the size case, 108 of them had magnitude 1, 22 had magnitude 2 and 1 had magnitude 3.

Table 7.2 shows the average time consumed to rank 5 objects for each instrument in the size case.

In the rating of their own performance, only 2 of the subjects felt that they did fewer errors with LIT than LI, while 3 felt they performed equally well with the instruments. Consequently, the remaining five subjects felt they performed better with LI than LIT.

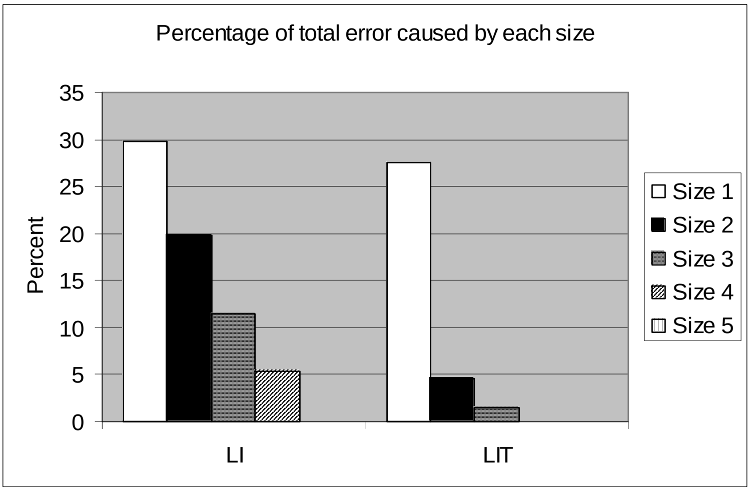

Figure 7.18: Plot showing the distribution of errors for each size.

Table 7.2: Average time consumption, size.

Instrument	Average time [s]
LI	347
LIT	388

7.6 Discussion

7.6.1 Performance

The remote palpation instrument was first evaluated by conducting some simple tests related to representation of shape, hardness and size.

When different shapes were pushed against the sensor array they were successfully rendered by the tactile display. The results were, however, dependent on the fact that the pressure was larger in the middle for all objects. Therefore, the response became somewhat graded towards the edges for objects with sharp edges. Another reason for this is that the lack of resolution results in aliasing, and hence information about sharp edges is not correctly represented. The grading is not as prominent with the cube as with the ball though, so a difference can be observed between these objects. Note that in the case of laparoscopic surgery, the ability to represent sharp edges is not so important since the interior of the body is mostly comprised of soft, rounded objects. Figure 7.4d illustrates that there is some crosstalk between the elements of the array since the area rendered on the tactile display seems to be somewhat larger than the actual area of the screw. This is probably due to the protective sheath around the sensor (which allows for safe disinfection of the device).

As far as size is concerned, the system was able to represent this in a good way, but the lack of resolution makes it difficult to differentiate between objects that are almost the same size.

Hardness can also be represented, but in the example shown here it should be noted that all the objects had the same size. This will not always be the case, and it may be necessary to provide additional information about the size of an object or the maximum pressure and total force applied to the sensor in order to make it useful for the surgeon.

The dynamic testing confirmed the findings about the limited bandwidth discussed in Chapter 5, so for high frequencies the response on the display becomes useless.

7.6.2 Psychophysical Evaluation

In Chapter 4.4, we suggested that it would be interesting to conduct the same experiments again when the tactile information could be presented to the finger and not via sensory substitution. The experiments in this chapter focused on investigating this in more detail. The study showed that the laparoscopic instrument with tactile feedback (LIT) was not significantly better than a conventional grasper in the hardness case (with a 95% confidence interval). In the size case, however, the hypothesis, H_0, that a conventional laparoscopic instrument and a laparoscopic instrument with tactile feedback would perform equally well, i.e. LI=LIT, was rejected when all 10 subjects were taken into consideration. The last 4 subjects used the same grasper during the whole experiment, but in half of the cases the tactile sensor and the tactile display were deliberately switched off. In comparison, the first 6 subjects used a grasper with a smaller end effector for the trials with LI. The analysis for only the last 4 subjects in the size case showed that the hypothesis,H_0, could not be rejected. Analysis of the 20 trials the last 4 subjects performed is obviously insufficient to reach a statistically significant conclusion, so the element of uncertainty must be taken into consideration. The results do, however, indicate that a larger end effector can be useful when a grasping technique is used in the search for irregularities in the tissue. Experienced surgeons often use a poking technique when estimating the size of objects, but as the results in Chapter 4 showed, they had trouble locating the two smallest sizes with this technique. It is possible that a larger grasper helps in these cases, since a larger portion of the tissue can be investigated at the same time. Another observation related to this is that although the instrument with sensor (LIT) had a smooth surface, while the grasper used by the first 6 subjects had a toothed surface, the smallest objects were more easily identified with LIT. This could be due to the size of the end effector, or it can imply that we actually detect very small objects in the exact moment they slip.

In the hardness case, the average and standard deviation of the error for LIT is slightly smaller than for LI. In the size case the standard deviation and average are considerably higher for LI than LIT, meaning that in the size case, the subjects performed better and with less variably with LIT than LI.

On the question about difficulty of the task, most subjects meant that it was appropriate, although some felt that it could have been easier for size and maybe more difficult for hardness. This also corresponds with the results, since the subjects made very few errors in the hardness case compared to the size case (40 versus 131).

Only 2 of the 10 subjects felt that it was distracting with the extra source of information provided by the tactile display. Both of them meant that more practice would help, since they sometimes found that it was difficult to interpret the response on the display. A couple of times the subjects also experienced that a tactel was stuck, and in these cases they reported that the information was confusing. The fact that the tactile display gave a response both when an object was found and when the water inside the finger cots were squeezed, caused some uncertainties. It is possible that a baseline subtraction to remove sensations when normal, homogeneous parts of the finger cots (water) are palpated could be useful.

In general, there was a high threshold for learning how to maneuver the instruments, but this seemed to affect the time spent on discrimination more than the error rate. The results for each individual subject show that the ability to discriminate the objects varied considerably, and this could be due to either thoroughness or the ability to control the instruments.

In the size case, the subjects did a lot of mistakes with the smallest ball, and in most cases they could not find the ball at all. The experiments suggest that our remote palpation instrument helps for discriminating between sizes. Despite this, the smallest ball was still difficult to find, meaning that there are considerable possibilities for improvements.

The average time for a trial in the hardness case was a lot lower than in the size case. In the hardness case, the difference between LI and LIT was around 30 seconds. This could be due to the fact that the subjects spend time correlating the information from the display with the haptic/tactile feedback from the grasper and the visual feedback from the camera. The increased average time for size is probably due to the time spent searching for the smallest balls. The average time decreased somewhat after the third subject because the view from the camera was changed, and this made the movements inside the simulator more intuitive.

In the rating of their own performance, the subjects often rated the instrument used last higher than the one used first, and this is not surprising keeping in mind that it requires some training to maneuver the instruments.

In Chapter 4, we found that the instrument with visual presentation of the tactile image (LIS) was most useful for hardness. In the experiment in this chapter, on the other hand, it seems that the laparoscopic instrument with tactile feedback (LIT) is most useful for size. Although the two experiments are not entirely comparable (since we exchanged the intestines with finger cots for the last experiment as well as the user profile of the subjects), this is somewhat surprising. Replacing the intestines with finger cots changed the surface of the objects from slippery (intestines) to more sticky (finger cots). This has impact on the technique used to identify the objects, since the sticky surface prevents the subjects from sliding the grasper along the surface and thereby corner the object under investigation. The change in user profile of the subjects should not be of too much concern when comparing the experiments since the results for the unexperienced subjects used in the study in Chapter 4 were comparable with the results of the experienced surgeons. The techniques used by both the unexperienced surgeons in Chapter 4 and the subjects in this experiment were more or less the same. Nevertheless, the results indicate that a combination of visual presentation of the tactile information and tactile feedback to the finger could be useful for the surgeon.

The subjects were invited to give subjective comments about the instruments and the experiment in general. Most of the subjects who found LIT better than LI felt that it was most useful in the size case. Only one of the subjects reported that he felt it was more useful for hardness. One of the persons also felt that it was easier to trust his own answers when LIT was used, and that it could confirm that he had a good grip of the object. Another observation was that the subjects did not find that the tactile display was too slow, since in most cases the actual palpation task was slower than the response on the display. All subject agreed that more training could have been useful.

In conclusion, LIT seem to work better than LI for palpation in the size case, but for hardness there was no significant difference.

Part V

Concluding Remarks

Chapter 8

Conclusions

8.1 Part II - Tactile Sensing

In Chapter 3, the design of a tactile sensor array based on piezoelectricity was described. The force range for the array was good and the size satisfactory for laparoscopic surgery. Piezoelectric material is also quite cheap, which makes the sensor array affordable. By amplifying frequencies close to DC response, low frequency signals could also be represented. We did, however, experience problems with crosstalk, resulting in reduced ability to differentiate between small objects and relatively large objects. Chapter 3 also presented the custom made TactArray system. The system has good sensitivity, an acceptable size and can be disinfected. Despite this, distinguishing objects with small variations in size is sometimes hard and the system is also quite expensive. Additionally, the electronics that come with the system is somewhat bulky, at least compared to the electronics made for the piezoelectric sensor array.

In Chapter 4, an experiment aiming at comparing palpation with gloved fingers, conventional laparoscopic instruments and an instrument with visual feedback of tactile information was described. The experiment considered both hardness and size, and it was found that gloved fingers were better than both the other two instruments for palpation. Despite this, a visual feedback of the tactile image seemed to be useful for the subjects who fully understood how to interpret the information, especially for hardness discrimination. It is quite surprising that the sensor worked well for hardness since it is presented as a shape and not as a compliant object. This indicates that humans are able to translate shape information into information about hardness in a useful way. It should be kept in mind, though, that in all the discrimination tasks for hardness, the objects had the same size.

In a real laparoscopic surgery, this will usually not be the case. It is not clear how crucial this information is, since the surgeon does receive some tactile and haptic cues related to the size of the object through the handle (given that the laparoscopic instrument does not have a relieve spring). Using active palpation (for instance by sliding back and forth over the object) will also provide the surgeon with information about the size. Frequently, the surgeons use the length of the end effector to measure the size of objects inside the body (given that the object is not hidden from view). This measure gives an estimate of the size, especially relative to other adjacent tissues or objects. If more accurate information about size is needed, measurements of the angle between the jaws of the end effector can be implemented by using a position sensor either on the handle or closer to the end effector (depending on the requirements for accuracy).

As mentioned in Chapter 4, it is debatable if the brain is able to translate visual images into meaningful tactile impressions fast enough for it to contribute to the surgeon's tactile understanding of the object under investigation. Sensory substitution is a mature research area, e.g. in the world of prosthetics, and in this field it was long assumed that the human mind has great powers of adaption that enables it to replace afferent signals by user's vision or other senses. For amputees, however, this assumption will often influence the ability to focus on other tasks, for instance indulging in intellectual activity at any but the trivial level (Simpson, 1973). At present, the concept of extended physiological proprioception (E.P.P.) introduced by David Simpson is considered to be more effective. In E.P.P. a control system is constructed such that the movement at a joint in for instance an artificial arm is made to correspond to the movement of, for example, one of the joints in the shoulder girdle. The information from the natural joint that corresponds to the angle of the appropriate joint in an artificial arm will then be sent to the central nervous system (Simpson, 1974). This concept has proved to reduce learning time significantly, and the findings are in accordance with our assumptions that a remote palpation instrument should put focus on feeding back the tactile sense rather than providing sensory substitution.

In Chapter 7, we touched on the problem that 2 different graspers were used in the LI and LIT case, and that the size or quality of the grasper probably affected the results. The same is the case for the experiments in Chapter 4. Therefore, it should be kept in mind that any improved results of LIS compared to LI could be due to both the visual presentation of the tactile image and the size or quality of the grasper.

8.1.1 Suggestions for Future Work

For the piezoelectric sensor array, the thickness could have been somewhat reduced. The spacing between the sensing elements can also possibly be made smaller by routing the cables differently, but most importantly, better channel separation has to be obtained. As mentioned in Chapter 3.2.4, this could be done by modeling the system more accurately and use the inverse model to find an appropriate filter to compensate for the dead zone included (to be able to display major changes between samples only). For the TactArray system, the main improvements would include increasing the resolution and reducing the size of the electronics package. To make the sensor array as sensitive as the human finger pad will be the ultimate goal for the future.

The experiments in Chapter 4 indicated that it could have been useful to give the subjects a training period with the new equipment before conducting the tests. A follow-up study to verify this will be important in the future. It would also be of interest to compare LI and LIS in more detail by using the same grasper for both LI and LIS, but with and without visual presentation of the tactile image.

8.2 Part III - Tactile Display

Chapter 5 gave a detailed description of a tactile display and its accompanying driver circuits. The tactile shape display consists of 32 small DC motors in a 4-by-8 array, with a center to center spacing of 2.7 mm. A key feature of the display was the size, which was restricted to 27 $mm \times$ 20 $mm \times$ 18 mm. Performance studies of the display revealed that a typical tactel could provide an active force of $0.4 - 0.5$ N at a frequency of close to 0.7 Hz at full excursion (3 mm). Additionally, the testing showed that the positioning resolution was approximately 0.04 mm, and that the stiffness was close to 50 N/mm. The chapter also considered some issues related to friction in tactile shape displays, and concluded that as much as 90% of the torque was lost due to friction. The estimate of friction found for the device will make it easier to construct similar devices in the future. The main limitations for the display are the restricted bandwidth and lack of robustness, but the size, weight, stiffness and positioning resolution are all properties that should be maintained in later versions. The small driver circuits work well and can be reused in future versions.

In Chapter 6, we hypothesized that the shape and size of the pins greatly affects the way information is rendered on a tactile display. Therefore, we conducted a psychophysical experiment to examine the perception of a line stimulus (sine, square or sawtooth wave) using 3 different pin shapes. Surprisingly, we found that there was no significant variation in perception with the different pin shapes investigated. The subjects even had trouble recognizing the signal shapes.

8.2.1 Suggestions for Future Work

Future work for the tactile display should focus on increasing the bandwidth of the display as well as making it more robust. Better lubrication, polished screws and using more optimal materials such as Teflon are all important factors to consider to be able to reduce the friction. Replacing the motors with faster and stronger motors would also be crucial. The motors are in fact the most vulnerable part of the system. The gears are only encapsulated in plastic, meaning that external force on the gear head, in either direction, would most likely destroy the gears. The mechanism for translating rotational motion to linear motion is also quite fragile. This can be exchanged by a commercially available system, such as the linear actuator 03A S3 in combination with the DC servomotor 0308 from Faulhaber. These actuators are somewhat larger than our tactel mechanism (3.4 mm), and the fastest variant can provide a speed of 2mm/s and a 0.47 mNm torque. The performance of the actuators have to be improved to make the system better with respect to bandwidth and torque, but it would be useful for increased robustness and reliability. Another possible improvement is to include position feedback in the system to allow for more accurate control of position.

For the experiment described in Chapter 6, it would be interesting to investigate the results in more detail by changing the classification task. Adding more than 1 column of tactels and the traditional spatial low pass filter could also give other results. Performing an experiment using the ”dual task paradigm” (where the subjects perform an unrelated task at the same time as the actual task to check the complexity of the task) could also be useful. Last but not least, focus could be put on how we can give the user the illusion that he is feeling a specific shape instead of reproducing the exact shape.

8.3 Part IV - Tactile Feedback

Chapter 7 described the communication between the tactile sensor array and the tactile display, as well as experiments for evaluating the performance of the system, both from a technical and psychophysical perspective.

A few simple experiments where different objects (with varying shape, hardness and size) were pressed against the display gave indications of the static performance. The rendering of objects with sharp edges was sometimes difficult due to the limited resolution of the display. For both size and hardness, the display rendered the objects satisfactory. The dynamic performance was investigated by pushing a lever arm against the array at increasing frequencies and in this case the performance suffered from the low bandwidth. When rolling an object slowly over the sensor array we saw that the signal was correctly rendered by the display, meaning that it can be useful for slow or static palpation tasks.

Finally, the performance of the remote palpation system was tested in a psychophysical experiment. The hypothesis was that a laparoscopic instrument with tactile feedback and a conventional laparoscopic grasper perform equally well for ranking objects with varying hardness and size. We found that the instrument with tactile feedback seemed to work better than conventional instruments for palpation in the size case, but for hardness there was no significant difference.

8.3.1 Suggestions for Future Work

Future work for the full remote palpation instrument includes conducting experiments with the tactile display attached to the grasper to check how this influences the results. Attaching the display to the grasper will enable the surgeon to use the same finger he is using to feel the tactile display in the actual grasping movement. This means that he will get the stimuli from the tactile display simultaneously as the haptic feedback already present in the grasper. This could allow for a more active palpation technique, and hence increase the usefulness of the tactile display. Testing with different tactel shapes and other spatial low pass filters will also be of interest. More importantly, experienced surgeons should be included in the experiments as soon as the system is sufficiently mechanically stable.

In the experiments in Chapters 4 and 7, we concluded that visual feedback of the tactile image was more useful for hardness, while tactile feedback was more useful for size discrimination. Future versions of such systems could include both sources of information, but to avoid confusion, the visual feedback should be merged on top of the camera image already presented to the surgeon, and the tactile display should be attached to the grasper. Another possibility for providing information about hardness is to use vibratory coding.

Bibliography

Begos, D. G. and Modlin, I. M.: 1994, Laparoscopic cholecystectomy: From gimmick to gold standard., *Journal of Clinical Gastroenterology* **19**(4), 325–330.

Berggren, U., Zathraeus, N., Arvidsson, D., Haglund, U. and Jonsson, B.: 1996, A cost-minimization analysis of laparoscopic cholecystectomy versus open cholecystectomy, *The American Journal of Surgery* **172**(4), 305–310.

Bholat, O. S., Haluck, R. S., Murray, W. B., Gorman, P. J. and Krummel, T. M.: 1999, Tactile feedback is present during minimally invasive surgery, *Journal of the American College of Surgeons* **189**(4), 349–355.

Bicchi, A., Canepa, G., Rossi, D. D., Iacconi, P. and Scilingo, E. P.: 1996, A sensorized minimally invasive surgery tool for detecting tissutal elastic properties, *Proceedings of the IEEE International Conference on Robotics and Automation*, Minneapolis, MN, pp. 884–888.

Blomqvist, A. M. K., Lönroth, H., Dalenbäck, J. and Lundell, L.: 1998, Laparoscopic or open fundoplication? A complete cost analysis, *Surgical Endoscopy* **12**(10), 1209–1212.

Boff, K. R., Kaufman, L. and Thomas, J. P. (eds): 1986, *Handbook of perception and human performance*, Wiley, chapter 11, by Sherrick and Cholewiak, pp. III–3 – III–7.

Box, G. E. P., Hunter, J. S. and Hunter, W. G.: 2005, *Statistics for experimenters*, John Wiley & Sons.

Broeders, I. A. M. J. and Ruurda, J. P.: 2002, Robotics in laparoscopic surgery: Current status and future perspectives, *Scandinavian Journal of Gastroenterology. Supplement.* (236), 76–80.

Buanes, T., Mjaaland, O., Waage, A., Solheim, K. and Færden, A.: 1995, The Norwegian national cholecystectomy registry. Practical quality assurance, *Tidsskrift for Den norske lægeforening* **115**(18), 2236–2239.

Caldwell, D. G., Tsagarakis, N. and Giesler, C.: 1999, An integrated tactile/shear feedback array for stimulation of finger mechanoreceptor, *Proceedings of the IEEE International Conference on Robotics and Automation*, Detroit, MI, pp. 287–292.

Cueto-García, J., Jacobs, M. and Gagner, M.: 2003, *Laparoscopic Surgery*, McGraw-Hill.

Cutkosky, M. R. and Howe, R. D.: 1990, Human grasp choice and robotic grasp analysis, *in* S. T. Venkataraman and T. Iberall (eds), *Dexterous Robot Hands*, Springer-Verlag, New York.

Dargahi, J. and Najarian, S.: 2004, Theoretical and experimental analysis of a piezoelectric tactile sensor for use in endoscopic surgery, *Sensor Review* **24**(1), 74–83.

Dargahi, J., Parameswaran, M. and Payandeh, S.: 2000, A micromachined piezoelectric tactile sensor for an endoscopic grasper - Theory, fabrication and experiments, *Journal of Microelectromechanical Systems* **9**(3), 329–335.

Darzi, S. A. and Munz, Y.: 2004, The impact of minimally invasive surgical techniques, *Annual Review of Medicine* **55**, 223–237.

den Boer, K. T., Herder, J. L., Sjoerdsma, W., Meijer, D. W., Gouma, D. J. and Stassen, H. G.: 1999, Sensitivity of laparoscopic dissectors, *Surgical Endoscopy* **13**, 869–873.

Egeland, O. and Gravdahl, J. T.: 2002, *Modeling and Simulation for Automatic Control*, Marine Cybernetics, Trondheim, Norway.

Eltaib, M. E. H. and Hewit, J. R.: 2003, Tactile sensing technology for minimal access surgery - A review, *Mechatronics* **13**, 1163–1177.

Engel, J., Chen, J. and Liu, C.: 2003, Development of polyimide flexible tactile sensor skin, *Journal of Micromechanics and Microengineering* **13**, 359–366.

Fischer, H., Trapp, R., Schuele, L. and Hoffmann, B.: 1997, Actuator array for use in minimally invasive surgery, *Journal de Physique IV (Colloque)* **7**, 609–614.

Frisken-Gibson, S. F., Bach-y-Rita, P., Tompkins, W. J. and Webster, J. G.: 1987, A 64-solenoid, four-level fingertip search display for the blind, *IEEE Transactions on Biomedical Engineering* **BME-34**, 963–965.

Fritschi, M., Buss, M., Drewing, K., Zopf, R. and Ernst, M. O.: 2004, Tactile feedback systems, Touch and Haptics Workshop at IEEE/RSJ International Conference on Intelligent Robots and Systems, Sendai, Japan.

Garry, R.: 2005, Laparoscopic surgery, *Best Practice & Research Clinical Obstetrics & Gynaecology* **19**, 1–16.

Guyton, A. C. and Hall, J. E.: 2000, *Textbook of Medical Physiology*, tenth edn, W.B. Saunders Company.

Hambley, A. R.: 2002, *Electrical Engineering Principles and Applications*, second edn, Prentice Hall.

Hayward, V., Astley, O. R., Cruz-Hernandez, M., Grant, D. and Robles-De-La-Torre, G.: 2004, Haptic interfaces and devices, *Sensor Review* **24**(1).

Hayward, V. and Cruz-Hernández, J. M.: 2000, Tactile display device using distributed lateral skin stretch, *Symposium on Haptic Interfaces for Virtual Environment and Teleoperator Systems*, Orlando, FL, pp. 1309–1314.

Howe, R. D.: n.d., Introduction to haptic display: Tactile display. http://haptic.mech.northwestern.edu/intro/tactile/lims.html.

Hu, T., Tholey, G., Desai, J. P. and Castellanos, A. E.: 2004, Evaluation of a laparoscopic grasper with force feedback, *Surgical Endoscopy* **18**(5), 863–867.

Iwamoto, T. and Shinoda, H.: 2005, Ultrasound tactile display for stress field reproduction - Examination of non-vibratory tactile apparent movement, *Proceedings of the First WorldHaptics Conference*, Pisa, Italy, pp. 220–228.

Jackman, S. V., Jarzemski, P. A., Listopadzki, S. M., Lee, B. R., Stoianovici, D., Demaree, R., Jarret, T. W. and Kavoussi, L. R.: 1999, The EndoHand: Comparison with standard laparoscopic instrumentation, *Journal of Laparoendoscopic & Advanced Surgical Techniques. Part A.* **9**(3), 253–258.

Jones, D. B., Wu, J. S. and Soper, N. J. (eds): 2004, *Laparoscopic Surgery. Principles and procedures*, Marcel Dekker, New York.

Kajimoto, H., Kawakami, N., Tachi, S. and Inami, M.: 2004, SmartTouch: Electric skin to touch the untouchable, *IEEE Computer Graphics and Applications* **24**(1), 36–43.

Kandel, E. R., Schwartz, J. H. and Jessell, T. M.: 2000, *Principles of Neural Science*, McGraw-Hill Companies, Inc.

Klatzky, R. L. and Lederman, S. J.: 2004, Touch, *in* A. F. Healy, R. W. Proctor and I. B. Weiner (eds), *Experimental Psychology. Handbook of Psychology, Volume 4*, John Wiley & Sons, New York, pp. 147–176.

Kolesar, E. S., Dyson, C. S., Reston, R. R., Fitch, R. C., Ford, D. G. and Nelms, S. D.: 1996, Tactile integrated circuit sensor realized with a piezoelectric polymer, *Proceedings of the 8th IEEE Conference on Innovative Systems in Silicon*, Austin, TX, pp. 372–381.

Krishna, G. M. and Rajanna, K.: 2004, Tactile sensor based on piezoelectric resonance, *IEEE Sensors Journal* **4**(5), 691–697.

Kyung, K., Ahn, M., Kwon, D. and Srinivasan, M. A.: 2005, A compact broadband tactile display and its effectiveness in the display of tactile form, *Proceedings of the First WorldHaptics Conference*, Pisa, Italy, pp. 600–601.

LaMotte, R. H. and Srinivasan, M. A.: 1991, Surface microgeometry: Tactile perception and neural encoding, *in* O. Franzen and J. Westman (eds), *Information processing in the somatosensory system*, MacMillan Press, London, pp. 49–58.

Lederman, S. J. and Klatzky, R. L.: 1987, Hand movements: A window into haptic object recognition, *Cognitive Psychology* **19**(3), 342–368.

Lederman, S. J. and Klatzky, R. L.: 1999, Sensing and displaying spatially distributed fingertip forces in haptic interfaces for teleoperator and virtual environment systems, *Presence: Teleoperators and Virtual Environments* **8**, 86–103.

Lee, J. M., Wagner, C. R., Lederman, S. J. and Howe, R. D.: 2003, Spatial low pass filters for pin actuated tactile displays, *Proceedings of the 11th International Symposium on Haptic Interfaces for Virtual Environment and Teleoperator Systems*, Los Angeles, CA, pp. 57–62.

Lehman, E. L.: 1975, *Nonparametrics. Statistical methods based on ranks*, Holden-Day.

Lowe, M., King, A., Lovett, E. and Papakostas, T.: 2004, Flexible tactile sensor technology: Bringing haptics to life, *Sensor Review* **24**(1), 33–36.

MacFarlane, M., Rosen, J., Hannaford, B., Pellegrini, C. and Sinanan, M.: 1999, Force-feedback grasper helps restore sense of touch in minimally invasive surgery, *Journal of Gastrointestinal Surgery* **3**(3), 278–285.

Makino, Y. and Shinoda, H.: 2005, Selective stimulation to superficial mechanoreceptors by temporal control of suction pressure, *Proceedings of the First WorldHaptics Conference*, Pisa, Italy, pp. 229–234.

Mårvik, R., Nesbakken, R., Langø, T., Yavuz, Y., Bjelland, H., Ottermo, M. V. and Stavdahl, Ø.: 2006, Ergonomic design criteria for a novel laparoscopic tool handle with tactile feedback. Submitted to Minerva Chirurgica.

Moy, G., Wagner, C. and Fearing, R. S.: 2000, A compliant tactile display for teletaction, *Proceedings of the IEEE International Conference on Robotics and Automation*, San Francisco, CA, pp. 3409–3415.

Napier, J. R.: 1956, The prehensile movements of the human hand, *Journal of Bone and Joint Surgery. British volume* (38B), 902–913.

Nesbakken, R.: 2004, Ergonomic guidelines in handle design - The challenges of laparoscopic surgical instruments. Student project report, NTNU.

Ottermo, M. V., Stavdahl, Ø. and Johansen, T. A.: 2004, Palpation instrument for augmented minimally invasive surgery, *Proceedings of the 2004 IEEE/RSJ International Conference on Intelligent Robots and Systems*, Sendai, Japan, pp. 3960–3964.

Ottermo, M. V., Stavdahl, Ø. and Johansen, T. A.: 2005, Electromechanical design of a miniature tactile shape display for minimally invasive surgery, *Proceedings of the First WorldHaptics Conference*, Pisa, Italy, pp. 561–562.

Ottermo, M. V., Stavdahl, Ø. and Johansen, T. A.: 2006a, Design and performance of a prototype tactile shape display for minimally invasive surgery. Submitted to Haptics-e.

Ottermo, M. V., Stavdahl, Ø. and Johansen, T. A.: 2006b, A remote palpation instrument for laparoscopic surgery: Design and performance. Submitted to IEEE Transactions on Biomedical Engineering.

Ottermo, M. V., Øvstedal, M., Langø, T., Stavdahl, Ø., Yavuz, Y., Johansen, T. A. and Mårvik, R.: 2006, The role of tactile feedback in laparoscopic surgery. Submitted to Surgical Laparoscopy, Endoscopy & Percutaneous Techniques.

Pagh, P., Heginbotham, W. B. and Page, C. J.: 1977, Novel techniques for tactile sensing in a three dimensional environment, *Ind. Robot.* pp. 35–48.

Pasquero, J. and Hayward, V.: 2003, STReSS: A practical tactile display system with one millimeter spatial resolution and 700 Hz refresh rate, *Proceedings of Eurohaptics 2003*, Dublin, Ireland.

Pawluk, D. T. V., Peine, W. J., Wellman, P. S. and Howe, R. D.: 1996, Simulating soft tissue with a tactile shape display, in B. Simon (ed.), Advances in Bioengineering, ASME BED-Vol. 36.

Pawluk, D. T. V., Son, J. S., Wellman, P. S., Peine, W. J. and Howe, R. D.: 1998, A distributed pressure sensor for biomechanical measurements, *Jornal of Biomechanical Engineering* **102**(2), 302–305.

Peine, W. J.: 1998, *Remote Palpation Instruments for Minimally Invasive Surgery*, PhD thesis, Harvard University, Cambridge, MA.

Peine, W. J., Wellman, P. S. and Howe, R. D.: 1997, Temporal bandwidth requirements for tactile shape displays, *Proceedings of the Symposium on Haptic Interfaces for Virtual Environment and Teleoperator Systems, ASME International Mechanical Engineering Congress and Exposition*, Dallas, TX, pp. 107–113.

Phillips, J. R. and Johnson, K. O.: 1981, Tactile spatial resolution. III. A continuum mechanics model of the skin predicting mechanoreceptor resonses to bars, edges, and gratings, *Journal of Neurophysiology* **46**(6).

Richard, C., Cutkosky, M. R. and MacLean, K.: 1999, Friction identification for haptic display, *Proceeding of the 1999 ASME IMECE*, Nashville, TN.

Rosen, J., Hannaford, B., MacFarlane, M. P. and Sinanan, M. N.: 1999, Force controlled and teleoperated endoscopic grasper for minimally invasive surgery - Experimental performance evaluation, *IEEE Transactions on Biomedical Engineering* **46**(10).

Sarakoglou, I., Tsagarakis, N. and Caldwell, D. G.: 2005, A portable fingertip tactile feedback array - Transmission system reliability and modelling, *Proceedings of the First WorldHaptics Conference*, Pisa, Italy, pp. 547–548.

Sedaghati, R., Dargahi, J. and Singh, H.: 2005, Design and modeling of an endoscopic piezoelectric tactile sensor, *International Journal of Solids and Structures* **42**, 5872–5886.

Sheskin, D. J.: 2000, *Handbook of Parametric and Nonparametric Statistical Procedures*, Chapman & Hall/CRC.

Simpson, D. C.: 1973, The control and supply of a multimovement externally powered upper limb prosthesis, *Proceedings of the 4th International Symposium on External Control of Human Extremities*, pp. 247–254.

Simpson, D. C.: 1974, The choice of control system for the multimovement prosthesis: Extended physiological proprioception (E.P.P.), *The control of Upper-Extremity Prostheses and Orthoses*, Thomas, chapter 15, pp. 146–150.

Srinivasan, M. A. and LaMotte, R. H.: 1987, Tactile discrimination of shape: Responses of slowly and rapidly adapting mechanoreceptive afferents to a step indented into the monkey fingerpad, *Journal of Neuroscience* **7**(6), 1682–1697.

Srinivasan, M. A. and LaMotte, R. H.: 1995, Tactual discrimination of softness, *Journal of Neurophysiology* **73**(1), 88–101.

Sugiyama, S., Kawahata, K., Yoneda, M. and Igarashi, I.: 1990, Tactile image detection using a 1k-element silicon pressure sensor array, *Sensors and Actuators* **A21-A23**, 397–400.

Tanie, K.: 1986, Advances in tactile sensors for robotics, *Proceedings of the 6th Sensor Symposium*, Japan, pp. 63–68.

Tendick, F. and Cavusoglu, M. C.: 1997, Human-machine interfaces for minimally invasive surgery, *Proceedings of the IEEE Engineering in Medicine and Biology Society*, Chicago, IL, pp. 2771–2776.

Tholey, G., Desai, J. P. and Castellanos, A. E.: 2005, Force feedback plays a significant role in minimally invasive surgery: Results and analysis, *Annals of Surgery* **241**(1), 102–109.

van Hemert tot Dingshof, V., Lazeroms, M., van der Ham, A., Jongkind, W. and Honderd, G.: 1996, Force reflection for a laparoscopic forceps, *Proceedings of the IEEE Engineering in medicine and biology society*, Amsterdam, The Netherlands, pp. 210–211.

Wagner, C. R., Lederman, S. J. and Howe, R. D.: 2004, Design and performance of a tactile shape display using RC servomotors, *Haptics-e: The Electronic Journal of Haptic Research* **3**(4).

Wagner, C. R., Stylopoulos, N. and Howe, R. D.: 2002, The role of force feedback in surgery: Analysis of blunt dissection, *Proceedings of the 10th International Symposium on Haptic Interfaces for Virtual Environment and Teleoperator Systems*, Orlando, FL.

Walpole, R. E., Myers, R. H. and Myers, S. L.: 1998, *Probability and statistics for engineers and scientists*, sixth edn, Prentice Hall.

Wellman, P. S., Peine, W. J., Favalora, G. E. and Howe, R. D.: 1997, Mechanical design and control of a high-bandwidth shape memory alloy tactile display, *International Symposium on Experimental Robotics*, Barcelona, Spain.

Yao, H., Hayward, V. and Ellis, R. E.: 2005, A tactile enhancement instrument for minimally invasive surgery, *Computer Aided Surgery* **10**(4), 233–239.

Øvstedal, M.: 2005, Taktil tilbakekobling i kikkhullskirurgi. Student project report, Department of Engineering Cybernetics, NTNU, English title: Tactile feedback in laparoscopic surgery.

Appendix A

Torque Constant Calculations

As mentioned in Chapter 5.2.4, we use three phases for the commutation instead of only two, which is done in normal operation. Therefore, we needed to calculate a new nominal torque constant. In the data sheet for the motor it is 13 mNm/A. The two cases are compared in Figure A.1.

We assume that COM is kept constant, so the current will be the same in all phases. Therefore, we relate the torque constant to COM. In our case, the magnetic field always points through the phase winding, so we assume an equivalent vector for the current (see Figure A.2).

The procedure for finding the new torque constant is as follows:

1. Determine the amount of torque each phase can generate (maximum when phase is perpendicular to rotor).

2. Use the new geometry (three phase case) to find torque as a function of phase current (assume 90° between rotor field and vector sum of the phase currents).

Part 1.

We know that the torque is proportional to the sine of the angle between the fields, so it will be maximum at 90° (between rotor and stator):

$$T_m = K_t I_m \tag{A.1}$$

Here K_t is the original nominal torque constant and I_m is the motor current.

By symmetry, we know that each of the two active phases (in the case where only two phases are used) contributes with half the torque:

$$T_1 = T_2 = \frac{T_m}{2} = \frac{1}{2} K_t I_1 = (\frac{1}{2} K_t I_2) \tag{A.2}$$

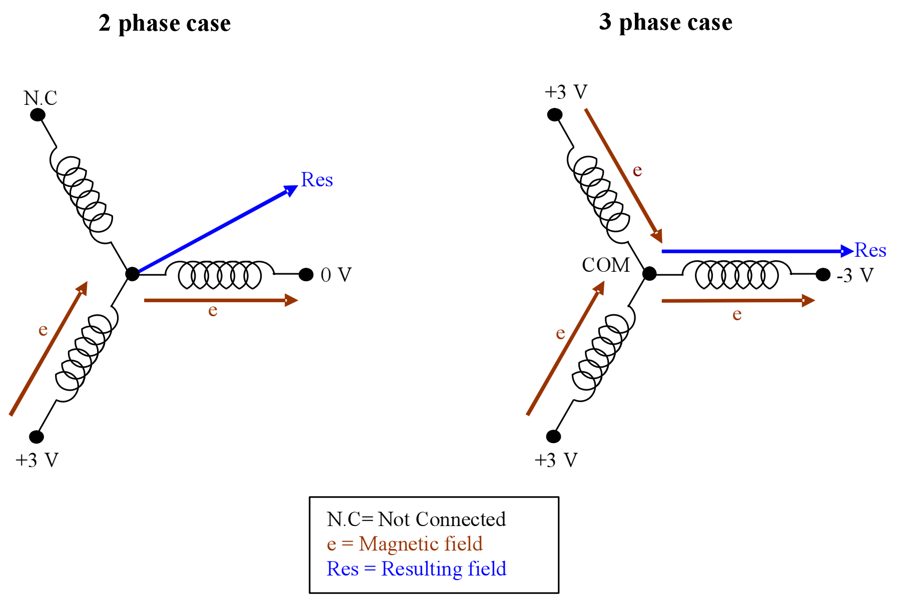

Figure A.1: Resulting field when using 2 and 3 active phases, respectively.

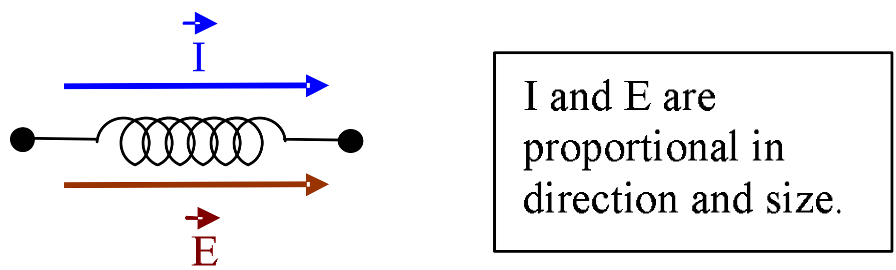

Figure A.2: Figure illustrating how I and B are proportional in size and direction.

where I_1 and I_2 are the phase currents. We also have:

$$T_{i,max} = K_p I_i \tag{A.3}$$

where K_p is the torque constant for one phase.

With an angle of 120° between the phase and the rotor we get:

$$T_{1,max} sin(120°) = \frac{1}{2} K_t I_1 \tag{A.4}$$

This gives:

$$T_{1,max} = \frac{K_t I_1}{2sin(120^o)} = K_p I_1 \tag{A.5}$$

$$K_p = \frac{K_t}{2sin(120°)} \tag{A.6}$$

With a torque constant of 13 $\frac{mNm}{A}$ we get:

$$K_p = \frac{13\ mNm/A}{2sin(120°)} = 7.5\ mNm/A \tag{A.7}$$

Part 2.

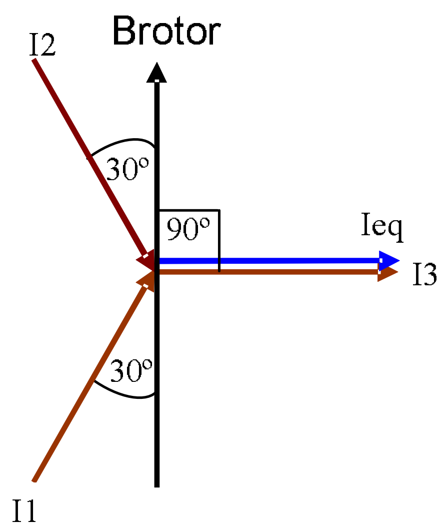

Figure A.3: Figure showing the geometry for the three phase case. The torque is at a maximum when the angle between the rotor and the phase is 90°.

For our geometry we get the situation indicated in Figure A.3 and calculate the torque as follows:

$$\begin{aligned} T_m &= T_{1,max} sin(90^\circ) + T_{2,max} sin(30^\circ) + T_{3,max} sin(30^\circ) \\ &= T_{i,max}(sin(90^\circ) + 2sin(30^\circ)) \end{aligned} \tag{A.8}$$

Recall from equation A.3 that $T_{i,max} = K_p I_i$. Since we have $sin(90^\circ) + 2sin(30^\circ) = 2$, we get:

$$T_m = K_p \cdot 2I_i = 15 \, \frac{mNm}{A} \cdot I_i \tag{A.9}$$

Hence the new torque constant is 15 mNm/A.

Appendix B

Statistics

B.1 Friedman's Test

In Chapter 4, a Friedman test was used to test the hypothesis H_0: F=LI=LIS. The alternative hypothesis is H_1: not H_0. Friedman's test is a two-way analysis of variance by ranks and is the nonparametric analog to one-way repeated ANOVA (Analysis of Variance). The test is an extension of the binomial sign test for two dependent samples to a design involving more than two dependent samples ($k > 2$). The reason why we use a nonparametric test is that we cannot assume that such a small data set has a normal (Gaussian) distribution. We have repeated measures since we test the same subject several times and more than two data sets (instruments), hence a Friedman test is suitable (Sheskin, 2000). If the result of the Friedman two-way analysis by ranks is significant, it indicates that there is a significant difference between at least two of the sample medians in the set of k medians (Sheskin, 2000). Although nonparametric tests are not based on assumptions of normality, randomization is still required, and the tests are less powerful than parametric tests.

The ranking procedure employed in Friedman's test requires that each of the scores of a subject be ranked within that subject. Since we have 3 observations for each instrument, we use the magnitude of the error for all 3 observations. The procedure for finding rank sums is as follows:

- Let X_k be the error observation for sample k
- Arrange the observations of each subject in ascending order and substitute a rank, R_k of $1, 2, .., k$ for each observation.

- In the case of identical observations, replace the observations by the mean of the ranks that the observations would have if they were distinguishable.

B.1.1 Hardness

The resulting ranking for our data set (for hardness) is shown in Table B.1 (where the sum of the magnitude of the error for all 3 observations for each subject is considered).

Table B.1: Table showing the rank order, (R_i), for Friedman's test for each subject in the hardness case. In the rank sum, FHF /FHLI/FHLIS, F stands for Friedman's test, H indicates hardness and F/LI/LIS indicates which instrument is considered. In FHFM/FHLIM/FHLISM, the M indicates that it is a mean.

Instrument	F		LI		LIS	
	X_1	R_1	X_2	R_2	X_3	R_3
Subject 1	0	1	4	2	8	3
Subject 2	8	1	15	3	10	2
Subject 3	0	1	8	3	2	2
Subject 4	0	1	10	2	17	3
Subject 5	0	1.5	6	3	0	1.5
Subject 6	0	1	2	3	1	2
Subject 7	0	1	2	2.5	2	2.5
Subject 8	0	1.5	6	3	0	1.5
Subject 9	2	1	8	3	4	2
Subject 10	0	1	6	3	2	2
Subject 11	0	1	9	3	2	2
Subject 12	2	1.5	2	1.5	4	3
Subject 13	2	1	3	2	4	3
Subject 14	0	1	8	3	2	2
Subject 15	0	1.5	0	1.5	4	3
Total		$FHF = 17$		$FHLI = 38.5$		$FHLIS = 34.5$
Mean		$FHFM = 1.13$		$FHLIM = 2.57$		$FHLISM = 2.30$

Based on these rank sums, the chi-square distribution is used to approximate the Friedman test statistic:

$$\begin{aligned}\chi_r^2 &= \frac{12}{nk(k+1)}(\sum_{j=1}^{k}(\sum R_j)^2) - 3n(k+1)\\ &= \frac{12}{15\cdot 3\cdot(3+1)}((17)^2) + (38.5)^2 + (34.5)^2) - (3\cdot 15\cdot(3+1))\\ &= 17.43 \end{aligned} \tag{B.1}$$

Here n is the number of subjects and k is the number of samples (instruments). The chi-square distribution provides an excellent approximation to the Friedman sampling distribution, but some sources recommend the use of exact probabilities for small sample sizes (Sheskin, 2000). From the look-up table of the chi-square distribution we find that $\chi^2_{0.05} = 5.99$ with a significance level, α, of 0.05. The number of degrees of freedom is $df = k - 1 = 2$. For $\alpha = 0.01$ we find $\chi^2_{0.01} = 9.21$. Since the computed value $\chi_r^2 = 17.43$ is greater than $\chi_{0.05} = 5.99$ and $\chi_{0.01} = 9.21$, the alternative hypothesis is supported at both the 0.05 and 0.01 level.

B.1.2 Size

The resulting ranking for our data set in the size case is shown in Table B.2. In the same way as for hardness, we test the hypothesis H_0: F=LI=LIS against the alternative hypothesis H_1: not H_0.

Based on these rank sums we find $\chi_r^2 = \frac{12}{15\cdot 3\cdot(3+1)}((16.5)^2) + (38.5)^2 + (33)^2) - (3\cdot 15\cdot(3+1)) = 19.23$. Recall that $\chi^2_{0.05} = 5.99$ and that $\chi^2_{0.01} = 9.21$. Since the computed value $\chi_r^2 = 19.23$ is greater than $\chi_{0.05} = 5.99$ and $\chi_{0.01} = 9.21$, the alternative hypothesis is rejected at both the 0.05 and 0.01 level.

B.2 Pairwise Comparison using Wilcoxon Two-sample Test

In the previous section, we compared all 3 instruments simultaneously, but when the value of χ_r^2 is significant it does not indicate whether just two or, in fact, more than two conditions differ significantly from each other. In this case, tests designed to compare only two samples provide a more effective alternative (Lehman, 1975). In our experiments we did not use paired observations but divided our subjects into blocks. A block is a portion (e.g. two seeds in the same pot) of the experimental material that is

Table B.2: Table showing the rank order, (R), for Friedman's test for each subject in the size case. In the rank sum, FSF /FSLI/FSLIS, F stands for Friedman's test, S indicates size and F/LI/LIS indicates which instrument is considered. In FSFM/FSLIM/FSLISM, the M indicates that it is a mean.

Instrument	F		LI		LIS	
	X_1	R_1	X_2	R_2	X_3	R_3
Subject 1	1	1	3	2	4	3
Subject 2	4	1	13	3	8	2
Subject 3	0	1	5	2	11	3
Subject 4	0	1	5	2	10	3
Subject 5	0	1	9	3	6	2
Subject 6	0	1	9	3	4	2
Subject 7	1	1	4	3	3	2
Subject 8	2	1	3	2	4	3
Subject 9	1	1	5	3	4	2
Subject 10	1	1	2	2	6	3
Subject 11	2	2	5	3	0	1
Subject 12	0	1	14	3	9	2
Subject 13	0	1	1	2.5	1	2.5
Subject 14	0	1	7	3	6	2
Subject 15	0	1.5	3	3	0	1.5
Total		$FSF = 16.5$		$FSLI = 39.5$		$FSLIS = 34$
Mean		$FSFM = 1.1$		$FSLIM = 2.63$		$FSLISM = 2.27$

expected to be more homogeneous than the aggregate (e.g. all seeds not in the same pot) (Box, Hunter and Hunter, 2005). By confining comparisons to those within blocks, greater precision is usually obtained because the differences between associated blocks are eliminated. We consider the results for each test subject (for hardness or size) as one block. Since we compare two instruments we get 6 observations in each block. Based on this, we can perform a Wilcoxon two-sample test and compute the rank sum for each of the instruments. The Wilcoxon two-sample test is an appropriate nonparametric alternative to the parametric two-sample t-test, which is extensively used in problems that deal with inference about the population mean or in problems that involve comparative samples (Walpole, Myers and Myers, 1998). Although we do not assume normality, randomization is still required in the same way as for Friedman's test.

The procedure for finding the rank sum for one test subject is as follows (when comparing for instance LI and LIS) (Walpole et al., 1998):

- Let f_1 be the number of observations for LI and f_2 the number of observations for LIS.
- Arrange the $f_1 + f_2$ observations of the combined samples in ascending order and substitute a rank of $1, 2, .., f_1 + f_2$ for each observation.
- In the case of identical observations, replace the observations by the mean of the ranks that the observations would have if they were distinguishable.

The mean or expected rank for one observation (with both instruments), μ , then becomes:

$$\mu = E(X) = \frac{f_1 + f_2 + 1}{2} \tag{B.2}$$

B.2.1 Analysis of F, LI and LIS in Chapter 4

Hardness

Table B.3 shows the rank sums for each subject for F, LI and LIS in the hardness case. Since we have 3 instruments, we also have 3 paired comparisons (F versus LI), (F versus LIS) and (LI versus LIS). After employment of Wilcoxon two-sample test, the total rank sums WHF, $WHLI$ and $WHLIS$, are assumed to be approximately normal (here W indicates the Wilcoxon two-sample test, H stands for hardness and F/LI/LIS indicates which instrument is considered). Hence, we end up with testing the following cases:

H_0: $WHF = WHLI$ versus H_1: $WHF < WHLI$
H_0: $WHF = WHLIS$ versus H_1: $WHF < WHLIS$
H_0: $WHLI = WHLIS$ versus H_1: $WHLIS < WHLI$

We have from equation B.2 that:

$$\mu = E(X) = \frac{3 + 3 + 1}{2} = 3.5 \tag{B.3}$$

As we have 3 observations (f) for all instruments in every block, and each block contains the results for one subject (for the two instruments we are comparing), we have 15 blocks (n). The expected value and variance for $WHF (= WHLI = WHLIS)$ then becomes:

$$\mu_{WHF} = f \cdot \mu \cdot n = 3 \cdot 3.5 \cdot 15 = 157.5 \tag{B.4}$$

Table B.3: Table showing the rank sums, $WHF_i/WHLI_i/WHLIS_i$ $(i = 1, 2, .., n)$, and the total rank sums, $WHF/WHLI/WHLIS$ from Wilcoxon two-sample test in the hardness case (from the experiments in Chapter 4).

Case	F versus LI		F versus LIS		LI versus LIS	
	WHF_i	$WHLI_i$	WHF_i	$WHLIS_i$	$WHLI_i$	$WHLIS_i$
Subject 1	9	12	6	15	8.5	12.5
Subject 2	7	14	9.5	11.5	12.5	8.5
Subject 3	9	12	9	12	11	10
Subject 4	6	15	7.5	13.5	9.5	11.5
Subject 5	6	15	10.5	10.5	15	6
Subject 6	9	12	9	12	13.5	7.5
Subject 7	9	12	9	12	10	11
Subject 8	7.5	13.5	10.5	10.5	13.5	7.5
Subject 9	6	15	9	12	13	8
Subject 10	6	15	9	12	13.5	7.5
Subject 11	6	15	9	12	14	7
Subject 12	10.5	10.5	9	12	9	12
Subject 13	9.5	11.5	9	12	9.5	11.5
Subject 14	6	15	9	12	7.5	13.5
Subject 15	10.5	10.5	7.5	13.5	7.5	13.5
Total rank sum	117	198	132.5	182.5	167.5	147.5

and

$$\sigma^2_{WHF} = f^2 \cdot \mu \cdot n = 3 \cdot 3 \cdot 3.5 \cdot 15 = 472.5 \tag{B.5}$$

F versus LI

Since we are testing the hypothesis H_0: $WHF = WHLI$ against the alternative that $WHF < WHLI$, we need a one-tailed test. With a significance level of $\alpha = 0.05$ we use the look-up table for the area under the normal curve to find the critical region $z_{0.05} < 1.645$.

We compute the value of the test statistic as follows (Walpole et al., 1998):

$$z = \frac{X - \mu}{\sqrt{\sigma^2}} \tag{B.6}$$

Hence we get the following critical region when comparing F and LI in the hardness case:

$$z_{WHF} = \frac{117 - 157.5}{\sqrt{472.5}} = -1.86 \tag{B.7}$$

Similarly, we find $z_{WHLI} = 1.86$ (due to symmetry of the normal distribution). Since $z_{WHLI} = 1.86 > 1.65 = z_{0.05}$, we can reject H_0 and conclude that F is significantly better than LI for hardness. From the table showing the area under the normal curve we can find the P-value, $P_{WHLI} = P(z > 1.86) = 0.0307$. The P-value is the lowest level of significance at which the observed value of the test statistic is significant. In other words, we can reject H_0 at a level of significance of approximately 0.03.

F versus LIS

Performing the same analysis for F versus LIS yields:

$$z_{WHF} = \frac{132.5 - 157.5}{\sqrt{472.5}} = -1.15 \tag{B.8}$$

Similarly, we find $z_{WHLIS} = 1.15$, and since $z_{WHLIS} = 1.15 < 1.65 = z_{0.05}$, we cannot reject H_0. This means that we can conclude that F is not significantly better than LIS for hardness.

LI versus LIS

When comparing LI and LIS we get:

$$z_{WHLIS} = \frac{147.5 - 157.5}{\sqrt{472.5}} = -0.46 \tag{B.9}$$

We find $z_{WHLI} = 0.46$ in the same way, and since $z_{WHLI} = 0.46 < 1.65 = z_{0.05}$, we cannot reject H_0. Hence, we can conclude that LIS is not significantly better than LI for hardness.

Size

Table B.4 shows the rank sums, $WSF/WSLI/WSLIS$, for each subject for F, LI and LIS in the size case (W indicates the Wilcoxon two-sample test, S stands for size and F/LI/LIS indicates which instrument is considered). The hypotheses for comparison of the instruments are the same as in the hardness case:
H_0: $WSF = WSLI$ versus H_1: $WSF < WSLI$
H_0: $WSF = WSLIS$ versus H_1: $WSF < WSLIS$
H_0: $WSLI = WSLIS$ versus H_1: $WSLIS < WSLI$

Table B.4: Table showing the rank sums, $WSF_i/WSLI_i/WSLIS_i$ ($i = 1, 2, .., n$), and the total rank sums, $WSF/WSLI/WSLIS$ from Wilcoxon two-sample test in the size case.

Case	F versus LI		F versus LIS		LI versus LIS	
	WSF_i	$WSLI_i$	WSF_i	$WSLIS_i$	$WSLI_i$	$WSLIS_i$
Subject 1	7.5	13.5	7	14	9	12
Subject 2	7	14	9	12	12	9
Subject 3	7.5	13.5	6	15	7.5	13.5
Subject 4	7.5	13.5	6	15	8	13
Subject 5	6	15	7.5	13.5	12	9
Subject 6	6	15	6	15	15	6
Subject 7	7.5	13.5	7.5	13.5	12	9
Subject 8	9.5	11.5	8.5	12.5	9.5	11.5
Subject 9	8.5	12.5	8	13	10.5	10.5
Subject 10	9	12	8	13	8.5	12.5
Subject 11	8	13	12	9	15	6
Subject 12	6	15	6	15	13	8
Subject 13	9	12	9	12	10.5	10.5
Subject 14	6	15	6	15	11.5	9.5
Subject 15	9	12	10.5	10.5	12	9
Total rank sum	114	201	117	198	166	149

F versus LI

We find the following critical region when comparing F and LI in the size case:

$$z_{WSF} = \frac{114 - 157.5}{\sqrt{472.5}} = -2.01 \tag{B.10}$$

Similarly, we find $z_{WSLI} = 2.01$, and since $z_{WSLI} = 2.01 > 1.65 = z_{0.05}$, we can reject H_0 and conclude that F is significantly better than LI for size. From the table showing the area under the normal curve we find $P_{WSLI} = P(z > 2.01) = 0.0222$. In other words, we can reject H_0 at a level of significance of approximately 0.02.

F versus LIS

Performing the analysis for F versus LIS yields:

$$z_{WSF} = \frac{117 - 157.5}{\sqrt{472.5}} = -1.86 \tag{B.11}$$

We also find $z_{WSLIS} = 1.86$ meaning that $z_{WSLI} = 1.86 > 1.65 = z_{0.05}$. Hence we can reject H_0 and conclude that F is significantly better than LIS for size.

LI versus LIS

When comparing LI and LIS we get:

$$z_{WSLIS} = \frac{149 - 157.5}{\sqrt{472.5}} = -0.39 \tag{B.12}$$

Similarly, we find $z_{WSLI} = 0.39$, and since $z_{WSLI} = 0.39 < 1.65 = z_{0.05}$, we cannot reject H_0 and conclude that LIS is not significantly better than LI for hardness.

B.2.2 Analysis of LI and LIT in Chapter 7

The procedure for comparing LI and LIT is the same as described in the previous section. Since we have 5 observations of each instrument for each person we find the mean or expected rank, μ, for one observation (with both instruments):

$$\mu = E(X) = \frac{f_1 + f_2 + 1}{2} = \frac{5 + 5 + 1}{2} = 5.5 \tag{B.13}$$

Hardness

In Table B.5, the rank sums for each subject for LI and LIT in the hardness case are shown. Under the hypothesis H_0: $WHLI = WHLIT$, we can assume that the total rank sums, $WHLI$ and $WHLIT$, are approximately normal. In the same way as in Section B.2.1, W indicates the Wilcoxon two-sample test, H stands for hardness and LI/LIT indicates which instrument is considered.

For hardness we had 5 observations (f) for both instruments in every block. Since one block contains the results for one test person, we have 10 blocks (n). The expected value and variance for $WHLI$ then becomes:

$$\mu_{WHLI} = f \cdot \mu \cdot n = 5 \cdot 5.5 \cdot 10 = 275 \tag{B.14}$$

$$\sigma^2_{WHLI} = f^2 \cdot \mu \cdot n = 5 \cdot 5 \cdot 5.5 \cdot 10 = 1375 \tag{B.15}$$

Table B.5: Table showing the rank sums from Wilcoxon two-sample test for each subject in the hardness case.

	$WHLI_i$	$WHLIT_i$
Subject 1	22.5	32.5
Subject 2	28	27
Subject 3	27.5	27.5
Subject 4	27.5	27.5
Subject 5	32.5	22.5
Subject 6	27.5	27.5
Subject 7	27.5	27.5
Subject 8	34.5	20.5
Subject 9	30	25
Subject 10	32.5	22.5
Total rank sum	$WHLI = 290$	$WHLIT = 260$

We test the hypothesis H_0: $WHLI = WHLIT$ against the alternative that $WHLI > WHLIT$. With a significance level, $\alpha = 0.05$, we find the critical region $z_{0.05} < 1.645$.

We compute the value of the test statistic:

$$z_{WHLI} = \frac{290 - 275}{\sqrt{1375}} = 0.41 \tag{B.16}$$

Similarly, we find $z_{WHLIT} = -0.41$ (due to symmetry of the normal distribution). Since $z_{WHLI} = 0.41 < 1.65 = z_{0.05}$, we do not reject H_0 and conclude that LIT is not significantly better than LI for hardness. From the table showing the area under the normal curve we can find $P_{WHLI} = P(z > 0.41) = 0.6591$. $P_{WHLI} = 0.6591$ is the probability of obtaining a value of z as large or larger (in magnitude) than 0.41, and hence the evidence in favor of H_0 is strong.

Size

Table B.6 shows the rank sums for each test person for LI and LIT in the size case. In the same way as for hardness, we test the hypothesis H_0: $WSLI = WSLIT$ against the alternative that $WSLI > WSLIT$.

With a significance level of $\alpha = 0.05$, we have the same critical region as in the hardness case ($z_{0.05} < 1.645$). We compute the value of the test statistic $z_{WSLI} = \frac{344-275}{\sqrt{1375}} = 1.86$. Since $z_{WSLI} = 1.86 > 1.65 = z_{0.05}$, we can reject H_0 and conclude that LIT is significantly better than LI for hardness. From the table showing the area under the normal curve we find

Table B.6: Table showing the rank sums from Wilcoxon two-sample test for each subject in the size case.

	$WSLI_i$	$WSLIT_i$
Subject 1	39.5	15.5
Subject 2	40	15
Subject 3	37.5	17.5
Subject 4	36.5	18.5
Subject 5	36	19
Subject 6	29	26
Subject 7	28	27
Subject 8	32.5	22.5
Subject 9	35	20
Subject 10	30	25
Total rank sum	$WSLI = 344$	$WSLIT = 206$

$P_{WSLI} = P(z > 1.86) = 0.0307$. In other words, we can reject H_0 at a level of significance of approximately 0.03.

As mentioned in Chapter 7.5.2, the last 4 subjects that conducted the experiments used a different grasper for LI than the previous 6 subjects. Therefore, the same analysis as above is used on the last 4 subjects to check if the size of the end effector or the quality of the grasper influenced our results.

We have $WSLI4 = 125$ and $WSLIT4 = 94.5$ (where the 4 in $WSLI4$ and $WSLIT4$ indicates that only the last 4 subjects are considered). The expected value and variance for $WSLI4$ then becomes (with 4 blocks):

$$\mu_{WSLI4} = 5 \cdot 5.5 \cdot 4 = 110 \tag{B.17}$$

$$\sigma^2_{WSLI4} = 5 \cdot 5 \cdot 5.5 \cdot 4 = 550 \tag{B.18}$$

Similarly, the value of the test statistic is:

$$z_{WSLI4} = \frac{125.5 - 110}{\sqrt{550}} = 0.66 \tag{B.19}$$

Since $z_{WSLI4} = 0.66 < 1.65 = z_{0.05}$, we cannot reject H_0 in this case.